



US Army Corps  
of Engineers

TECHNICAL REPORT CERC-92-15

# CRESCENT CITY INSTRUMENTED MODEL DOLOS STUDY

## Coastal Model Investigation

by

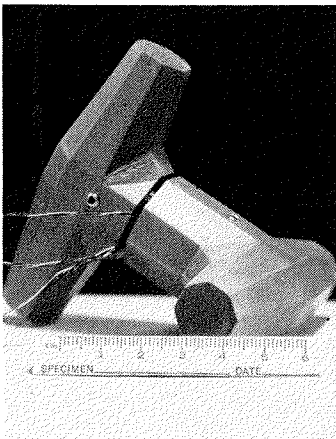
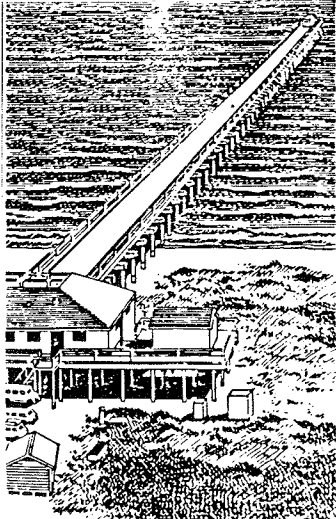
Dennis G. Markle, Homer C. Greer III

Coastal Engineering Research Center

DEPARTMENT OF THE ARMY

Waterways Experiment Station, Corps of Engineers  
3909 Halls Ferry Road, Vicksburg, Mississippi 39180-6199

# CERC LIBRARY



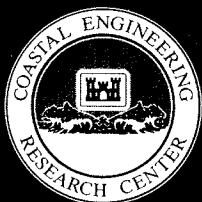
December 1992

Final Report

Approved For Public Release; Distribution Is Unlimited

# CERC LIBRARY

Prepared for DEPARTMENT OF THE ARMY  
US Army Corps of Engineers  
Washington, DC 20314-1000



**Destroy this report when no longer needed. Do not return  
it to the originator.**

**The findings in this report are not to be construed as an official  
Department of the Army position unless so designated  
by other authorized documents.**

**The contents of this report are not to be used for  
advertising, publication, or promotional purposes.  
Citation of trade names does not constitute an  
official endorsement or approval of the use of  
such commercial products.**

REPORT DOCUMENTATION PAGE			Form Approved OMB No. 0704-0188	
Public reporting burden for this collection of information is estimated to average 1 hour per response, including the time for reviewing instructions, searching existing data sources, gathering and maintaining the data needed, and completing and reviewing the collection of information. Send comments regarding this burden estimate or any other aspect of this collection of information, including suggestions for reducing this burden, to Washington Headquarters Services, Directorate for Information Operations and Reports, 1215 Jefferson Davis Highway, Suite 1204, Arlington, VA 22202-4302, and to the Office of Management and Budget, Paperwork Reduction Project (0704-0188), Washington, DC 20503.				
1. AGENCY USE ONLY (Leave blank)	2. REPORT DATE December 1992	3. REPORT TYPE AND DATES COVERED Final report		
4. TITLE AND SUBTITLE Crescent City Instrumented Model Dolos Study; Coastal Model Investigation			5. FUNDING NUMBERS	
6. AUTHOR(S) Dennis G. Markle Homer C. Greer III				
7. PERFORMING ORGANIZATION NAME(S) AND ADDRESS(ES) USAE Waterways Experiment Station Coastal Engineering Research Center 3909 Halls Ferry Road Vicksburg, MS 39180-6199			8. PERFORMING ORGANIZATION REPORT NUMBER  Technical Report CERC-92-15	
9. SPONSORING/MONITORING AGENCY NAME(S) AND ADDRESS(ES)  US Army Corps of Engineers Washington, DC 20314-1000			10. SPONSORING/MONITORING AGENCY REPORT NUMBER	
11. SUPPLEMENTARY NOTES Available from National Technical Information Service, 5285 Port Royal Road, Springfield, VA 22161				
12a. DISTRIBUTION / AVAILABILITY STATEMENT  Approved for public release; distribution is unlimited			12b. DISTRIBUTION CODE	
13. ABSTRACT (Maximum 200 words)  One task of the Prototype Dolos Study was to develop a transfer function between incident wave conditions and the pulsating loads they produce in the instrumented prototype dolosse. The purpose of the physical model investigation was to develop and verify model technology for measuring wave-induced moments and torques at small scale. This objective was approached in the model investigation in the following manner. <ul style="list-style-type: none"> <li>a. Reactivate the three-dimensional (3-D) breakwater stability model used during the 1985 model tests, modify the breakwater structure to match the geometry of the 1986 dolos rehabilitation, and remold the bathymetry seaward of the breakwater to match the most recent survey information.</li> <li>b. Develop and construct instrumented model dolosse that reproduce the 42-ton prototype dolosse at the stability model scale and that are capable of measuring wave-induced pulsating loads.</li> <li>c. Incorporate the instrumented dolosse into the model and measure and</li> </ul> <p style="text-align: right;">(Continued)</p>				
14. SUBJECT TERMS Armor Units Breakwater Concrete			Dolos Hydraulic Model Wave Stability	15. NUMBER OF PAGES 101
			16. PRICE CODE	
17. SECURITY CLASSIFICATION OF REPORT UNCLASSIFIED	18. SECURITY CLASSIFICATION OF THIS PAGE UNCLASSIFIED	19. SECURITY CLASSIFICATION OF ABSTRACT	20. LIMITATION OF ABSTRACT	

13. (Concluded).

record the pulsating loads induced in the dolosse by irregular wave realization of the discrete spectra that were measured in the prototype.

- d. Develop a transfer function between incident model waves and the pulsating loads they induce in the instrumented model dolosse in a similar manner as done for the prototype data.
- e. Compare the model and prototype transfer function and if needed, develop a scaling relation between them.

## PREFACE

The study reported herein was one of many tasks of the Crescent City Prototype Dolosse Study. Authority and funding to conduct this study were granted the US Army Engineer Waterways Experiment Station (WES) Coastal Engineering Research Center (CERC) by Headquarters, US Army Corps of Engineers (HQUSACE). This report was reviewed, edited, and published under the Civil Works Research Work Unit 32536, "Concrete Armor Unit Design," Coastal R&D Program, authorized by USACE. The HQUSACE Technical Monitors were Messrs. John H. Lockhart, Jr; John G. Housley; Barry Holiday; and David Rollig. Ms. Carolyn M. Holmes was the CERC Program Manager.

Physical model tests were developed and conducted during the period June 1987 to July 1989 under the general direction of Dr. James R. Houston, Director, CERC, and Mr. Charles C. Calhoun, Jr., Assistant Director, CERC; and under the direct supervision of Mr. C. E. Chatham, Chief, Wave Dynamics Division (WDD), and Mr. D. D. Davidson, Chief, Wave Research Branch (WRB). The model investigation was designed and carried out by Mr. Dennis G. Markle, Wave Processes Branch (WPB), assisted by Messrs. Donald L. Ward, Jeffrey A. Melby, C. Ray Herrington, and Raymond Reed, all of WRB, Messrs. Homer C. Greer III, Barry W. McCleave, S. Wallace Guy, and Joseph C. Ables, all of the WES Instrumentation Services Division, Mr. Tommy L. Bevins, WES Structures Laboratory, and Mr. Marshall P. Thomas, WPB. This report was prepared by Messrs. Markle and Greer. Technical review was provided by Dr. Stephen A. Hughes, Senior Scientist in WDD.

At the time of publication of this report, Director of WES was Dr. Robert W. Whalin. Commander was COL Leonard G. Hassell, EN.

## CONTENTS

	<u>Page</u>
PREFACE.....	1
CONVERSION FACTORS, NON-SI TO SI (METRIC)	
UNITS OF MEASUREMENT.....	3
PART I: INTRODUCTION.....	4
The Prototype.....	4
Purpose and Approach of the Model Investigation.....	7
PART II: THE MODEL.....	10
Model-Prototype Scale Relationships.....	10
Breakwater Construction Material.....	10
Test Facility.....	11
Model Breakwater Construction.....	11
Local Bathymetry.....	13
Instrumented Model Dolosse.....	15
Wave Gage System.....	30
Automated Data Acquisition System.....	33
PART III: TESTS AND TEST RESULTS.....	34
Selection of Test Conditions.....	34
Calibration of the Wave Basin.....	34
Placement of Instrumented Model Dolosse.....	35
Model Operation.....	40
Tests.....	45
Data Analysis.....	45
PART IV: CONCLUSIONS.....	58
REFERENCES.....	59
TABLES 1-5	
APPENDIX A: NOTATION.....	A1
APPENDIX B: PROTOTYPE BREAKWATER AND BATHYMETRY DATA.....	B1
APPENDIX C: ADACS.....	C1

CONVERSION FACTORS, NON-SI TO SI (METRIC)  
UNITS OF MEASUREMENT

Non-SI units of measurement used in this report can be converted to SI (metric) units as follows:

<u>Multiply</u>	<u>By</u>	<u>To Obtain</u>
degrees (angle)	0.01745329	radians
Fahrenheit degrees	5/9 (F-32)	Celcius degrees or Kelvins
feet	0.3048	metres
foot-pounds (force)	1.355818	metre-newtons
inches	25.4	millimetres
miles (US statute)	1.609347	kilometres
pounds (force) per square inch	68947.6	dynes per square centimetre
pounds (force) per cubic foot	157.087467	newtons per cubic metre
tons (force)	8896.444	newtons

---

\* To obtain Celsius (C) temperature readings from Fahrenheit (F) readings, use the following formula:  $C = (5/9)(F-32)$ . To obtain Kelvin (K) readings, use:  $K = (5/9)(F-32) + 273.15$ .

CRESCENT CITY INSTRUMENTED MODEL DOLOS STUDY

Coastal Model Investigation

PART I: INTRODUCTION

The Prototype

1. Crescent City Harbor, California, is located on the northern California coastline, approximately 17 miles\* south of the Oregon-California border (Figure 1). The existing outer breakwater is 4,670 ft long with the main stem 3,670 ft long, and the easterly extension (dogleg) 1,000-ft-long. The original project did not call for the dogleg but intended for the main stem of the breakwater to extend out to Round Rock. However, the main stem of the original breakwater, beyond sta 37+00, sustained severe damage and was reconstructed on two occasions. Finally, this portion of the main stem was abandoned and the 1,000-ft-long dogleg referred to above was added. Two-dimensional stability tests were conducted of the tetrapod breakwater designs proposed for the trunk portion of the dogleg (Hudson and Jackson 1955, 1956). In 1957, 1,836 twenty-five-ton, unreinforced tetrapods were placed on the sea-side slope from sta 41+20 to the end of the dogleg (sta 46+70), and 140 of the same size tetrapods were stockpiled on the sea-side slope of the first 200 ft of the dogleg, adjacent to the main stem (sta 37+00 to 39+00). Model tests were not conducted for the severe breaking wave action that occurs around the elbow of the breakwater and most of the tetrapods have been broken and/or displaced from this area, while to date, only three of the tetrapods placed on the last 550 ft (sta 41+20 to 46+70) of the dogleg have been reported broken. In 1974, 246 forty-ton unreinforced dolosse were placed on the sea-side slope of the last 230 ft of the breakwater's main stem (sta 34+70 to 37+00). A survey conducted in August 1982 found that approximately 70 of the original 240 dolosse were broken.\*\* Of this number, it was certain that 22 were broken during placement and/or during storm conditions that occurred while

---

\* A table of factors for converting non-SI units of measurement to SI (metric) units is presented on page 3.

\*\* Memorandum for Record, September 1982, "Crescent City Harbor, California - 20 August 1982 Inspection of Outer Breakwater Dolos Section," J. R. Edminsten, US Army Engineer Division, South Pacific, San Francisco, CA.

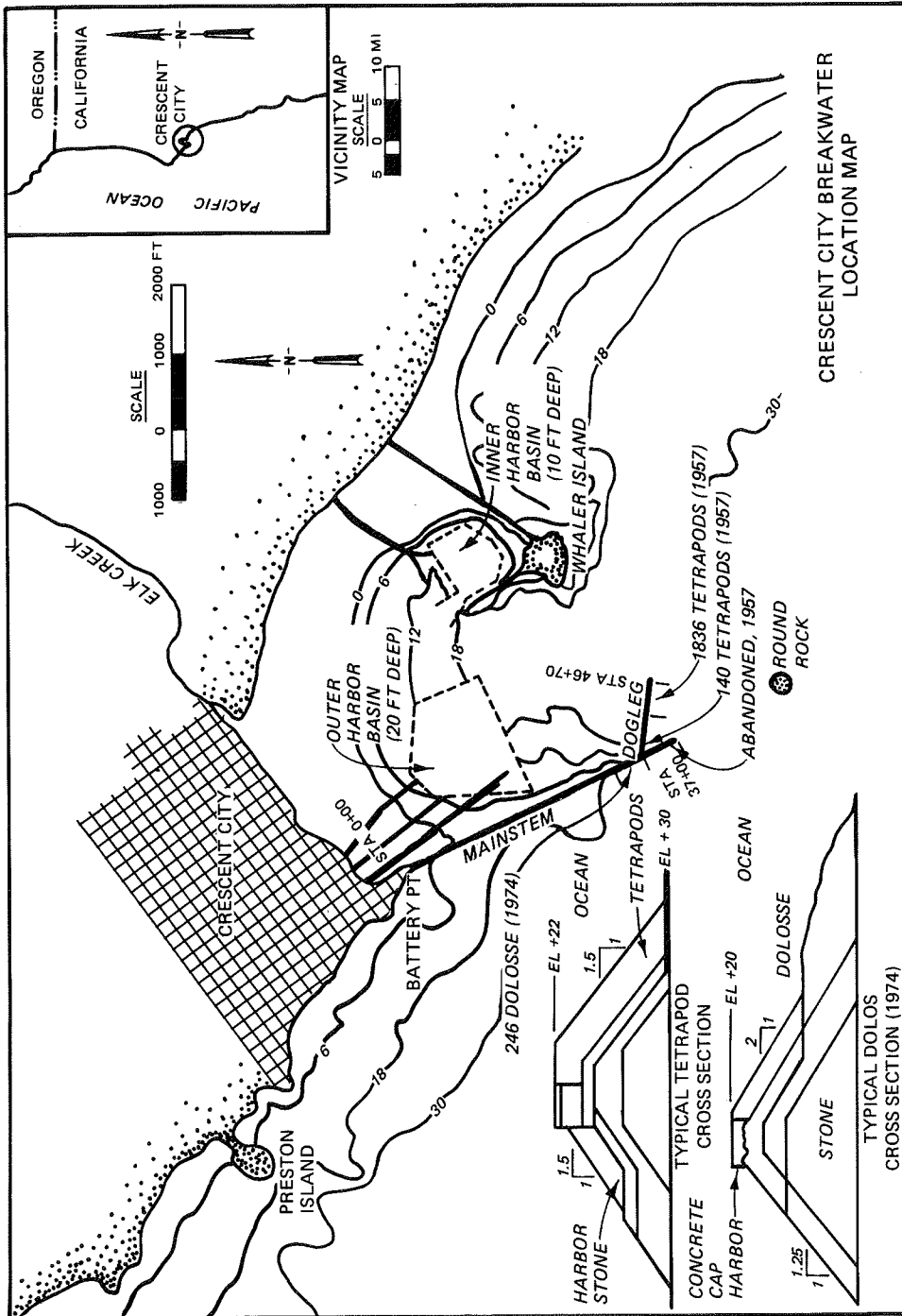


Figure 1. Vicinity and location map, Crescent City breakwater

construction was ongoing (Markle and Davidson 1984). Storms during the winter of 1983 caused significant amounts of additional dolos breakage and deterioration of the outer portions of the breakwater main stem. From July 1984 through March 1985 a series of physical model stability tests were conducted at the Waterways Experiment Station's (WES's) Coastal Engineering Research Center (CERC) to develop a hydraulically stable rehabilitation design for the damaged breakwater (Baumgartner, Carver, and Davidson 1985). Specifically, the model study objective was to determine the number of reinforced, 42-ton dolosse required and the geometry they should be placed in to stabilize the breakwater between sta 34+00 and 37+00.

2. In 1986, 760 fiber-reinforced, 42-ton dolosse were cast, and 680 placed on the sea-side slope of the main stem from sta 34+00 to approximately 105 ft beyond sta 37+00. The remainder of the units were stockpiled on the harbor side of the structure. Figure 2 shows the plan view geometry of the dolos rehabilitation work as recommended by the 1985 physical model investigation. Twenty of the 680 dolosse placed on the sea-side face were instrumented to collect moments and torques induced at the fluke-shank interface on one end of the dolos and selected dolosse out of these 20 contained accelerometers to monitor dolos motion. The instrumented units were placed near the center of the repair area. Four of the dolosse were placed in the bottom layer and the remaining sixteen were positioned in the top layer. Figures 3 and 4 show the delivery and subsequent deployment of the first instrumented dolos. The dolosse were linked to a land-based data acquisition system. Wave monitoring devices were placed at locations seaward of the dolos repair section and pressure transducers were positioned within the breakwater to monitor internal pressure fluctuations. During the two years following the repair, a wealth of incident wave conditions and dolos moment and torque data were collected. Details of the prototype dolos instrumentation and data acquisition and analysis work are presented in Howell et al. (in preparation). An aerial view of the rehabilitated structure is shown in Figure 5. Instrumented units can be seen in the darker area at approximately the center of the sea-side slope.

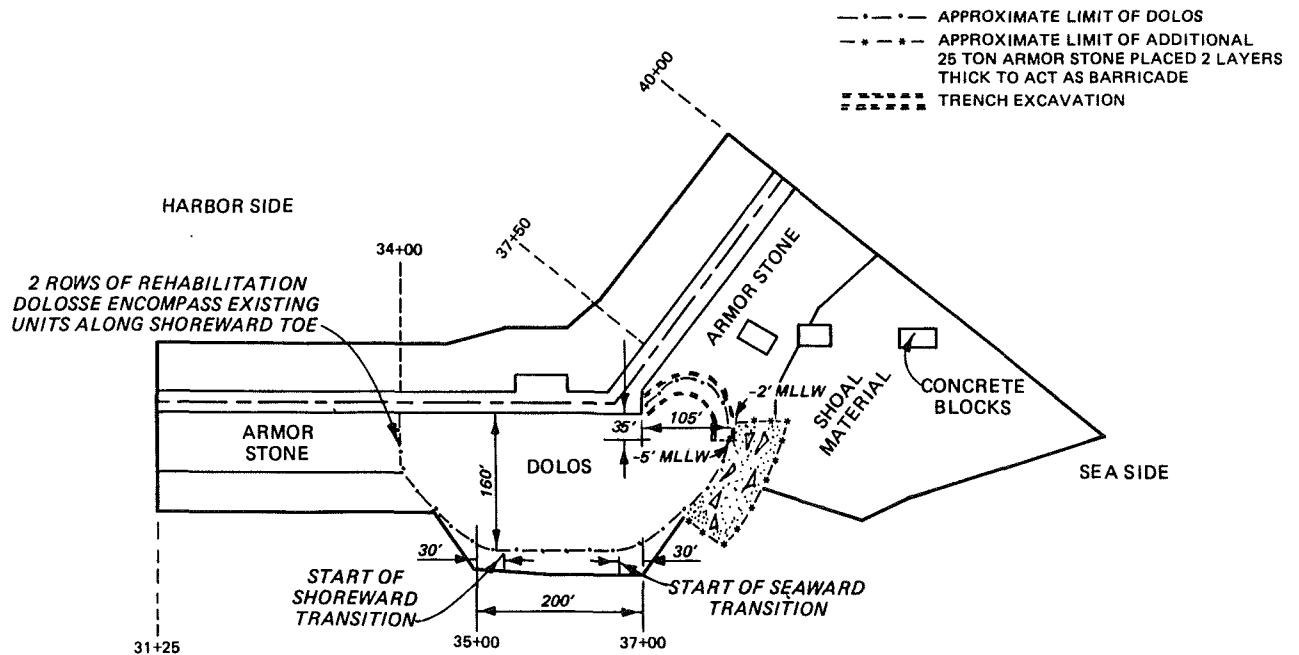


Figure 2. Dolos rehabilitation design as recommended by 1985 model study

Purpose and Approach of the Model Investigation

3. One task of the Prototype Dolos Study was to develop a transfer function between incident wave conditions and the pulsating loads they produce in the instrumented prototype dolosse. The purpose of the physical model investigation was to develop and verify model technology for measuring wave-induced moments and torques at small scale. This objective was approached in the model investigation in the following manner:

- a. Reactivate the three-dimensional breakwater stability model used during the 1985 model tests, modify the breakwater structure to match the geometry of the 1986 dolos rehabilitation, and remold the bathymetry seaward of the breakwater to match the most recent survey information.
- b. Develop and construct instrumented model dolosse that reproduce the 42-ton prototype dolosse at the stability model scale and that are capable of measuring wave-induced pulsating loads.
- c. Incorporate the instrumented dolosse into the model, and measure and record the pulsating loads induced in the dolosse by irregular wave realization of the discrete spectra that were measured in the prototype.



Figure 3. Delivery of first instrumented dolos



Figure 4. Deployment of first instrumented unit

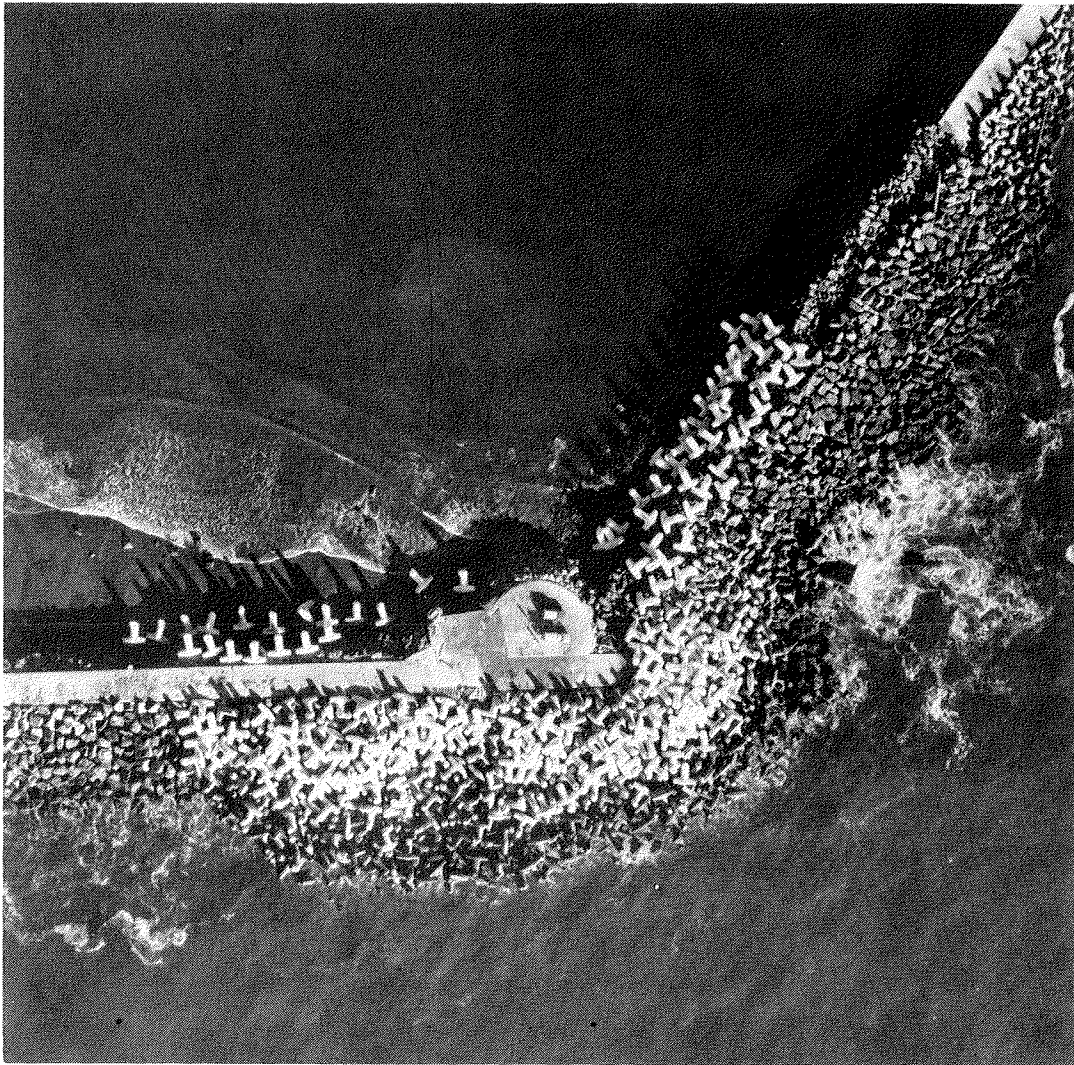


Figure 5. December 10, 1986 aerial view of Crescent City breakwater's dolos rehabilitation

- d. Develop a transfer function between incident model waves and the pulsating loads they induce in the instrumented model dolosse in a similar manner as done for the prototype data.
- e. Compare the model and prototype transfer functions and, if needed, develop a scaling relation between them.

## PART II: THE MODEL

### Model-Prototype Scale Relationships

4. Tests were conducted at a geometrically undistorted linear scale of 1:57.5, model to prototype. Scale selection was determined during the 1985 model tests (Baumgartner, Carver, and Davidson 1985) based on the following conditions: (a) absolute size of model breakwater sections necessary to ensure preclusion of stability scale effects (Hudson 1975), (b) capabilities of the available test facility, and (c) the depth of water at the toe of the breakwater. Based on Froude model law (Stevens et al. 1942) and the 1:57.5 scale, the following model-to-prototype relations were derived. Dimensions are in terms of force (F), length (L), and time (T).\*

<u>Characteristic</u>	<u>Dimension</u>	<u>Model-Prototype Scale Relation</u>
Length	L	$L_r = 1:57.5$
Area	$L^2$	$A_r = L_r^2 = 1:3,306$
Volume	$L^3$	$V_r = L_r^3 = 1:190,109$
Time	T	$T_r = L_r^{1/2} 1:7.6$
Fluid Weight	F	$W_r = L_r^3(64/62.4) = 194,984$

### Breakwater Construction Material

5. The specific weight of the fresh water used in the model was assumed to be 62.4 pcf and that of seawater 64.0 pcf; specific weights of model breakwater construction materials were not identical to their prototype counterparts, but the density of the model dolos material was chosen to minimize scale effects arising from using fresh water in the model. The weights of individual armor units and underlayer stone were determined using the following transference equation:

---

\* Symbols and abbreviations are listed in the Notation (Appendix A).

$$\frac{(W_a)_m}{(W_a)_p} = \frac{(\gamma_a)_m}{(\gamma_a)_p} \left( \frac{L_m}{L_p} \right)^3 \left[ \frac{((S_a)_p - 1)}{((S_a)_m - 1)} \right]^3 \quad (1)$$

$W_a$  = weight of an individual armor stone or unit, pounds. Subscripts m,p = model and prototype quantities, respectively

$\gamma_a$  = specific weight of an individual armor stone or unit, pounds per cubic foot

$L_m/L_p$  = linear scale of model

$S_a$  = specific gravity of an individual armor stone or unit relative to water in which the breakwater is constructed (i.e.,  $S_a = \gamma_a/\gamma_w$ , where  $\gamma_w$  is the specific weight of water, pounds per cubic foot)

### Test Facility

6. All model tests were conducted in the L-shaped wave basin (Figure 6). This was the same facility used during the 1985 stability model tests, but subsequent to the 1985 tests, the test facility's monochromatic wave generator was replaced with a computer-controlled wave generator capable of producing both monochromatic and irregular waves.

### Model Breakwater Construction

7. The model breakwater test section used during the 1985 model tests had been maintained in a remote area of the test basin and was moved back into the test area for the study reported herein. Therefore, the detailed description of model construction reported by Baumgartner, Carver, and Davidson (1985) is the same for this study. Figure 2 shows details of the breakwater as reproduced in the 1985 model tests, along with the recommended rehabilitation design. Using results of photogrammetric and hydrographic surveys conducted on 25 November 1986 and 11-14 November 1986, respectively, female model templates were constructed and positioned over the model breakwater (Figure 7) so that dolos placement geometry, elevations, and coverage area would approximate the 1986 rehabilitation work as actually constructed. Details of the prototype breakwater cross sections between sta 32+00 and sta 36+75 are presented in Appendix B, "Prototype Breakwater and Bathymetry Data."

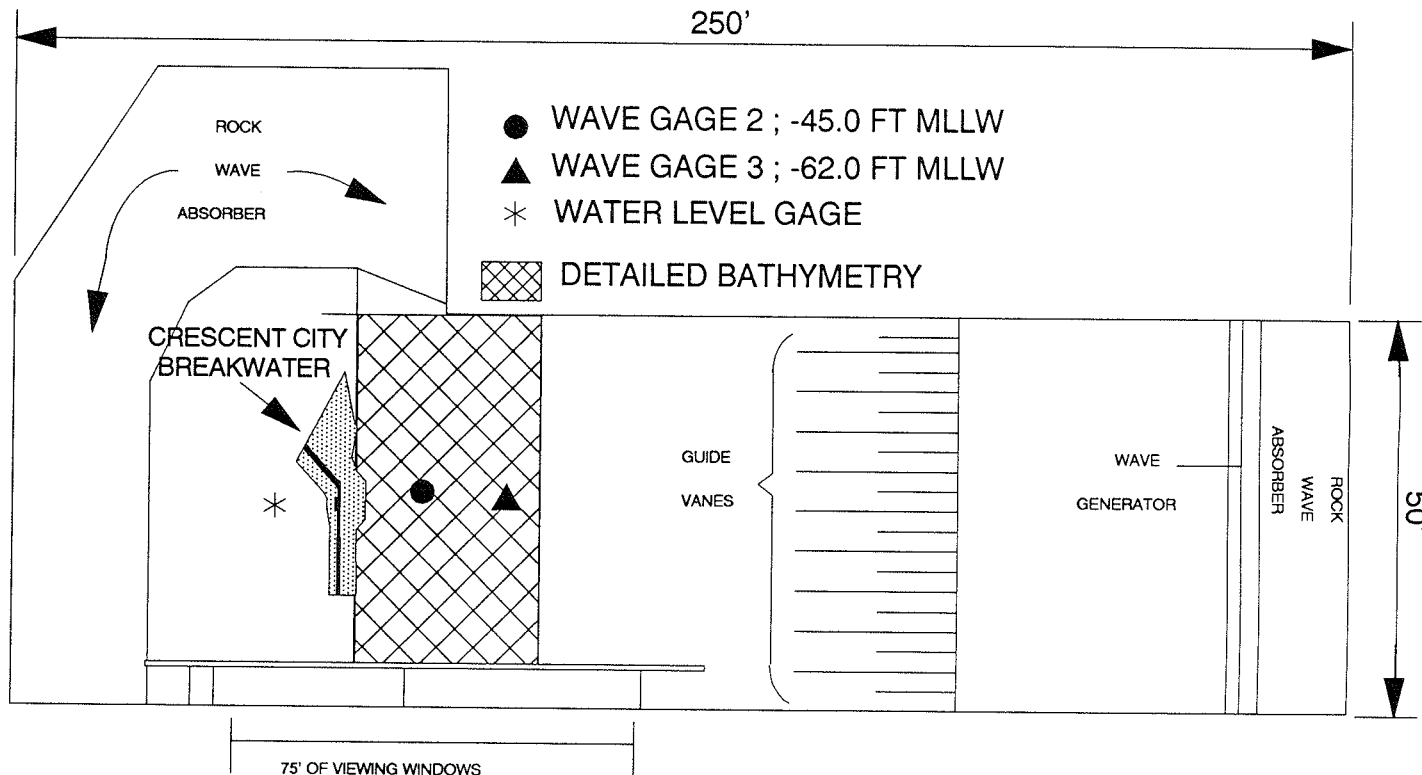


Figure 6. Plan view of L-shaped wave basin showing breakwater model, detailed bathymetry, and wave gage locations

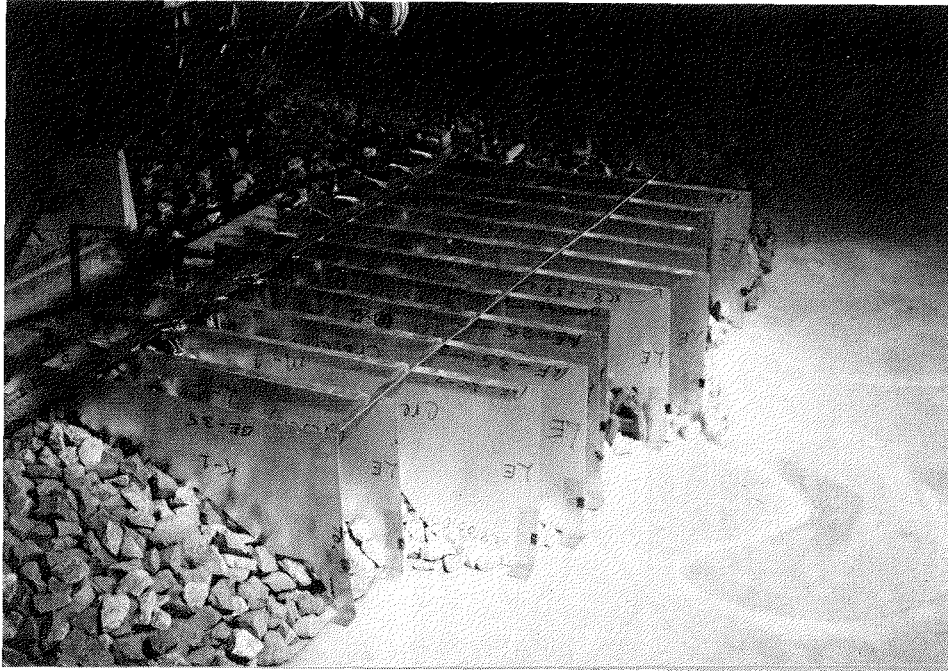


Figure 7. Templates used to control dolos elevations and placement area on breakwater model

The dolos armor layers were constructed using random placement in all areas except for the outer perimeter, where special placement was used to match the interlocking recommended by the 1985 model study and specified in the rehabilitation construction specifications. The number of dolosse placed in the model matched the existing prototype count within  $\pm 3$  to 5 units. Figure 8 provides geometric details and material sizing of the model, while Figure 9 provides a view of the breakwater model.

#### Local Bathymetry

8. During the 1985 model tests, bathymetry seaward of the breakwater toe was represented in the model by an idealized bathymetry so that the breakwater structure could be turned to test wave attack from two incident wave directions. As will be discussed in a later section, it was determined that only one incident wave direction was needed for this test series. This determination made it possible to reproduce the actual prototype bathymetry lying seaward of the breakwater toe, in a water depth of approximately -29 ft mean lower low water (mllw), and extending out to a depth of approximately

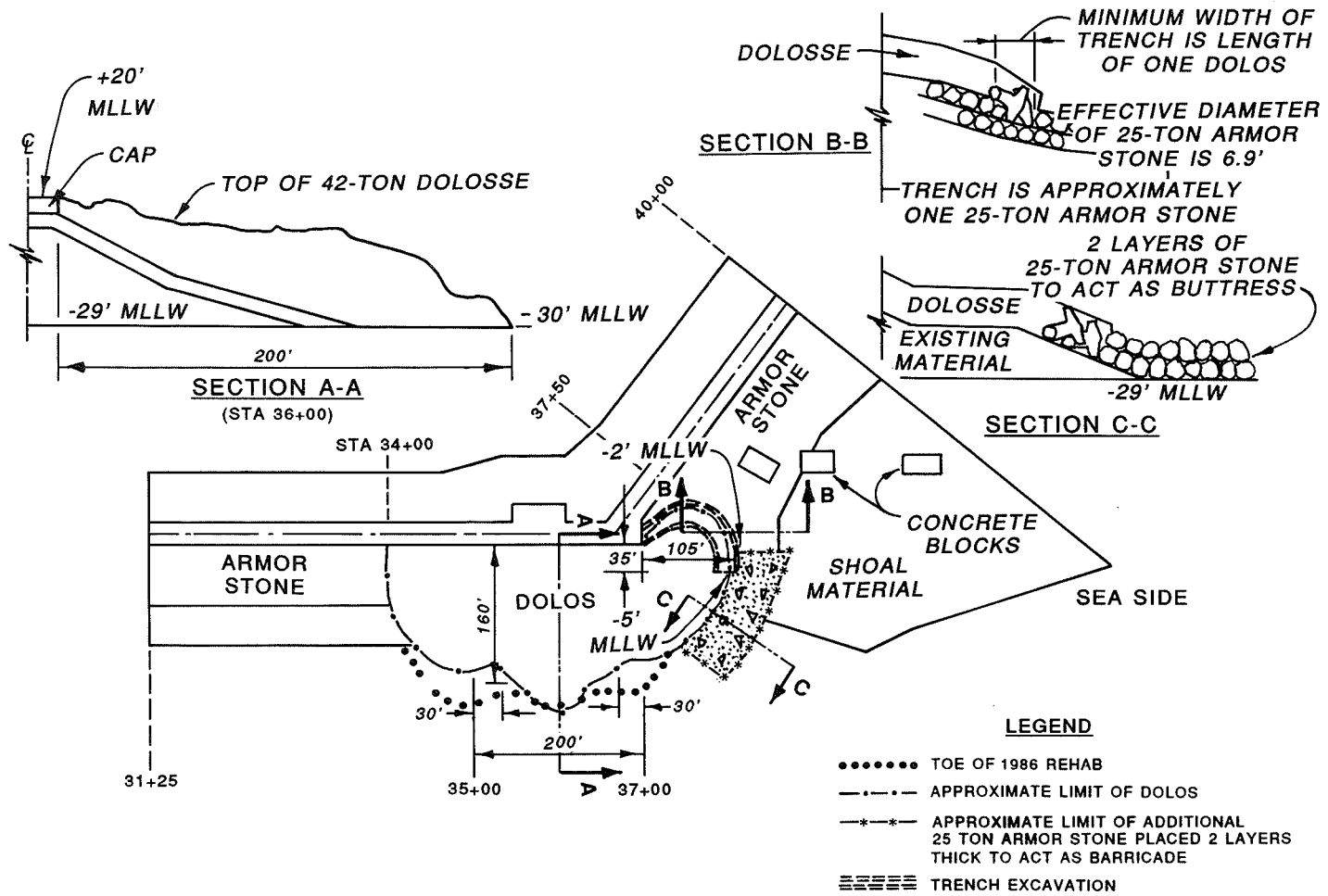


Figure 8. Plan view and cross section of breakwater as reproduced in model (Additional breakwater cross sections in Appendix B)

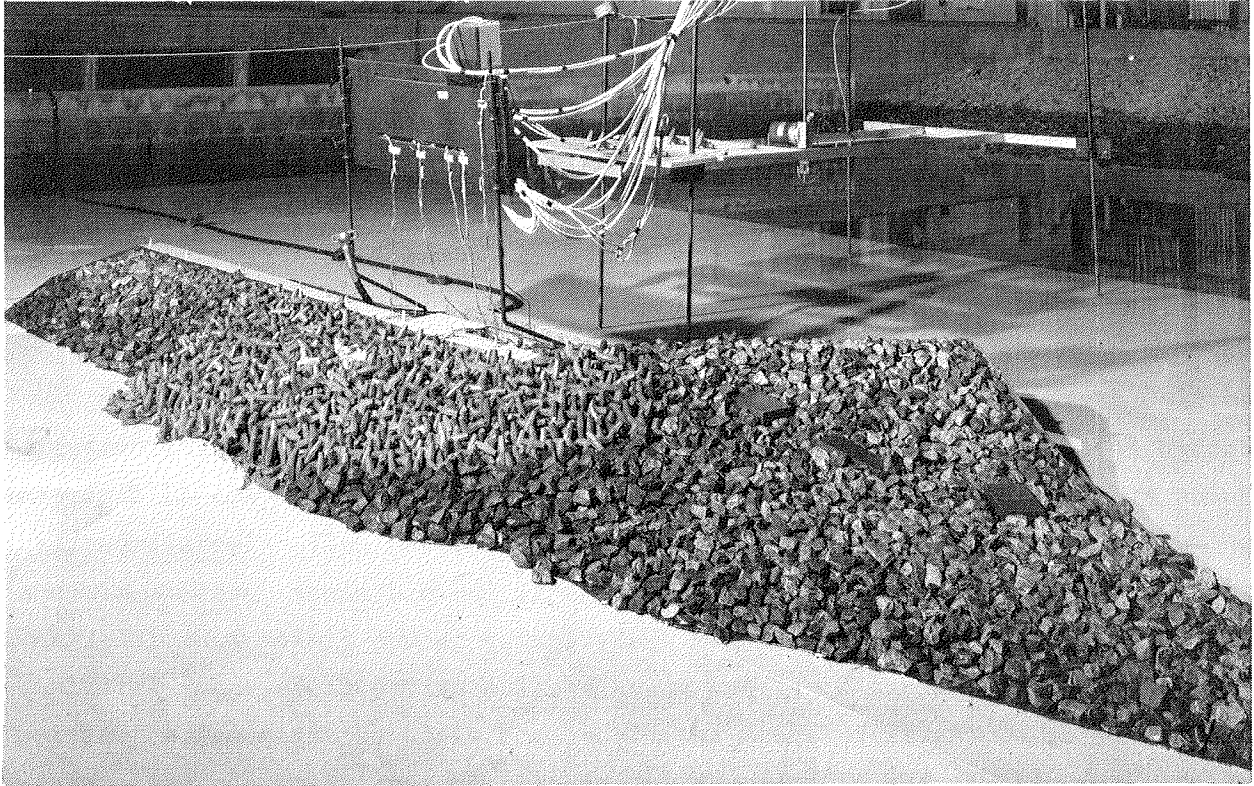


Figure 9. View of breakwater stability model looking shoreward from end of breakwater main stem

51 ft mllw. Seaward of this, the model bathymetry dropped off on a 1V on 20H slope until it intersected the existing wave basin floor at an elevation of approximately -87 ft mllw (Note that depths are expressed in equivalent prototype units.). Details from the hydrographic surveys referred to in paragraph 7, along with the most current bathymetric charts available, were used to define the bottom bathymetry. See Appendix B for details.

#### Instrumented Model Dolosse

9. Instrumentation in the prototype dolosse was positioned in the manner necessary to monitor two moments and a torque at the shank-fluke interface. Details of prototype dolos instrumentation and data acquisition and analysis are presented by Howell et al. (in preparation). Previous model dolos instrumentation has been carried out by both Canadian and European laboratories (Scott 1986; Scott, Turke, and Baird 1986; and Delft Hydraulics Laboratory 1980). These studies, along with others that are not mentioned herein, used either strain gages on the surface of the model dolos and/or an

instrumented load cell that was placed inside the model dolosse. The model study reported herein used the load cell approach.

10. The geometric and material configuration of the load cell was designed by WES engineers from CERC, the Structures Laboratory (SL), and the Instrumentation Services Division. SL engineers specified load cell geometry, strain gage locations on the load cell, and positioning of the load cell inside the dolos. Figure 10 shows positioning of the load cell, model dolos geometry, and convention for horizontal and vertical moments and torque as used in both the prototype and model studies. The cylindrical, thin-walled section of the load cell had a flexural rigidity, composite EI, that was scaled to match that of the octagonal cross section of the 42-ton, prototype dolos at the 1:57.5 model scale. SL engineers conducted analysis to determine where to cut the model dolos for placement of the load cell. Two approaches were considered, one being to cut the dolos at the mid-shank, measure moments and torques, and then transfer them analytically to the fluke-shank interface. The second was to assume a uniform cross section at the fluke-shank interface, cut the dolos at the fluke-shank interface, and place the thin-walled portion of the load cell at the fluke-shank interface. In the latter approach, the moments and torques would be defined at the same point as the prototype, and no analytical transfer function would be needed. Analysis of both approaches showed that even though the responses at mid-shank are more predictable, no accurate linear relation could be developed to relate the responses at the two locations. Thus, it was determined that it would be more appropriate to assume a linear cross section at the fluke-shank interface and measure the moments and torque at the same point as they were measured in the prototype, than it would be to measure at mid-shank and use a linear function to transfer the responses to the fluke-shank interface.

11. The load cell was machined from solid 7075 aluminum round stock to the dimensions shown in Figure 11. Dolosse were machined to accept the load cells so that the center of the thin-walled, gaged section was in the plane of the shank-fluke interface. The load cell was held in place in the dolos unit with a near press fit and set screws (Figure 12).

12. The strains induced in the load cell for expected magnitudes of moments and torque were quite small and this required the use of semi-conductor strain gages having gage factors on the order of 130. These gages were arranged in a Wheatstone bridge generating a bridge factor of 520, thereby producing a bridge output 4 times that of a single semi-conductor

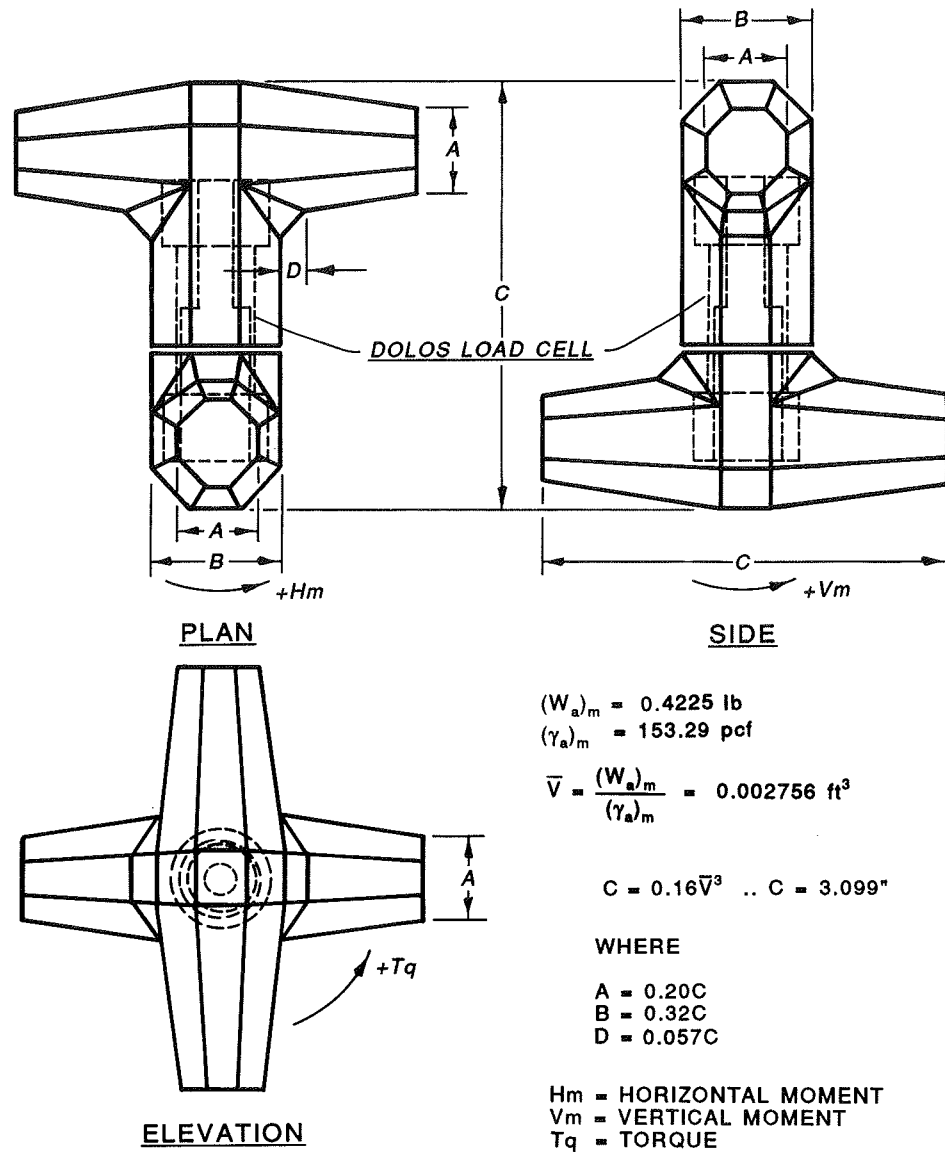


Figure 10. Definition of horizontal and vertical moments,  $H_m$  and  $V_m$ , respectively, and torque,  $T_q$ , as used in prototype and model.

Model dolos specifications and load cell positioning

gage and 260 times that of metal foil gage. Unfortunately, to gain this sensitivity, a trade-off in temperature instability had to be accepted. In the region of 75 to 100  $\mu\text{in./in.}$ , this is devastating even to near-term accuracy when temperature is allowed to drift by only a few degrees Fahrenheit. A silicon temperature sensor, similar in size to the strain gages, was installed on the gaged section to sense the load cell temperature, so that temperature effects could be corrected during data analysis.

13. Kulite strain gages, type UEP-350-060 (a large element gage in the form of a "U"), were used to instrument the dolos load cell. This

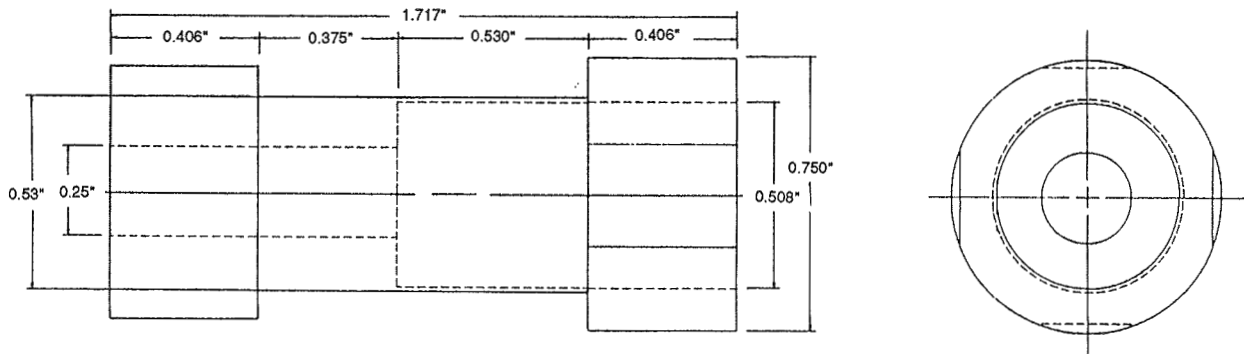


Figure 11. Dolos load cell geometry

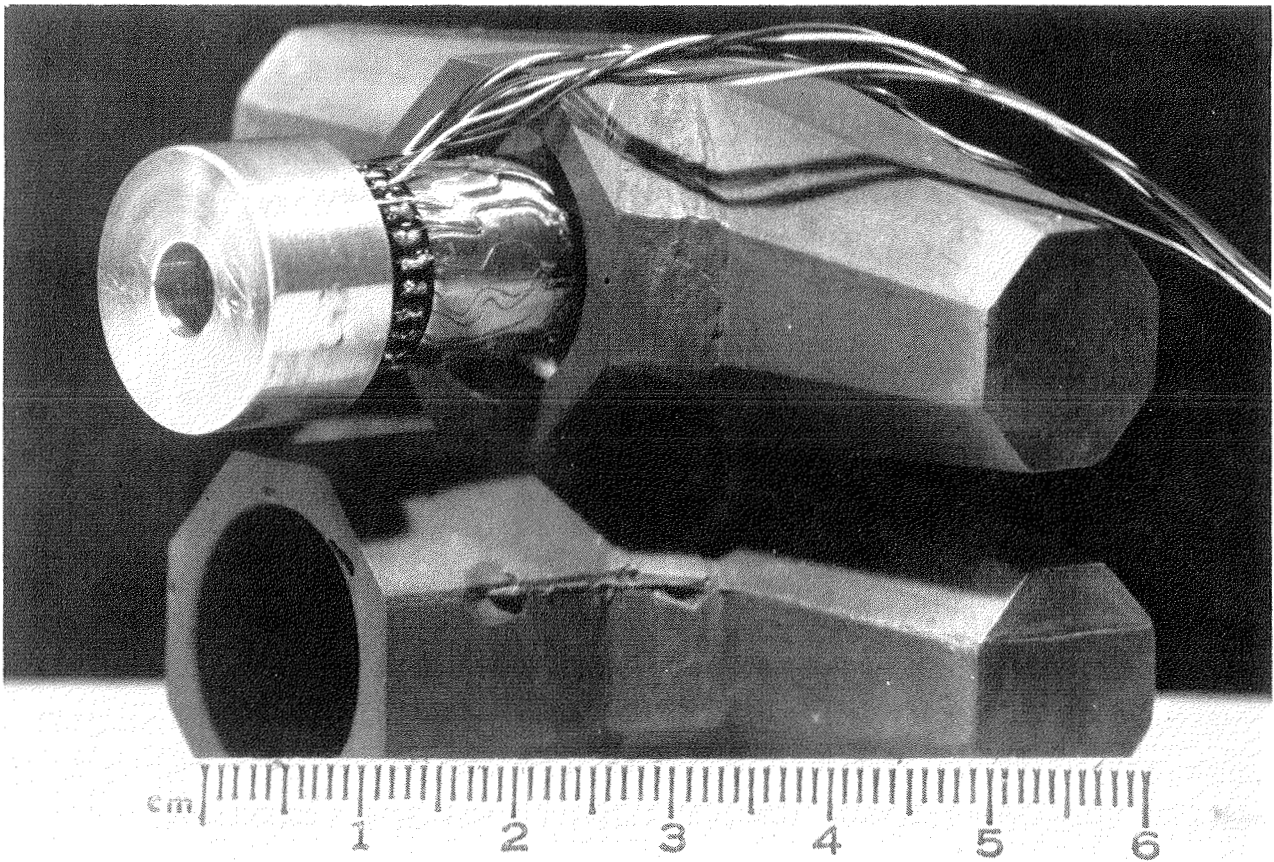


Figure 12. Dolos load cell unioned with dolos fluke

construction was designed for maximum resistance in a minimum size with single-ended lead configuration. Bare gages ensured the most intimate contact of the sensor to the bonded surface, but did require considerable experience in handling and bonding. A gage was 0.060 in. long and 0.020 in. wide.

14. Strain gage size allowed two gages to be bonded at the quarter points about the circumference of the gaged section. The gages bonded at the quarter points were oriented to sense strain parallel to the axial center line of the cylinder and were wired so they would sense the horizontal and vertical moments acting on the cylinder. The gages, bonded 90 deg to each other and 45 deg to a line on the circumference parallel to the axial center line of the cylinder, were wired to measure the torque action around the cylinder. The torque transducer was not sensitive to axial forces and bending moments. The moment transducers were insensitive to axial forces and torques. The wiring diagram and gage locations for the torque and moment circuits are shown in Figure 13.

15. High quality strain gage application techniques had to be strictly adhered to during bonding and waterproofing of the gages. The bare unbacked semi-conductor strain gages were very fragile and had to be handled with extreme care. Only an experienced technician should attempt to install these gages since special hand tools and a microscope were required to accurately place and bond the gages. The gages could not withstand the application of pressure and shattered if any pressure was applied directly to the crystal or as a torque to the leads. The gage was placed in bonding adhesive in a liquid state, which allowed it to float down to a previously applied adhesive layer that was partially cured. Care had to be taken when the leads were cut and formed for connections with internal wiring. Each application of adhesives and coatings had to be fully cured before advancing to the next procedure since many of the chemicals would react with others to destroy the desired insulating qualities. Enamel-coated-solid copper wire, No. 36 AWG, was used for internal bridge wiring. Gage placement and wiring before waterproofing are shown in Figure 14.

16. Several different coatings of materials were applied to the gaged area to provide insulation and waterproofing for the bridge circuits (Figure 15). The cables or lead wires, which were later attached to transducers, were submerged in water for several days. During this period, insulation readings made each day determined any drop in insulation caused by leakage. Wires were discarded when insulation fell below 10,000 megohms. After the

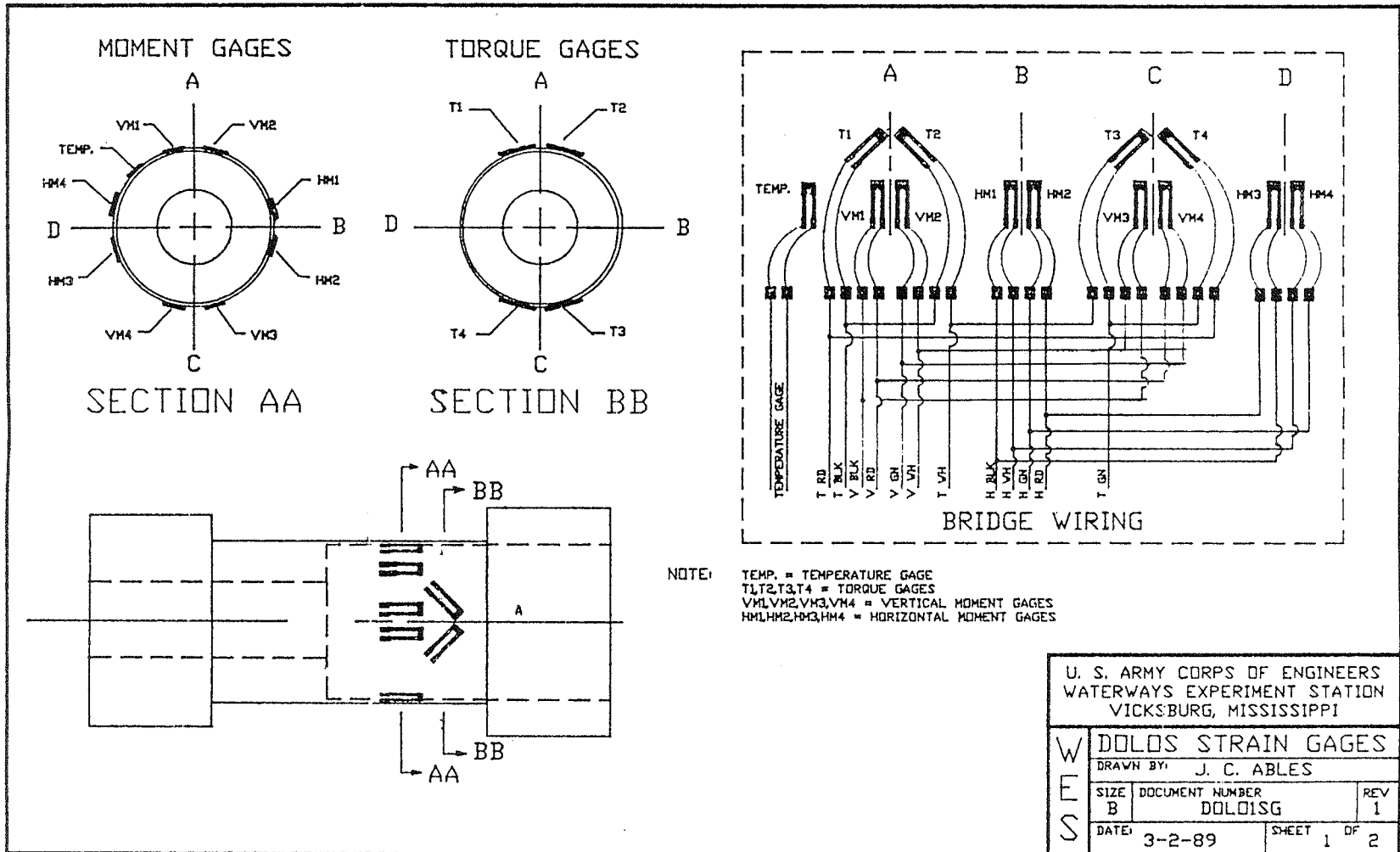


Figure 13. Dolos load cell strain gage and temperature gage locations and wiring diagram

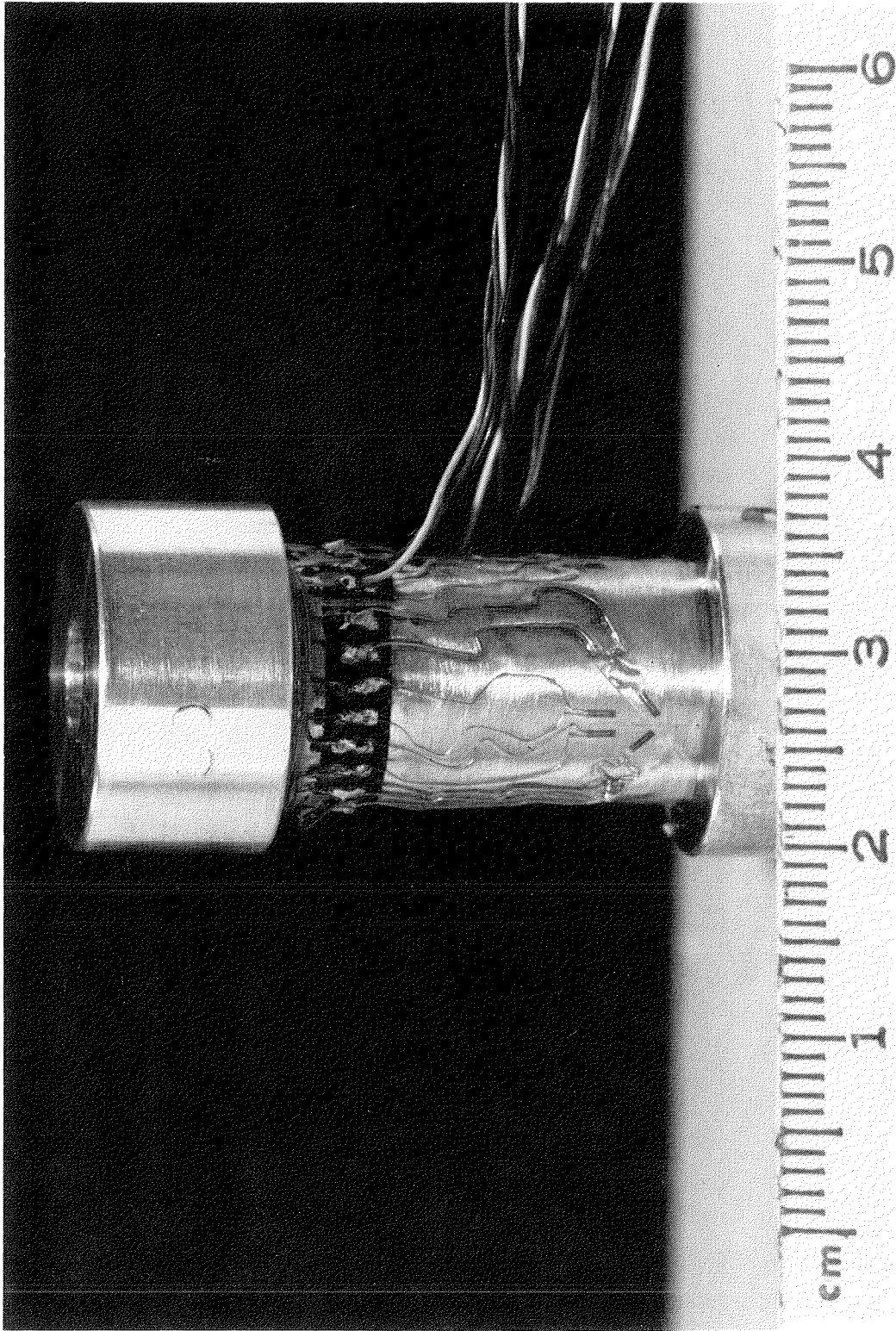
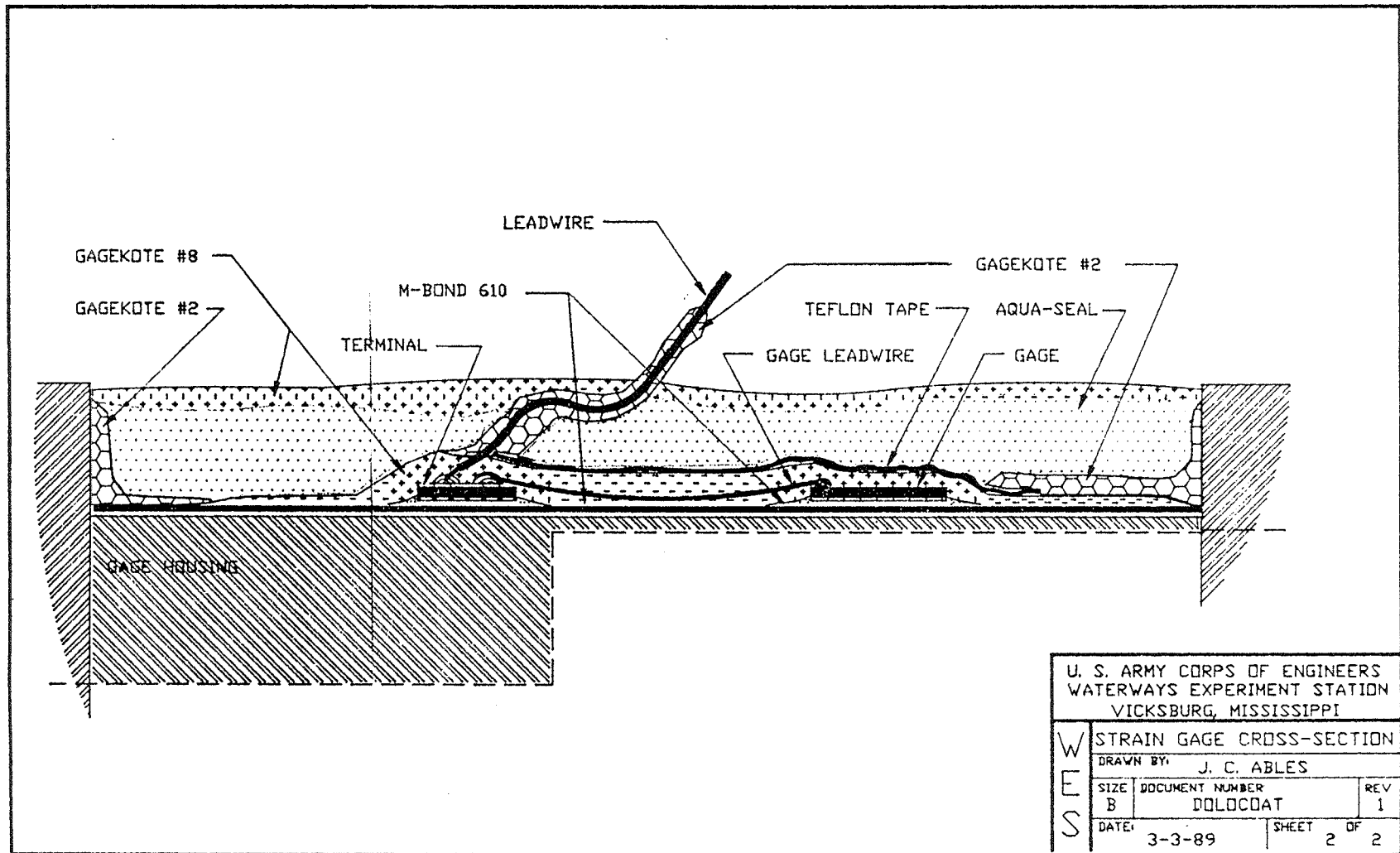


Figure 14. Dolos load cell with gages installed but prior to waterproofing



U. S. ARMY CORPS OF ENGINEERS WATERWAYS EXPERIMENT STATION VICKSBURG, MISSISSIPPI			
W E S	STRAIN GAGE CROSS-SECTION		
	DRAWN BY: J. C. ABLES		
	SIZE	DOCUMENT NUMBER	REV
	B	DOLCOAT	1
DATE:	3-3-89	SHEET	2 OF 2

Figure 15. Dolos load cell waterproofing

lead wires were attached to the transducer, final coats of waterproofing compounds were applied to the whole surface area and the interface of the lead wires exit. The transducer and lead wires were submerged in 1-1/2 ft of water for a period of 4 days with only the bare cable ends exposed so that insulation of the complete unit could be checked. If the insulation failed, the unit was examined to determine where the leakage had occurred. Repairs were made, the unit again was submerged in water, and insulation readings were taken. This process was repeated until an insulation of 5,000 megohms could be maintained for a period of 4 days.

17. The fully instrumented and insulated load cell was installed in a machined dolos and the complete assembly (Figure 16) was calibrated to measure moments and torque at the fluke-shank interface. The ranges of moments and torques measured were on the magnitude of those that are developed by a dolos's distributed weights and points of support. The values were very small and resulted in strains of only about 100  $\mu\text{in./in.}$  In this range of sensitivity, the temperature sensitivity was paramount and had to be accounted for; therefore, the transducers also had to be calibrated for temperature.

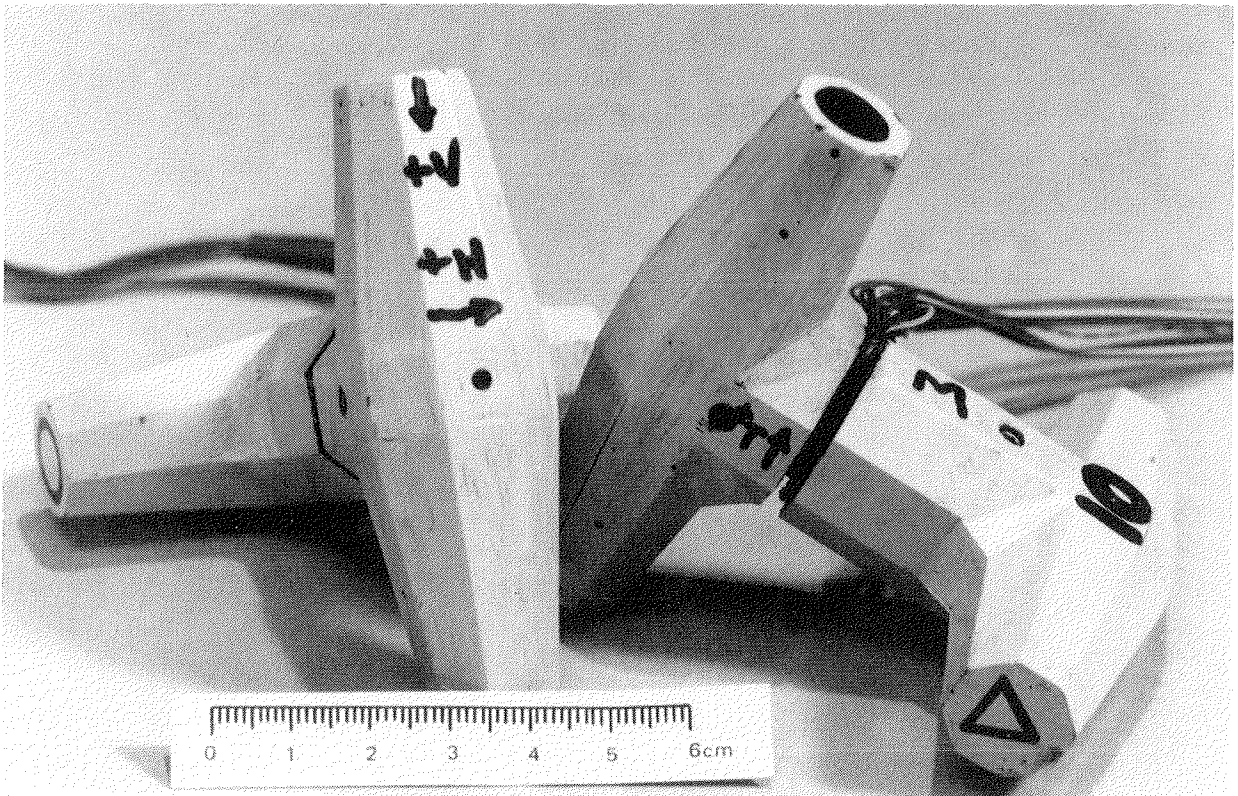


Figure 16. Instrumented model dolosse

18. The first step in dolos transducer calibration was the temperature sensor. This was accomplished by suspending the dolos so that its shank was held vertical, no load position, in a water bath. The initial temperature of the water bath was near 32 °F and by the addition of warmer water, the temperature was raised over the range that data were expected to be recorded. Using a precision electronic thermometer, the water temperature was set at several intervals. At these intervals, temperature sensor voltage outputs were recorded along with water bath temperature on a Data Acquisition System (DAS) consisting of an IBM-compatible personal computer complete with an analog-to-digital converter. From the values recorded, the linear equation for the temperature sensor output as a function of temperature sensor output voltage and temperature was computed. The linearity of the sensor was also computed with respect to the best straight line that could be fit through all the data points (Figure 17).

19. Gage factor temperature compensation was the second step in the load cell calibration. This was accomplished with the use of a controlled temperature chamber, thermometer, microvolt meter, a fixture to support the dolosse, precision gram weights, and several precision resistors that would be

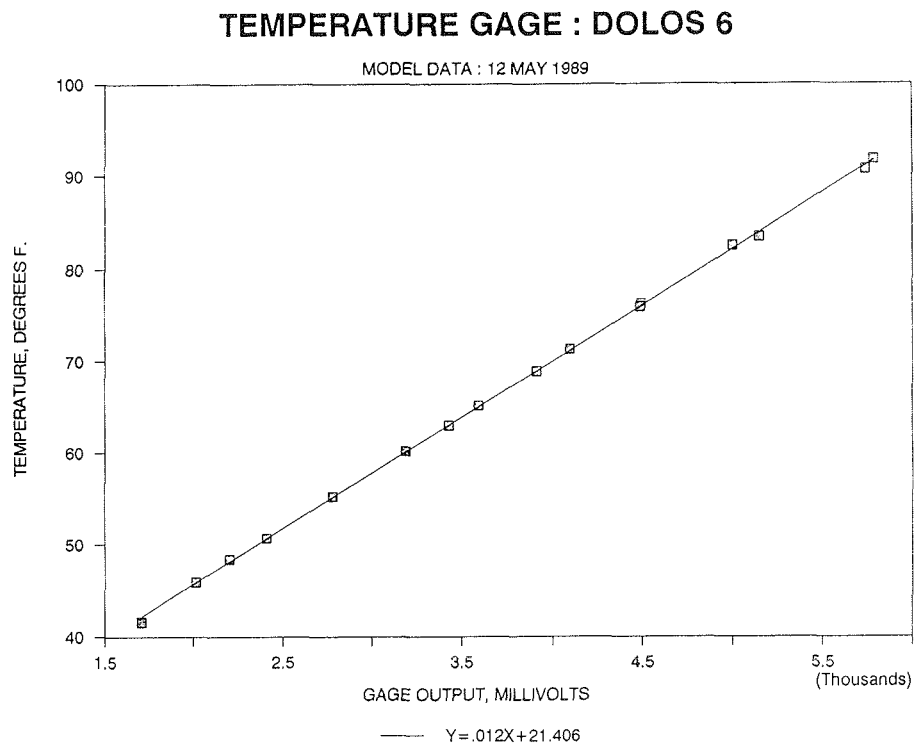


Figure 17. Example of dolos load cell temperature sensor calibration

placed in serial with one arm of the bridge and its excitation source. The dolos was installed in the support fixture so that weights could be hung from a specific location to induce known loads in the torque transducer. The temperature chamber was set at the lowest temperature that data were expected to be taken. When the temperature sensors on the gaged section indicated agreement with the thermometer reading, the temperature of the chamber, an unloaded output voltage from the torque transducer, was measured with the millivoltmeter. The instrumented dolos then was loaded with a known torque and another output reading taken. The temperature then was raised to the highest temperature that data were expected to be recorded and similar measurements were repeated. These loaded and unloaded measurements, along with bridge excitation voltage, temperature, and serial resistance, were recorded on a data sheet. These data sheets also defined the dolos number, transducer type (torque, horizontal moment, or vertical moment), serial number, date, calibrator's name, job number, and project name. The differences between the loaded and the unloaded bridge outputs were calculated for the different serial resistor values. The resistor that produced the least output change was selected for gage factor compensation and was permanently attached to the positive excitation corner of the bridge. This procedure was carried out for the horizontal and vertical moment transducers, which completed the gage factor compensation of the bridge.

20. Load cell calibration for bridge output variations as a function of temperature was the third step in the calibration process and was conducted with the same equipment that was used for calibration of the temperature sensor. Each dolos was suspended in a water bath so that its fluke was horizontal and its shank was vertical, forcing the torque and moment transducers into an unloaded condition. As a result, variations in bridge output were a function of temperature alone. The dolos was submerged in a water bath that was initially at the lowest temperature that data were expected to be recorded during actual model tests. The water temperature was raised in steps to the highest temperature that data were expected to be recorded. The water was stirred at each temperature step to maintain an isothermal condition throughout the bath. The outputs of the transducers and the temperature sensor were recorded by the DAS at each discrete step. The DAS computed the least squares best fit straight line through the points and tabulated the percent deviation of the data from best fit for each point. In general, bridge output was quite linear for temperatures above 45 to 50 °F, but showed some pronounced

nonlinearities below these temperatures. During actual model tests, operating temperatures ranged from 70 to 80 °F and this allowed the use of a best fit straight line through the higher (i.e., more linear) temperature range. Figure 18 shows an example of a thermal compensation calibration used during actual model tests.

21. The final stage in the load cell calibration was determining bridge output as a function of known moments and torques. Vertical moment calibration equipment included a tilt table calibrated in degrees of rotation, a voltmeter, a microvoltmeter, a bridge excitation power supply, precision gram weights and hanger, and a DAS. The dolos was mounted to the tilt table with a specially designed fixture. The table was set for 0 deg and the dolos was mounted so that the gages sensing the vertical moment were oriented at 12 o'clock and 6 o'clock. The tilt table and the dolos were leveled by leveling screws referenced to a spirit level. The excitation voltage was monitored and set with the voltmeter and the output of the temperature sensor and the three transducers were read with a voltmeter and the DAS. Data were recorded on the DAS with no load (zero moment) applied to the transducer. Since the maximum weight to be hung on the transducer was about one half the

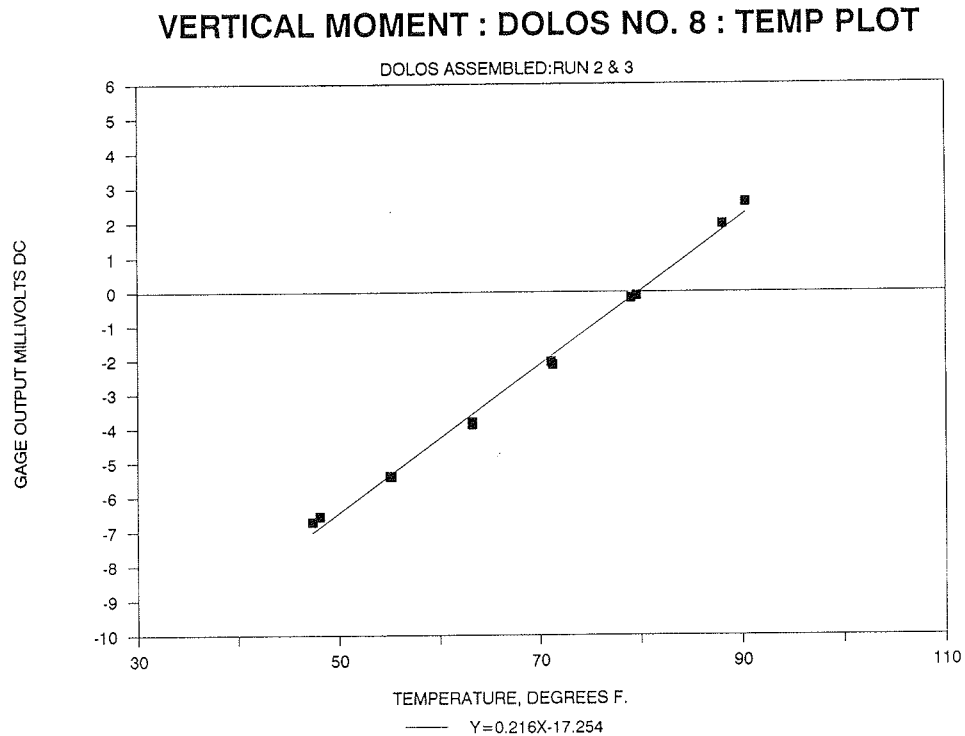


Figure 18. Example of dolos load cell thermal compensation calibration

weight of the instrumented dolos, all weights, including the tray, wire, and the screw used to support the gram weights, had to be included in the total. A tray of known weight was attached to the dolos at a known distance from the gages. This was the first point in the calibration. The DAS recorded the outputs from the three transducers and the temperature sensor. Several known weights were added and recordings on the DAS were taken with the addition of each weight change. The weights were taken off in reverse order and similar recordings were made with each change in weight. The tilt table was then rotated 180 deg so that a calibration for the other sensitive axis could be done. The same calibration procedure was followed as described above. During all calibrations, data were recorded from the three transducers to define any cross-axis sensitivity. When the output voltage of the vertical moment transducer was plotted against the applied moment, as shown in Figure 19, it was obvious that the resulting lines had the same slope but were offset from each other. This separation was the gravitational effect on the distributed self weight of the dolos, due to rotation, on the moment transducer. Adjustment was made for this condition by calculating the difference in the no-load voltages and dividing it by two to determine the offset from zero for no load. This half difference was subtracted from the larger upper line and added to the lower line, resulting in a self-weight-corrected, best-fit linear calibration curve as shown in the middle of Figure 19. To calibrate the horizontal moment transducer, the dolos was rotated so the strain gages sensing the horizontal moment were at 12 o'clock and 6 o'clock. The same procedures that were used in calibrating the vertical moment transducer were repeated.

22. Conformity to the cosine law defines how well the resultant of the horizontal and vertical components, the values measured by the horizontal and vertical transducers, agrees with the value of the ideal resultant. The law of cosines,  $A^2 = B^2 + C^2 - 2BC \cos \beta$ , (Figure 20) reduces to  $A^2 = B^2 + C^2$  in the case of quadrature components. Therefore, the ideal response would inscribe a circle with radius  $A = (B^2 + C^2)^{1/2}$ . To check the load cells' conformity to the cosine law, a known weight was hung on the fluke at the axial center line of the shank. The dolos was plumbed with the vertical moment sensors at 12 and 6 o'clock with the tilt table set at 0 deg. With the known weight removed from the dolos, the table was rotated counterclockwise in 15-deg increments through 360 deg. The DAS recorded the output of the moment transducers and the angle of rotation. This procedure produced outputs from the

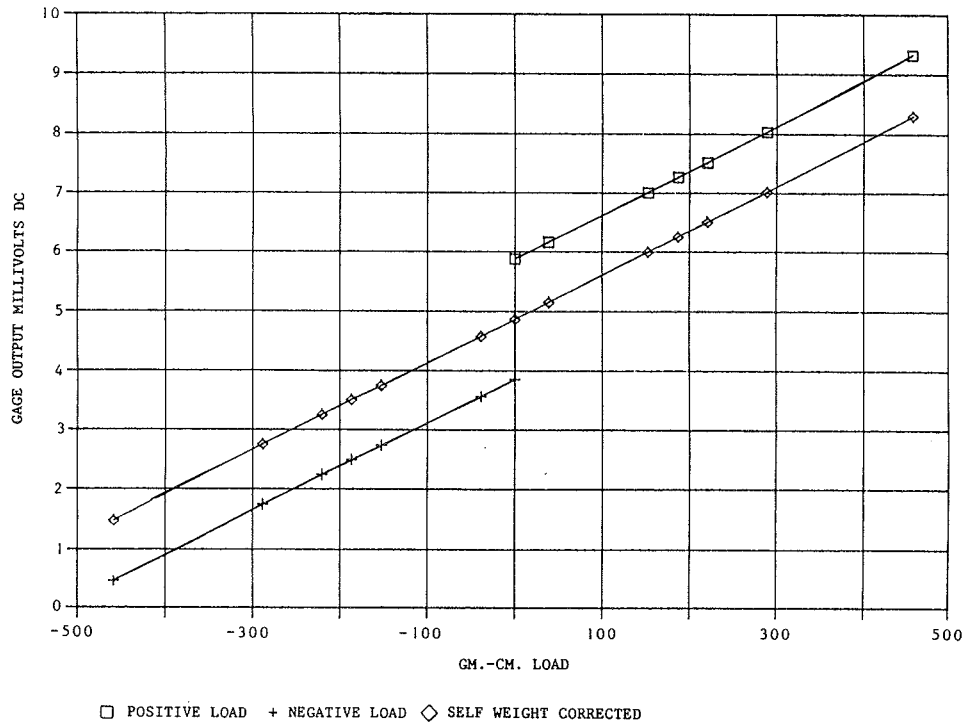


Figure 19. Example plot of dolos load cell vertical moment calibration

$$A^2 = B^2 + C^2 - 2BC \cos \theta$$

if  $\theta = 90^\circ$

$$A^2 = B^2 + C^2$$

$$\therefore A = (B^2 + C^2)^{1/2}$$

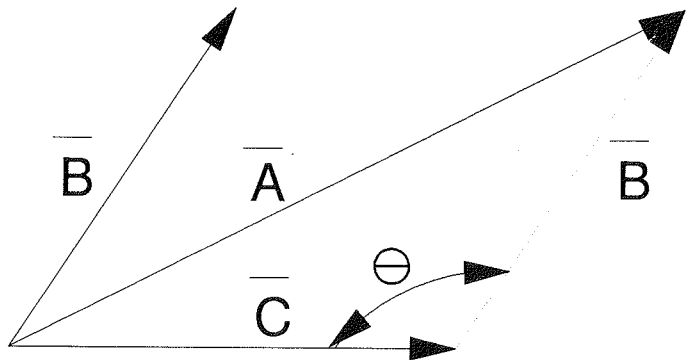


Figure 20. Definition sketch of cosine law

moment transducers proportional to the moments generated by the gravitational forces acting on the distributed mass of the dolos. The known weight was hung on the dolos and it was again rotated through 360 deg in 15-degree increments with the same measurements recorded as described above. This calibration was a function of the known load and the gravitational influences on the distributed mass. The data from both procedures were zero corrected, then the incremental values of the unloaded data were subtracted from the total moment, to arrive at the moment proportional to the known load. The resultants of the values at each 15-deg increment were plotted on the same graph and at the same scale as the ideal responses. The deviation of these actual calibration values from the ideal was very small, as shown by one example in Figure 21. All other units exhibited similar cosine response.

23. For calibration of the torque transducer, the dolos was mounted to the tilt table as it was during the moment calibration. Previously, during machining of the dolosse to accept the load cells, points on both sides of the top of the horizontal fluke were marked at a distance of 1 in. from its midpoint. A known weight was attached to the horizontal fluke at this point to produce a counterclockwise torque equal to the maximum expected test value. Incremental amounts of weight were removed one at a time, the DAS recorded the output of the torque and moment transducers and the temperature sensor, and the calculated value of the applied torque was entered from the keyboard. With all weights removed, a zero load condition was recorded. The weights were then added in ascending order to the other side of the horizontal fluke, generating a clockwise torque, and the same type measurements were recorded by the DAS. Analysis of these data produced best fit straight lines through the data that defined the torque transducer output as a function of torque for each instrumented dolos. Figure 22 shows an example of a dolos load cell torque transducer calibration.

24. In summary, calibration of each instrumented dolos created seven pieces of calibration information, each defined by a linear function:

- a. Load cell temperature in degrees Fahrenheit as a function of temperature sensor output.
- b. Vertical moment transducer output as a function of vertical moment.
- c. Vertical moment transducer output as a function of temperature.

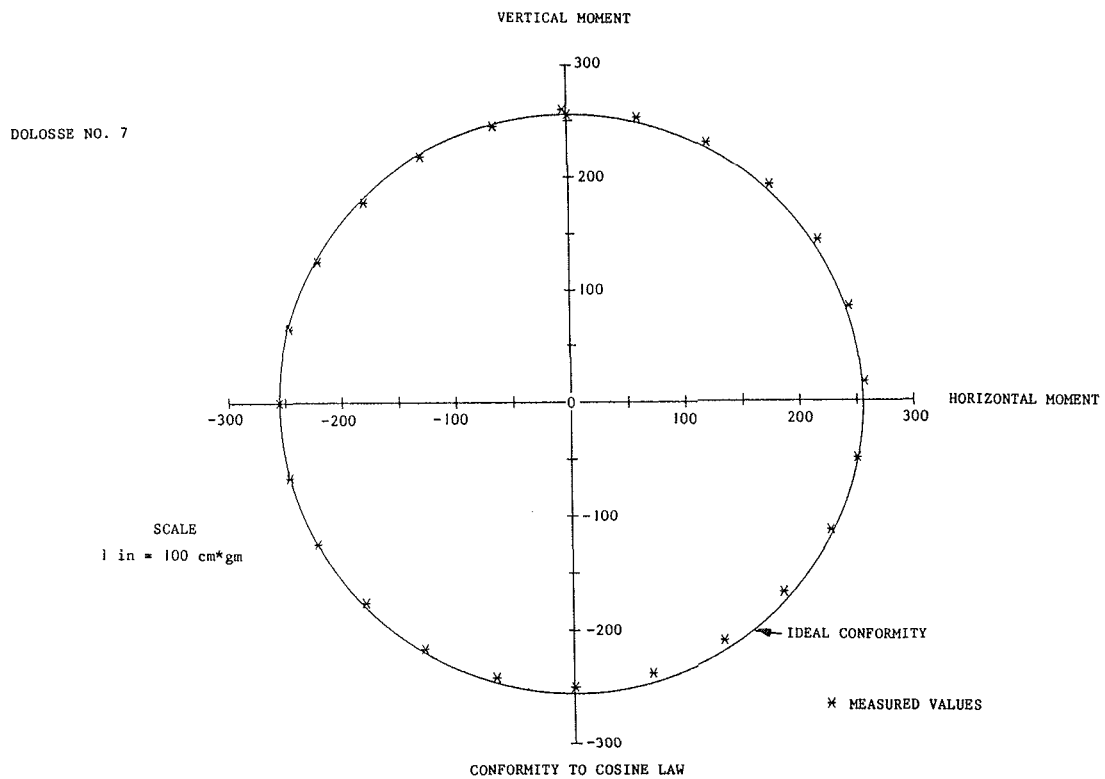


Figure 21. Example of load cell vertical and horizontal moments' conformity to cosine law

- d. Horizontal moment transducer output as a function of horizontal moment.
- e. Horizontal moment transducer output as a function of temperature.
- f. Torque transducer output as a function of torque.
- g. Torque transducer output as a function of temperature.

#### Wave Gage System

25. The wave gage system was based on capacitive sensor techniques and consisted of four main parts: (a) wave staff, (b) oscillator card, (c) interface card, and (d) voltage-to-frequency card.

26. The wave staff, Figure 23, consisted of a wire drawn taut in a stainless steel tube bow. The insulation of the wire served as a capacitor between the inner conductor and ground. The capacitance between the conductor and ground varied linearly with changes in water surface elevation. The insulation had to be uniform along the wire's length and free of holes. The conductor of the wire was connected directly to a variable oscillator on the

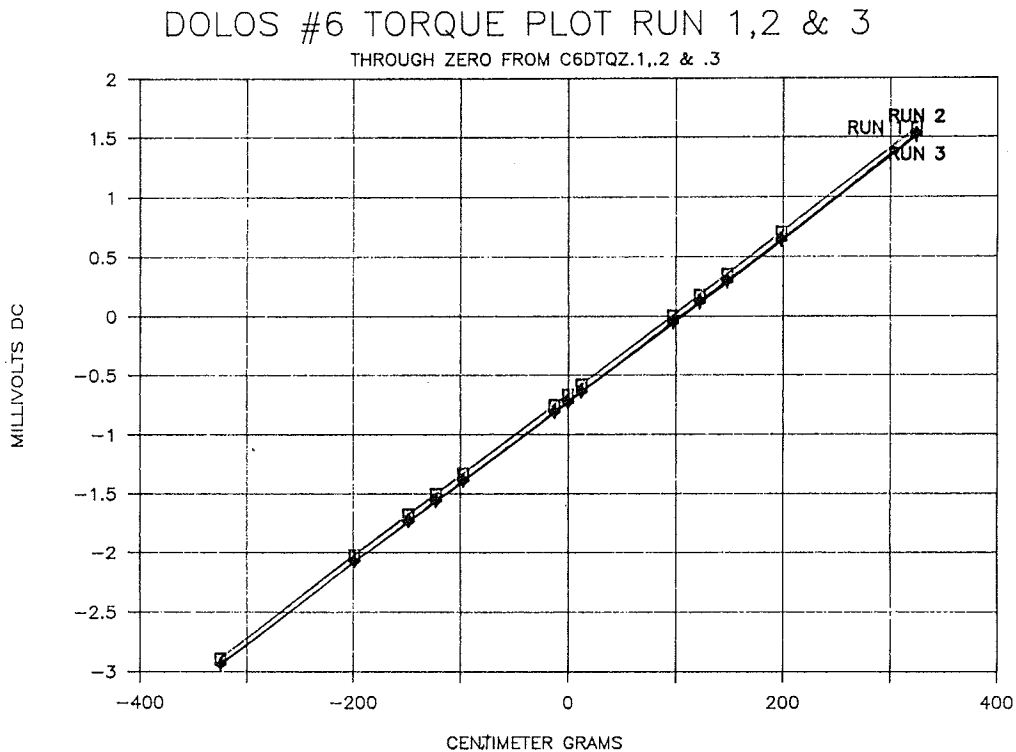


Figure 22. Example plot of dolos load cell torque calibration oscillator card to minimize stray capacitances that could have affected frequency stability.

27. The oscillator card consisted of two identical oscillators, a frequency divider, and an optical isolator line driver. The oscillator card produced a frequency-modulated output proportional to water surface elevation.

28. The interface card had components to adjust the voltages driving the position feedback and isolated regulated DC-DC voltage converter power, the oscillator board, and a test point for output of the oscillator card.

29. The frequency-to-voltage card accepted the frequency-modulated signal from the oscillator card via the interface card and converted it to a voltage analog that was compatible with the analog-to-digital converter in the Microvax computer recording system, where the wave data were stored for analysis at a later time.

30. The wave gage system was designed for maximum isolation between its own parts, the data acquisition system, and other electrical equipment. Each oscillator card was isolated from all others by means of an isolated DC-to-DC converter. The oscillator card output also featured isolation in its output circuit with an optical isolator and a current output. This isolation

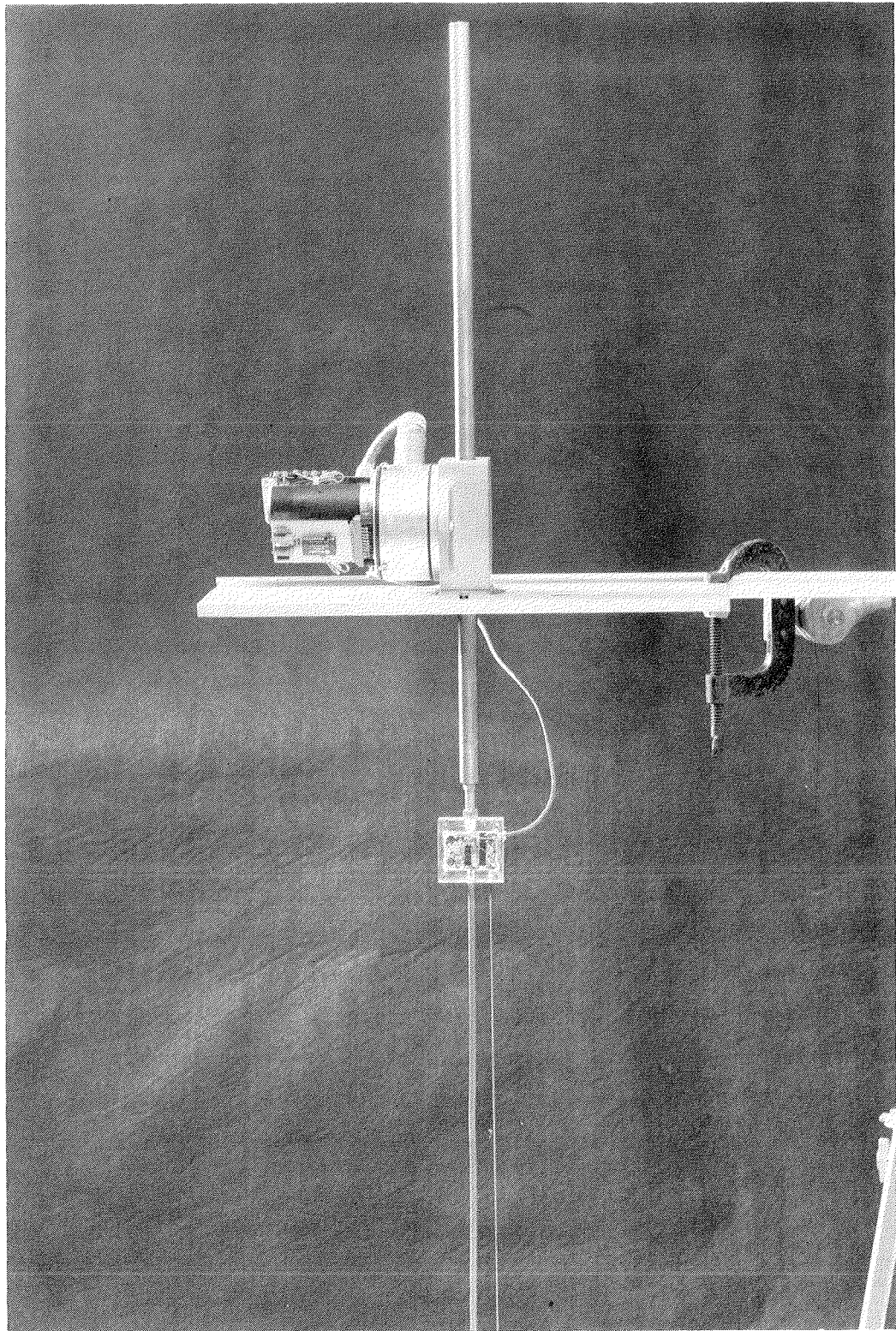


Figure 23. Wave staff

produced a high signal-to-noise ratio, which allowed very high signal resolution and accuracy. The wave gage system was tested over a two-month period and data showed very high stability indicated by the consistency of the linear calibration coefficients listed in Table 1.

#### Automated Data Acquisition System (ADACS)

31. The test facility's Automated Data Acquisition System (ADACS) consisted of amplifiers, gain multiplexers, and a Microvax II computer and peripherals. The amplifiers were designed and constructed specifically for the Crescent City Instrumented Model Dolos Study. Each of the amplifiers had a differential input for noise rejection, 10 switchable, fixed-gain steps varying in steps from 1 to 1,000, with an optional gain factor of 2 increasing the total gain from 2 to 2,000, an anti-aliasing 8-pole Bessel filter, a coded output for the gain, and a  $\pm 10$ -volt and 10-milliampere output.

32. Outputs proportional to moment, torque, dolos temperature, water surface elevation variations with time, and wave heights were individually routed to special channels in the analog-to-digital converter for recording and analysis. The coded output for the gain was routed through multiplexers to the digital inputs in the data acquisition computer. Photographs and/or schematics of various wave gage system and ADACS' components are presented in Appendix C, "ADACS."

## PART III: TESTS AND TEST RESULTS

### Selection of Test Conditions

33. Selection of wave and water level conditions to reproduce in the physical model was based on the highest water levels and most severe wave conditions for which prototype dolos moment and torque data were available. A search of the prototype data revealed that the first 5 hr of 11 January 1988 offered the best set of data. As shown in Table 2, data were available for up to six individual dolosse during 1 hr of the storm. Two prototype wave gages were in place and collecting data on that day. Wave gage 2 was located 867 ft seaward of the center line of the breakwater cap in a water depth of 45 ft and wave gage 3 was 1,266 ft seaward of gage 2 in a water depth of approximately 62 ft. Water level data were available from a tide gage positioned in the lee of the inner Crescent City breakwater. Tabulated results from analysis of the prototype wave and water level data are presented in the top half of Table 3.

34. During the storm hours of 11 January 1989, directional wave data were gathered at Monterey Bay, California. Examination of these data revealed that the mean deep water wave direction during this period of time was best defined as 280 deg relative to True North. No shallow-water wave direction data were collected near the Crescent City breakwater during this time period. In the absence of these data, an estimated shallow-water wave direction was determined using information from a Crescent City water wave refraction, diffraction, and shoaling study conducted at CERC by Hales (1985). Considering the peak periods of the selected test spectra and the 280-deg deepwater wave direction, Hales' study indicated that incident waves approach essentially perpendicular to the crest of the main stem of the breakwater. Thus it was determined that the model bathymetry and structure should be constructed and oriented such that incident waves in the model would approach perpendicular to the cap on the breakwater's main stem.

### Calibration of the Wave Basin

35. The prototype wave spectra were defined by discrete spectral energy density versus frequency data sets, one spectrum for each hour of the storm to be reproduced in the model. These discrete spectra were transformed into the

wave machine time history command signals necessary to reproduce both the time domain and frequency domain wave statistics matching the prototype wave statistics at gages 2 and 3. Wave gage arrays (three gages) were placed in the model at the points corresponding to the prototype gages (Figure 6). Wave gage arrays were used so that both incident and reflected spectra could be resolved. With the model breakwater in place and the still-water level set at the appropriate elevation for the selected storm hour, the wave spectra command signal was run for a sufficient time to collect data at gages 2 and 3 that corresponded to approximately 30 min of prototype time. Thirty minutes of data were collected during each hour that prototype data were collected. Both frequency and time domain analysis of the data were conducted and the results were compared to prototype data. During wave basin calibration and subsequent tests, the water level was monitored and recorded through a gage placed on the lee side of the model breakwater (Figure 6). Adjustments were made to the command signal, it was rerun, and the data were reanalyzed until a close match was obtained between the model and prototype time domain and frequency domain wave statistics. This approach was used until acceptable wave machine command signals had been developed for each hour of prototype storm. The model wave and water level statistics were scaled to prototype and are presented on the bottom half of Table 3. The time domain statistics at wave gages 2 and 3 are plotted in Figures 24-27 and graphs comparing the model and prototype spectral energy density versus frequency at gage 2 are presented for each hour of the storm in Figures 28-32. The single-channel frequency analyses in Figures 28-32 do not separate incident and reflected model spectra, while the Goda spectral analyses in the same figures show only the portions of the model spectra that are incident on the breakwater.

#### Placement of Instrumented Model Dolosse

36. Subsequent to wave basin calibration and prior to conducting tests to collect dolos data, a portion of the model dolos cover layer was reworked in an effort to position dolosse in the approximate positions, orientations, and elevations defined by the prototype dolos boundary condition study described by Howell et al. (in preparation). Figure 33 is an aerial view of the prototype instrumented dolosse in the top layer. Table 4 lists prototype survey data on the elevations of three points each on dolosse C, E, G, N, and

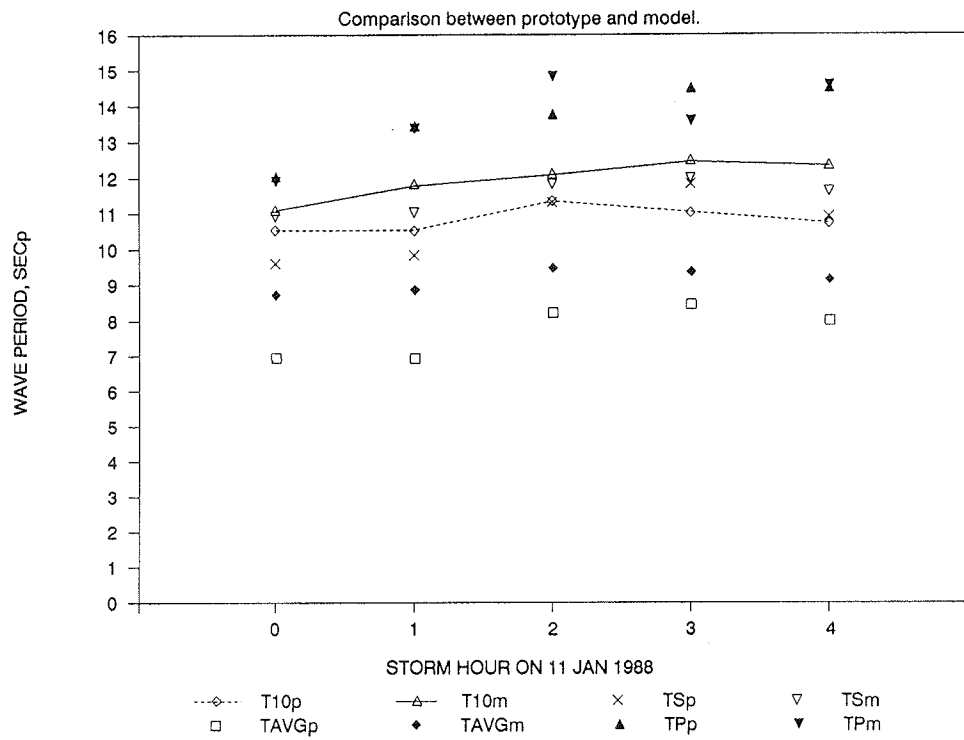


Figure 24. Wave period versus storm hour as measured in model and prototype at gage 2

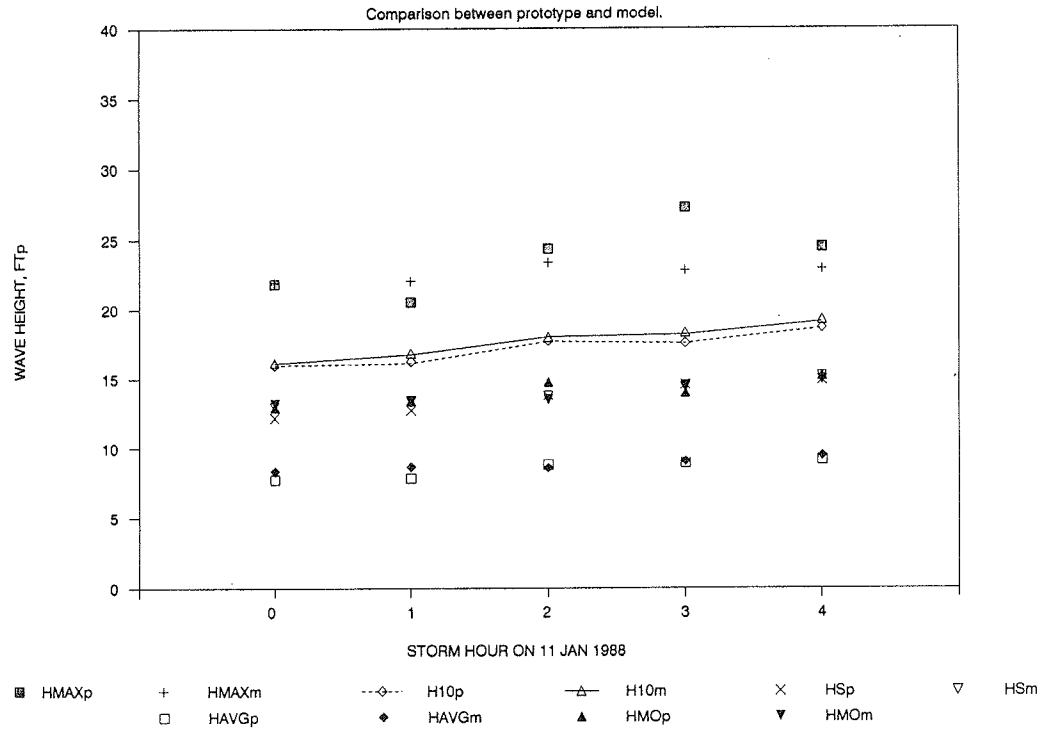


Figure 25. Wave heights versus storm hour as measured in the model and prototype at gage 2

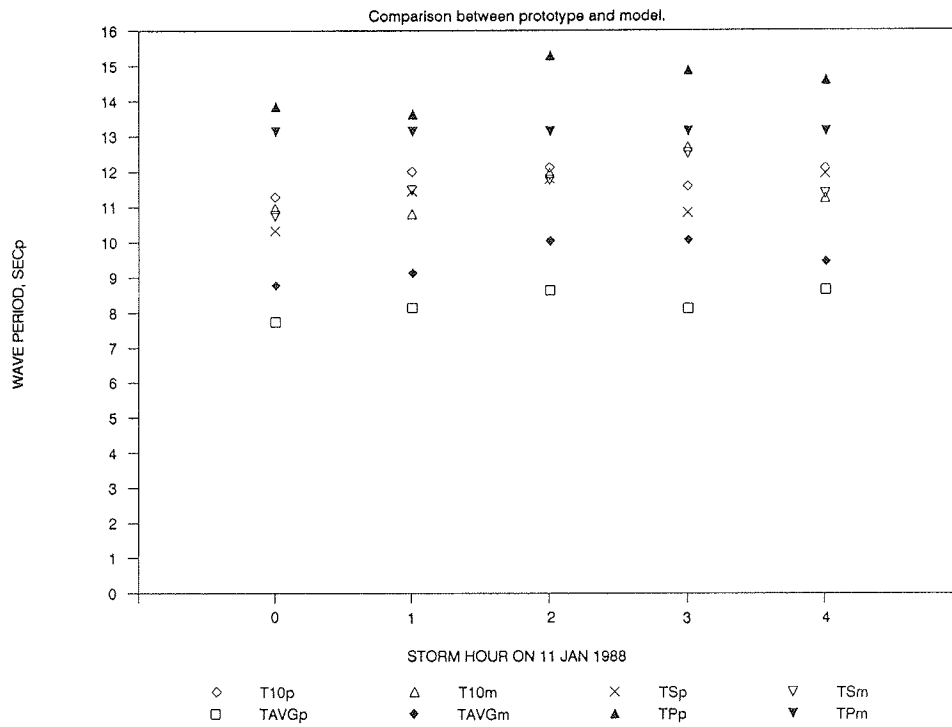


Figure 26. Wave period versus storm hour as measured in model and prototype at gage 3

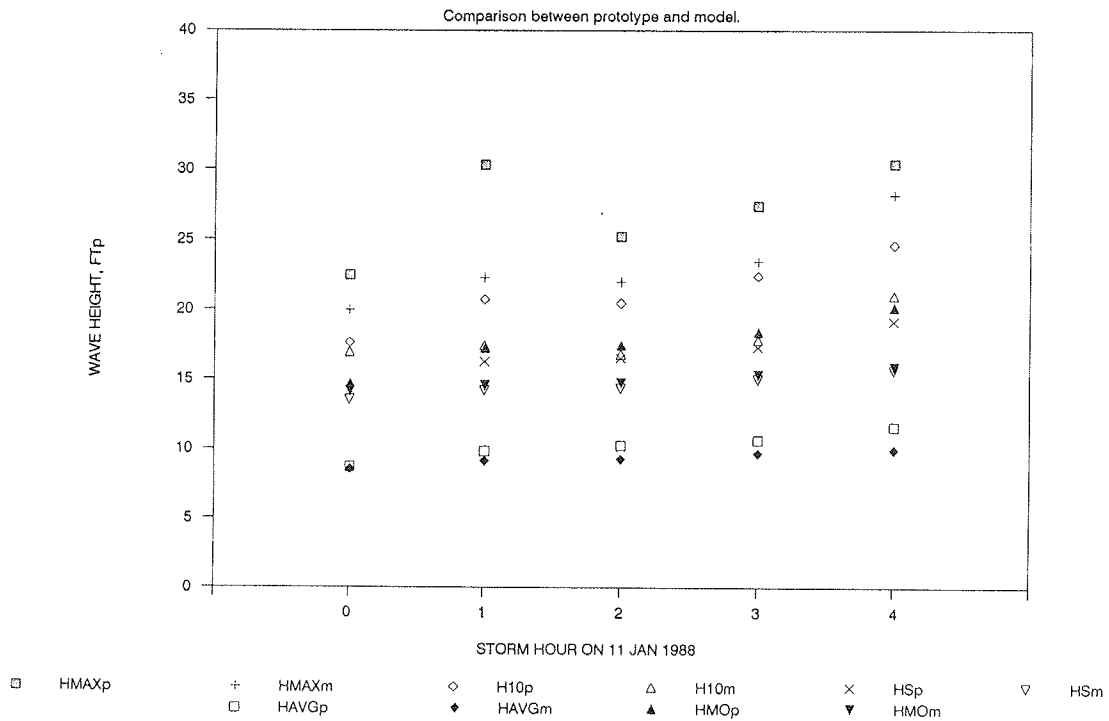


Figure 27. Wave heights versus storm hour as measured in the model and prototype at gage 3

11 JANUARY 1988

TEST047 : GAGE 2

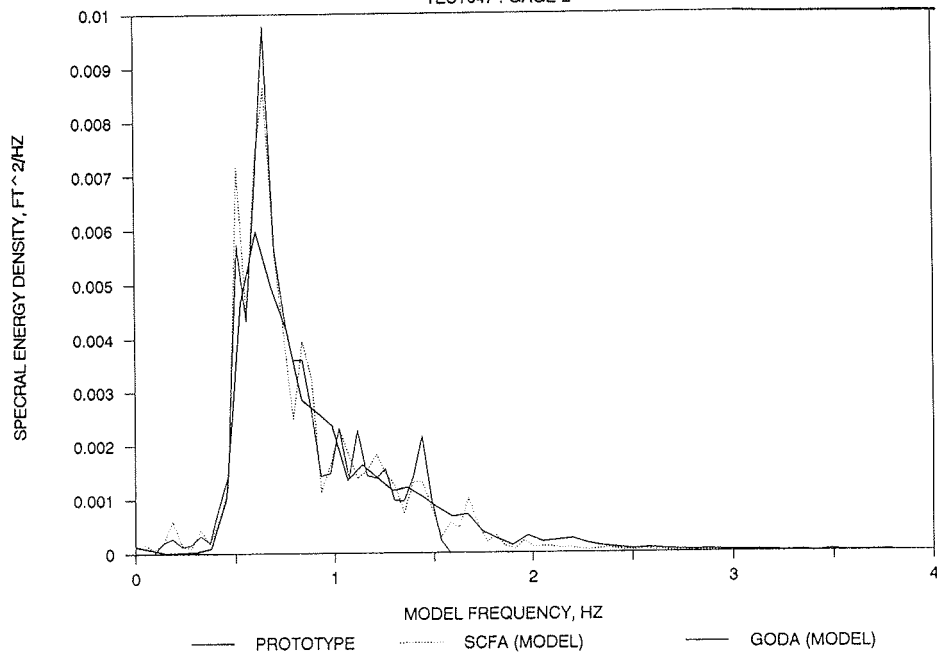


Figure 28. Spectral energy density versus frequency plots comparing model and prototype measurements for storm hour 0

11 JANUARY 1988

TEST049 : GAGE 2

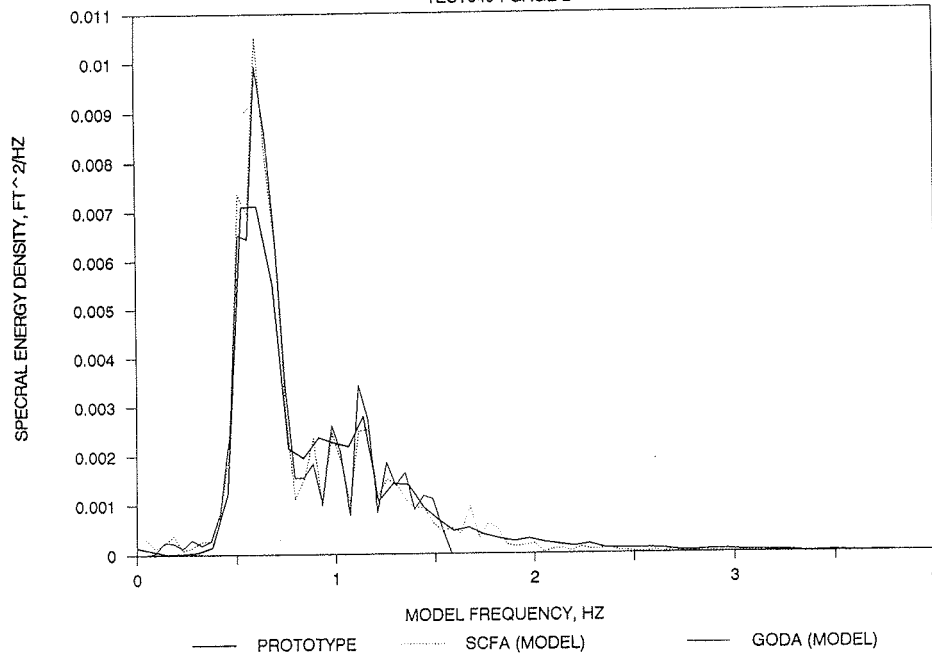


Figure 29. Spectral energy density versus frequency plots comparing model and prototype measurements for storm hour 1

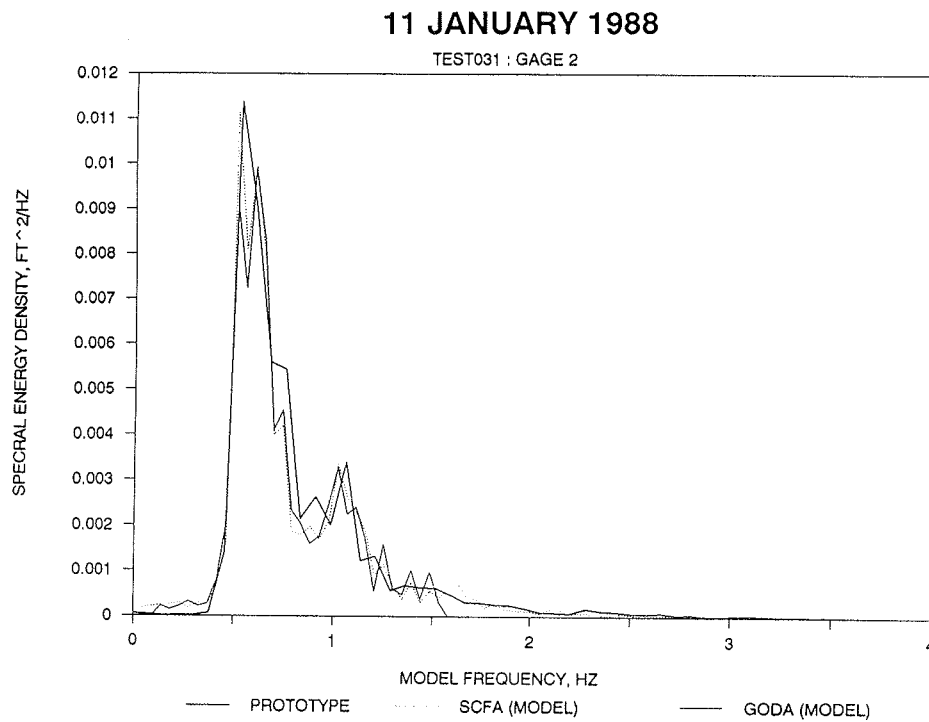


Figure 30. Spectral energy density versus frequency plots comparing model and prototype measurements for storm hour 2

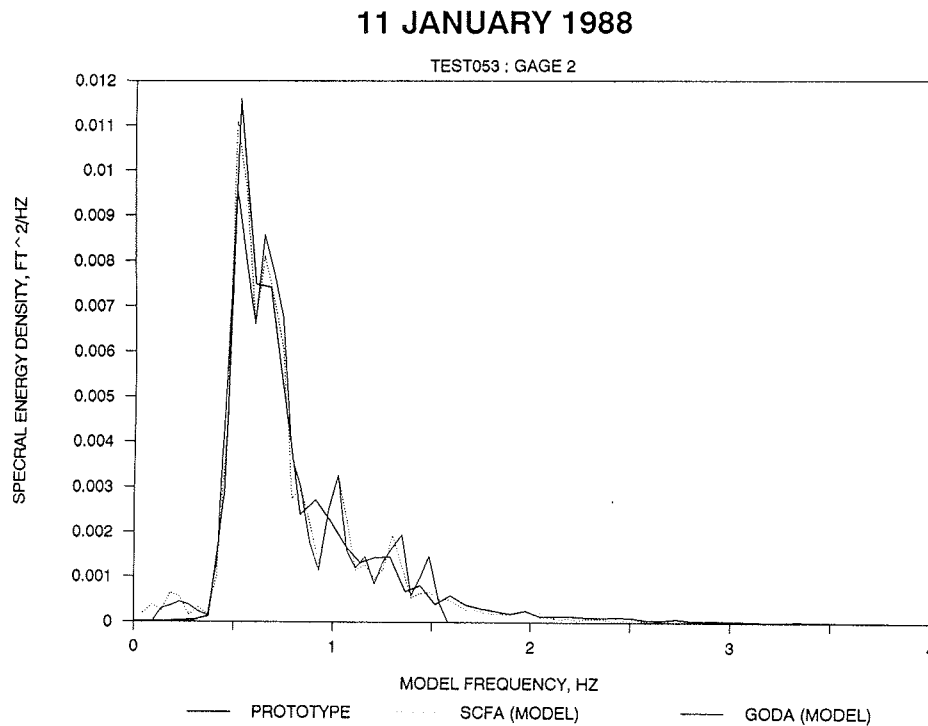


Figure 31. Spectral energy density versus frequency plots comparing model and prototype measurements for storm hour 3

11 JANUARY 1988

TEST055 : GAGE 2

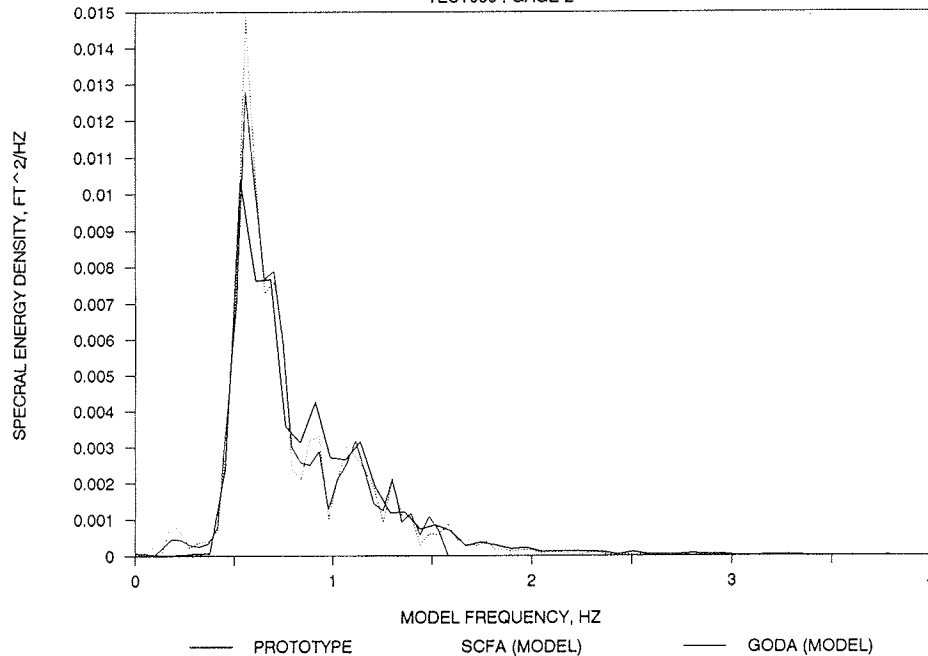


Figure 32. Spectral energy density versus frequency plots comparing model and prototype measurements for storm hour 4

P taken in April 1987 and dolosse D and M taken in January 1987. After reworking the model dolosse, the three points on each model dolos corresponding to the prototype survey points were checked for elevation and these results are presented adjacent to the prototype data in Table 4. Figure 34 shows the instrumented dolosse in position on the model. In Figure 34, the alpha characters near mid-shank of the instrumented model dolosse correspond to the prototype dolosse they are representing and the numerals on the flukes are the model dolosse identification numbers.

#### Model Operation

37. Once the instrumented model dolosse had been installed on the model and interfaced with the ADACS, a series of quality control tests were conducted to insure the accuracy of the moment and torque data to be collected. These tests consisted of mounting each dolos back in the calibration device, which had been positioned in the lee of the model breakwater, and loading the units with known moments and torques. Data were collected and analyzed and



Figure 33. . Aerial view of instrumented prototype dolosse on Crescent City breakwater

compared to the expected values. This gave confidence that the thermal correction routines in the data analysis software were working correctly and that the interfacing of the units with the ADACS had in no way altered the transducer outputs. The results of these tests showed that for the instrumented dolosse used to collect data on the model, the measured output varied from the expected for any given data channel by a maximum of 2.57 percent and some channels showed exact matches when compared to the third decimal place to the expected values.

38. The five storm command signals were run in sequence starting with hour zero. The water level was increased to the appropriate elevation, and the water in the wave basin was allowed to reach a calm state between each storm level. From day to day, the instrumented dolosse were kept out of the water on a platform behind the breakwater. Before they were placed on the breakwater, they were placed in a rack in the water behind the structure (Figure 35). In the rack, the dolosse were in a no-load position and immersed in model water. Once the dolos units had stabilized at the model water temperature, a data set was collected that defined the temperature of each dolos and the output of each data channel that could be referenced to this no-load configuration and beginning temperature. These values were used to correct data channel outputs for thermal drift and output voltages associated with no load.

39. Once the zero reference test was completed, the instrumented dolosse were placed on the breakwater and the instrumentation wires were woven through the adjacent dolosse and up to the breakwater cap. This was done to minimize wire motion in the wave action in order to protect the wires from damage and to minimize the chance for wire motion that might influence load cell output. With the dolosse in place, the five wave conditions were run but no dolos data were collected. This was done to let the dolosse nest and settle into the structure. This is commonly referred to as shaking down the model and is carried out to simulate natural consolidation and armor unit adjustments that take place in the prototype subsequent to completion of new construction. The prototype dolosse had seen two winters of storms and were well nested into the structure before the January 1988 data were collected.

40. Following the shakedown, the model was run using the five storm wave board command signals. During days when data were collected, ambient air temperatures in the test facility reached 95 °F and the model water



Figure 34. Instrumented model dolosse in place on breakwater

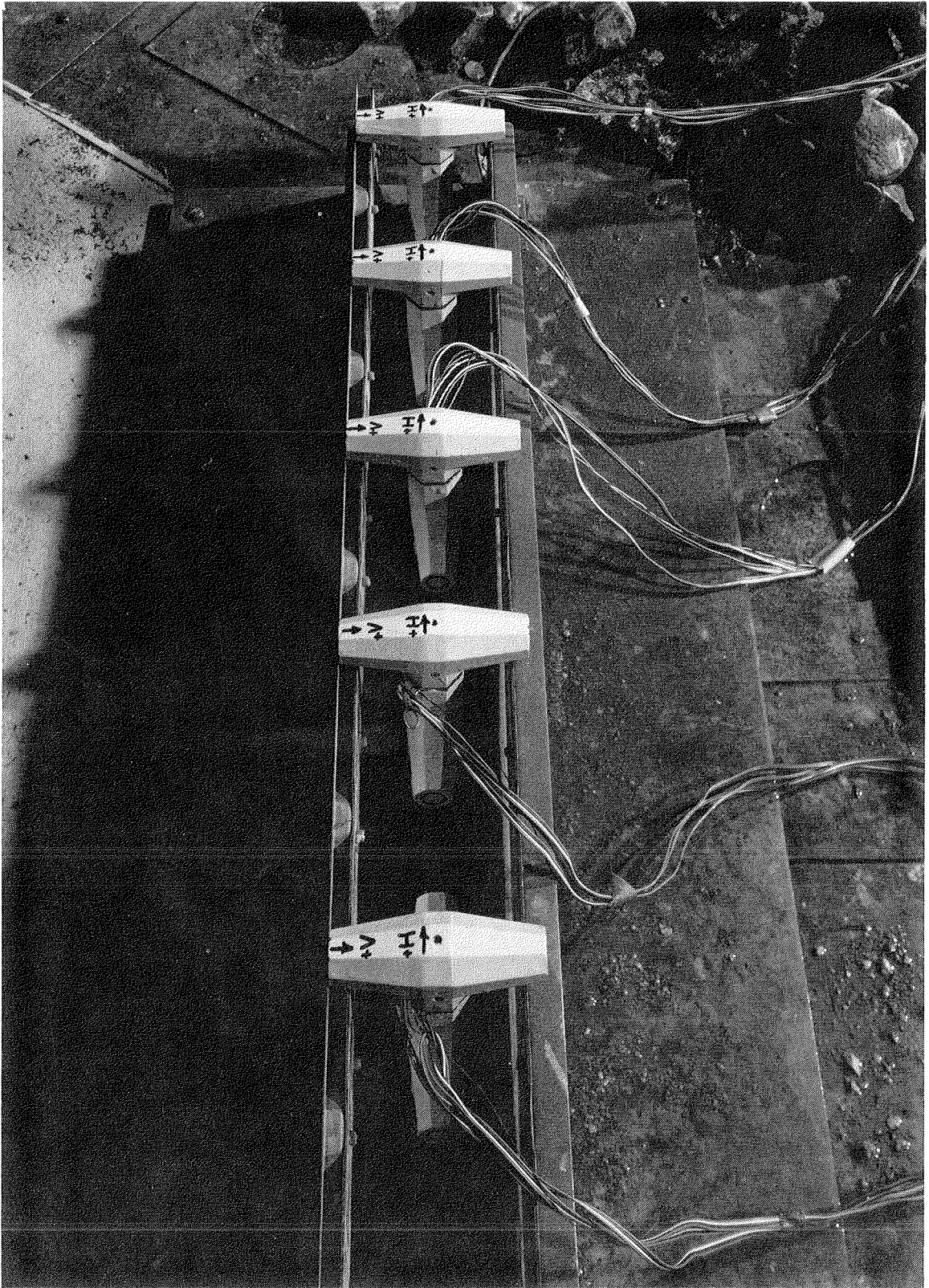


Figure 35. Instrumented dolosse in no-load rack behind model breakwater

temperature stayed in the mid 70's. A low-velocity water spray was directed on the instrumented units between runs to keep them at a temperature very near that of the model water. Even with the temperature-compensating software, it was determined that it would be better for the longevity of the units to minimize thermal shock. The dolosse were removed from the breakwater when a day's testing had been completed. As each instrumented dolos was removed, it was replaced with an uninstrumented unit. This was done to ensure that an instrumented unit could be repositioned at a future date so that repeat tests could be conducted.

### Tests

41. The 5-hour storm sequence and associated data collection were repeated six times, giving a total of thirty data sets. After analysis and close scrutiny of the data, it was determined that 27 tests contained good quality data. During early tests, seven instrumented dolosse were working and incorporated into the model. During latter stages of the study, the insulation levels had fallen below acceptable limits on two dolosse and they had to be pulled from the test section.

42. Each data set contained approximately 30 min, prototype time, of data defining the time histories of water surface elevations at wave gages 2 and 3 and the water level gage in the lee of the breakwater, and vertical and horizontal moments, torque, and temperature for each dolos activated for the test. The data sampling rate was 50 samples per second, model time, for all data channels. This rate was determined to be more than adequate to define variations in static loads and the wave-induced pulsations in the moments and torque being monitored in each dolos. A higher sampling rate would have been required if good resolution of impact data had been a goal of this study.

### Data Analysis

43. During preliminary analysis of the prototype data, it was determined that the two moments and the torque measured in each dolos could be used to define a principal stress  $\sigma$  and thus allow some simplification by only having to correlate one time-varying parameter with the incident wave environment, instead of three. The principal stress approach to the prototype data analysis was first presented by Burcharth and Howell (1988). A detailed

description of the assumptions associated with this approach and its application to the prototype data are presented in the Data Analysis section of Howell et al. (in preparation).

44. Principal stress calculations were carried out in the model in the same way as was done for the prototype data. The following equation defined principal stress:

$$\sigma = \frac{\sigma_x}{2} + \left[ \left( \frac{\sigma_x}{2} \right)^2 + \tau^2 \right]^{1/2} \quad (2)$$

where

$\sigma_x$  = normal stress, lb/in<sup>2</sup>

$\tau$  = shear stress, lb/in<sup>2</sup>

The normal stress is perpendicular to the plane that passes through the fluke-shank interface normal to the shank and the shear stress is at right angles to the normal stress and lying in the plane (Figure 36). The normal stress is defined as a function of the vertical and horizontal moments as follows:

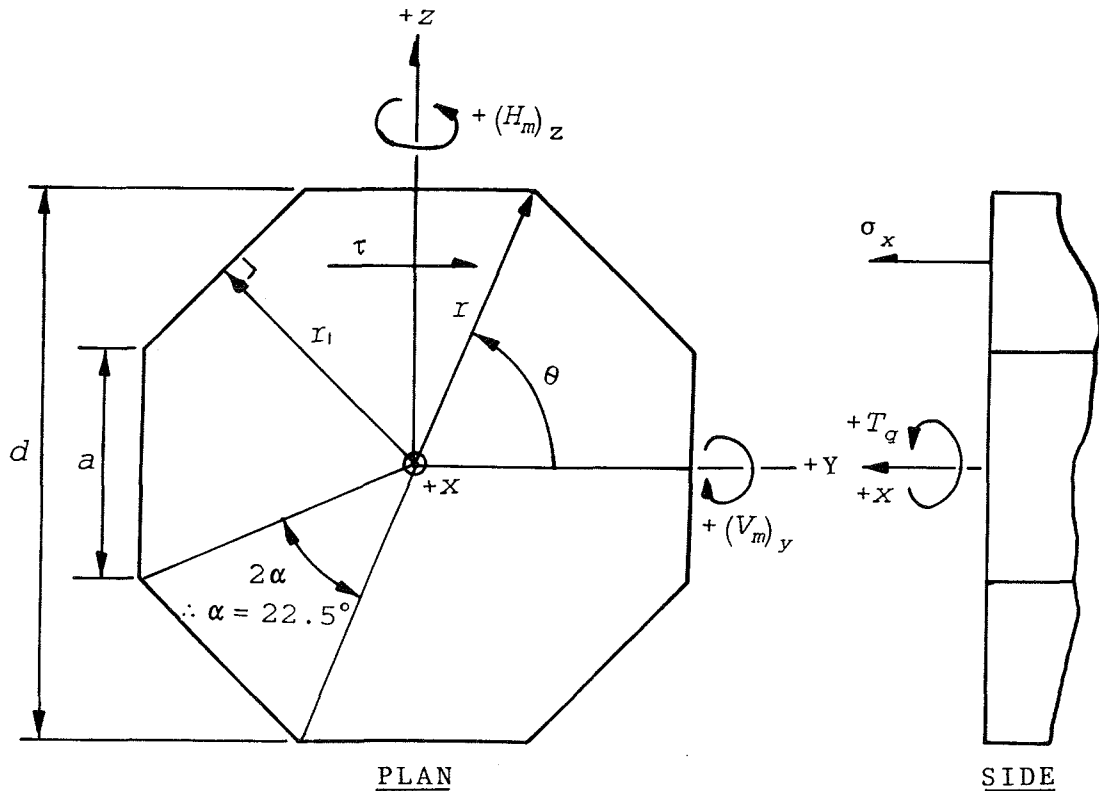


Figure 36. Plan and side views of fluke-shank interface and definitions of data analysis parameters for instrumented model dolosse

$$\sigma_x = \left[ \frac{-(H_m)_z y}{I_z} + \frac{(V_m)_y z}{I_y} \right] \div 144 \quad (3)$$

where

$(H_m)_z$  = horizontal moment, foot-pounds

$(V_m)_y$  = vertical moment, foot-pounds

$I_z = I_y$  = moment of inertia of the area defined by the cross section of the dolos shank, feet<sup>4</sup>

$y$  = distance measured along y axis, feet

$z$  = distance measured along z axis, feet

For the octagonal area

$$I = \frac{\text{Area} \times (12r_1^2 + a^2)}{48} \quad (4)$$

and

$$\text{Area} = 2d^2 \tan \alpha \quad (5)$$

See Figure 36 for variable definitions. Normal stress increases with distance from the neutral axis and is a maximum at the farthest point, which in the case of the octagonal, was at one of the eight corners on the surface of the shank at the fluke-shank interface. Thus, the maximum normal stress  $(\sigma_x)_{\max}$  was determined at data time-step  $t_1$  by calculating the normal stress at each corner of the octagon for the two moments measured at  $t_1$  and selecting the maximum value from these eight values. At each corner, magnitudes of  $x$  and  $y$  were calculated based on the values of  $r$  and  $\theta$  (Figure 36). The shear stress at the surface of the dolos shank created by torque, and referred to as  $\tau$  in Equation 3, was calculated as follows:

$$\tau = \frac{T_q r_2}{J} \div 144 \quad (6)$$

where

$T_q$  = torque, foot-pounds

$J$  = polar moment of inertia of a circle of radius  $r_2$ , and the circle has a moment of inertia  $I$  equal to that of the octagonal cross section of the dolos shank, ft<sup>4</sup>

It can be shown that

$$r_2 = 0.50499 d \quad (7)$$

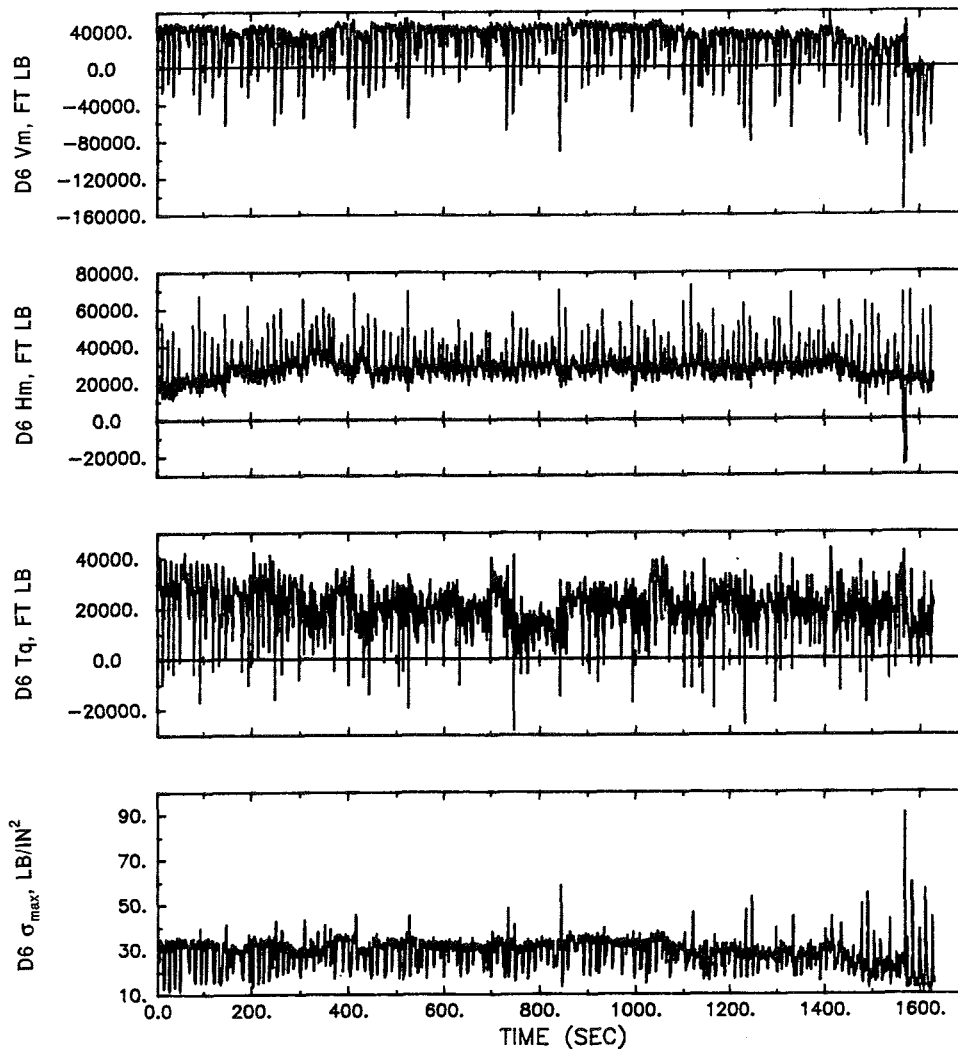
and thus,

$$J = \frac{\pi(r_2)^4}{64} = \frac{0.06503 \pi (d)^4}{64} \quad (8)$$

Substituting Equations 7 and 8 into Equation 6 along with the torque measured at time-step  $t_1$  gave the value of  $\tau$  at  $t_1$ . Substituting  $(\sigma_x)_{\max}$  and  $\tau$  for  $t_1$  into Equation 2 gave the maximum principal stress at time-step  $t_1$ ,  $(\sigma_{\max})_{t_1}$ .

45. Following the procedure described in the previous paragraph, the time histories of  $\sigma_{\max}$  were calculated for the moment and torque data on each dolos in each of the 27 data sets. Figure 37 shows examples of vertical and horizontal moment, torque, and maximum principal stress time histories for one dolos during the entire duration of one storm hour test condition. Calculated values were scaled to prototype units before plotting. The portion of the  $\sigma_{\max}$  associated with the pulsating loads induced by wave action was superimposed on top of  $\sigma_{\max}$  resulting from static loads induced by the dolos self weight combined with loads produced by contact with adjacent units in the dolos matrix. For the prototype data, the  $\sigma_{\max}$  values associated with pulsating loads were extracted from the prototype data by removing the mean from the  $\sigma_{\max}$  and creating what was referred to as the detrended  $\sigma_{\max}$  time history. This same approach was used to remove the static portion of  $\sigma_{\max}$  from the model data. A sliding linear detrending methodology was developed that removed the mean as well as any linear trends that were caused by a change in static loads that occurred during any test. Figure 38 shows an example of the detrended  $\sigma_{\max}$  time histories of three dolosse for a one-storm-hour data set. The time history of dolos 6 in Figure 38 is the  $\sigma_{\max}$  time history from Figure 37 after detrending. The detrended time histories then were analyzed, and the maximum value of maximum principal stress  $(\sigma_{\max})_m$  and the second-highest value of maximum principal stress  $(\sigma_{\max})_{m2}$  were extracted from each data set for each dolos. A listing of  $(\sigma_{\max})_m$  and  $(\sigma_{\max})_{m2}$  values for all tests is presented in Table 5. Measured values were scaled to prototype equivalent.

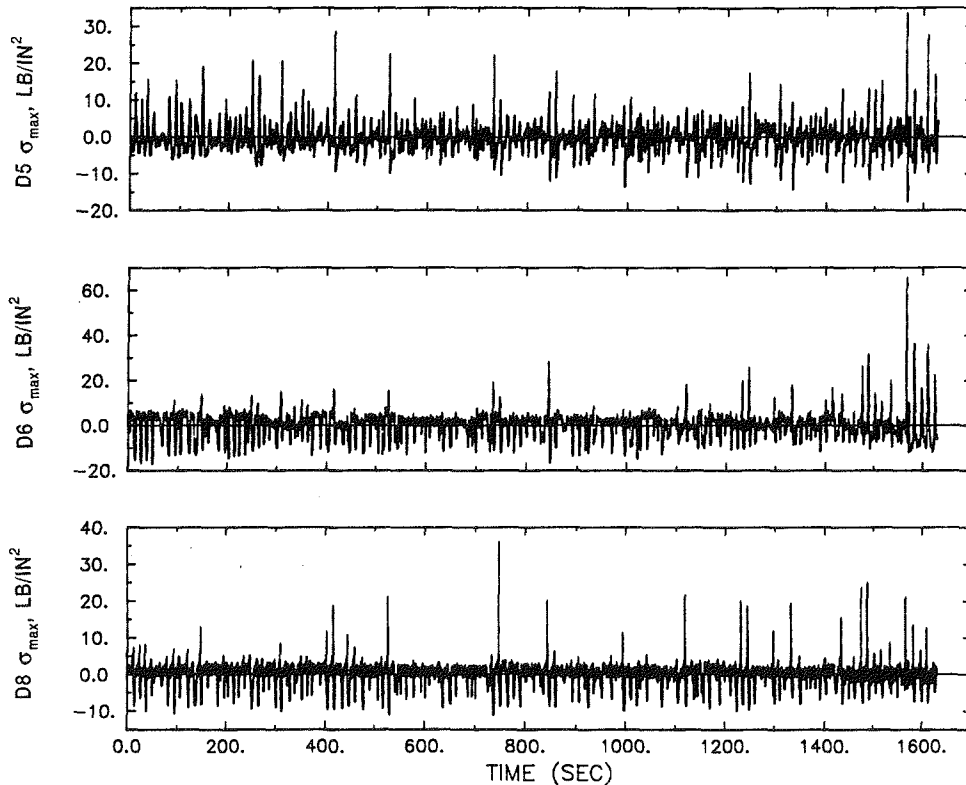
46. During analysis of the prototype data, the average of the maximum values of maximum principal stress were plotted against cellular ranges of



STORM HOUR 4  
TEST 88

Figure 37. Example of vertical and horizontal moments, torque, and maximum principal stress time histories for one dolos during one-storm-hour condition (dolos 6 from one of the latter repeat tests for storm hour 4)

$H_{10}$  and  $T_{10}$  (Figure 39) (Howell et al., in preparation). It was obvious from this plot that average maximum principal stress showed no consistent trend with wave period, but showed a general trend to increase with increasing values of  $H_{10}$ . Further, it was discovered that within a cellular range of  $H_{10}$  the exceedance probability distribution of  $(\sigma_{max})_m$  could be closely approximated by a Rayleigh exceedance probability distribution function (Figure 40).



STORM HOUR 4  
 DETRENDED PS  
 TEST 88

Figure 38. Example of detrended maximum principal stress time histories for three dolosse during one-storm-hour condition (dolosse 5, 6, and 8 from one of the latter repeat tests for storm hour 4)

47. The majority of the maximum principal stress data collected for the 5 hr of storm conditions reproduced in the model study fell within or very close to the prototype data cell defined by  $T_{10} = 12$  to 14 sec and  $H_{10} = 16.40$  to 19.69 ft. These data are presented in Figure 41. The average of the maximum values of maximum principal stress shows a close comparison to the prototype and the average of the highest two maximum principal stresses shows an even closer comparison to the prototype. Figures 42-45 show a comparison between measured model and predicted Rayleigh values of probability density, probability, cumulative probability, and exceedance probability of the maximum values of maximum principal stress  $(\sigma_{max})_m$ . As was found with the prototype data, the Rayleigh distributions can be used to predict distributions and

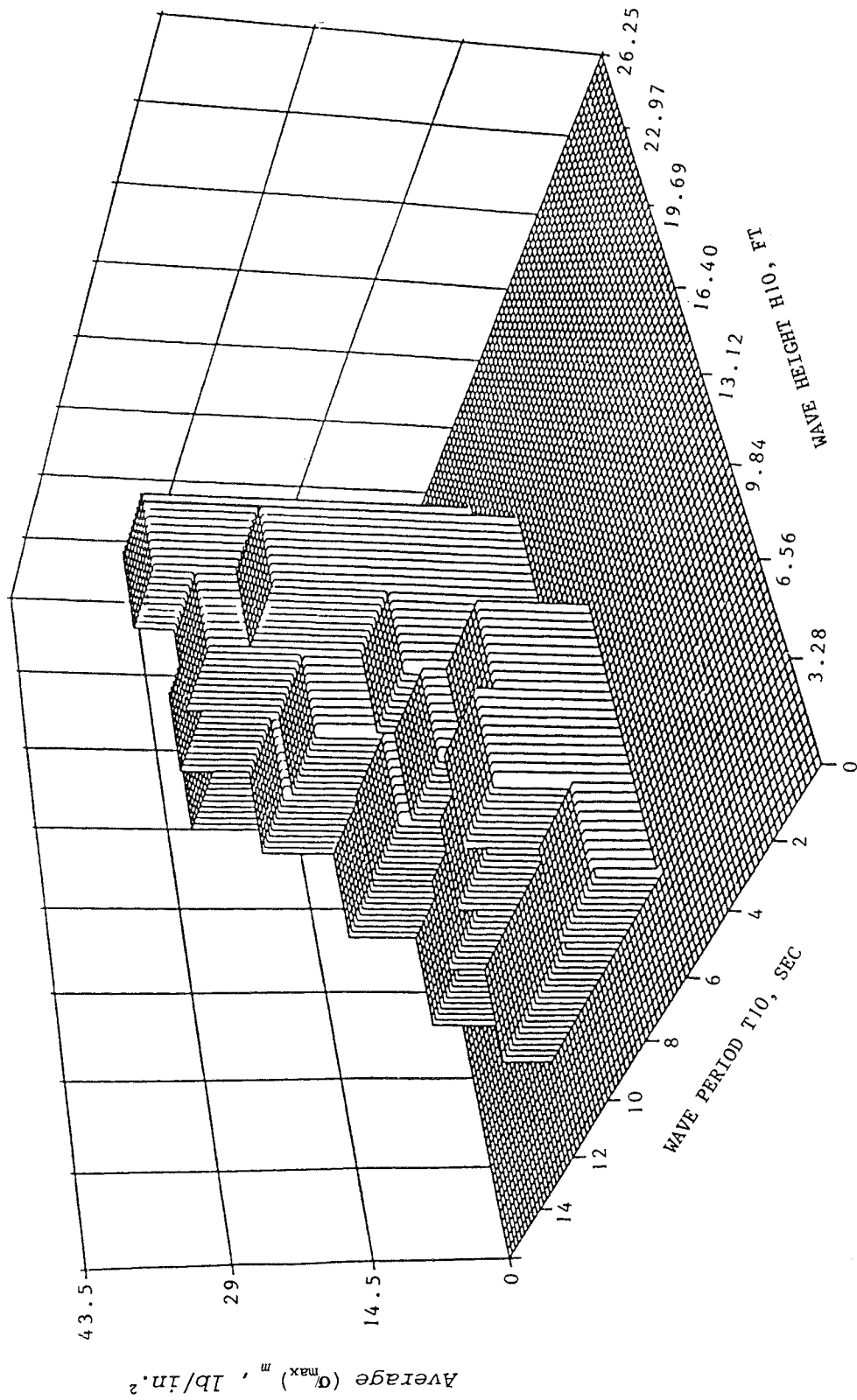


Figure 39. Prototype values of average of maximum values of maximum principal stress plotted against  $T_{10}$  and  $H_{10}$

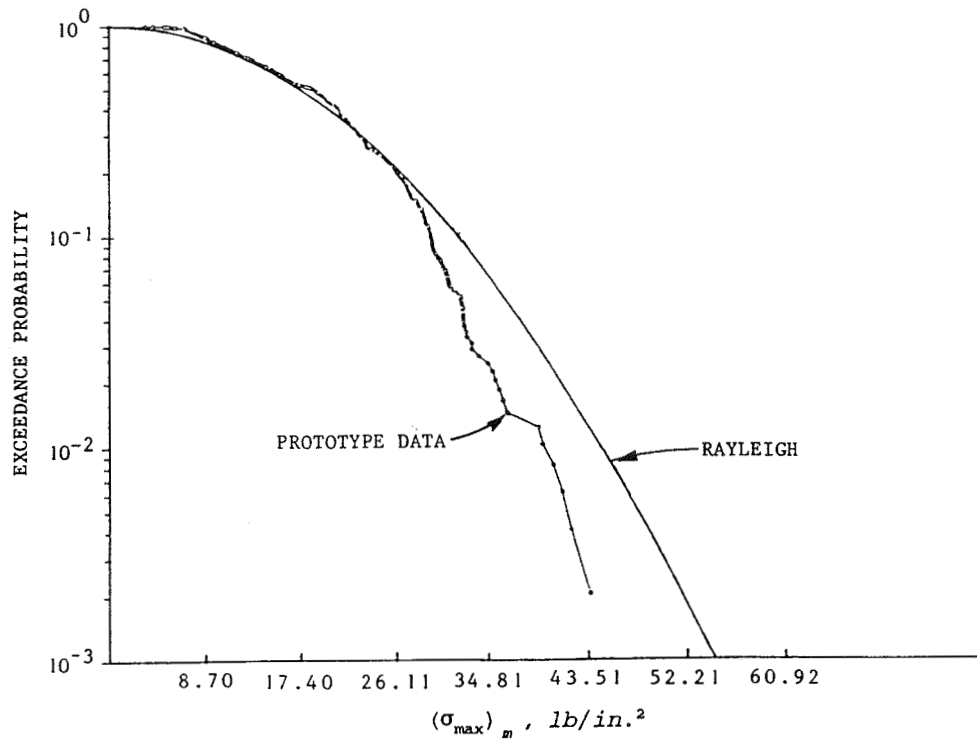


Figure 40. Prototype exceedance probability of  $(\sigma_{max})_m$  for  $H_{10} = 11.48$  to  $14.76$  ft

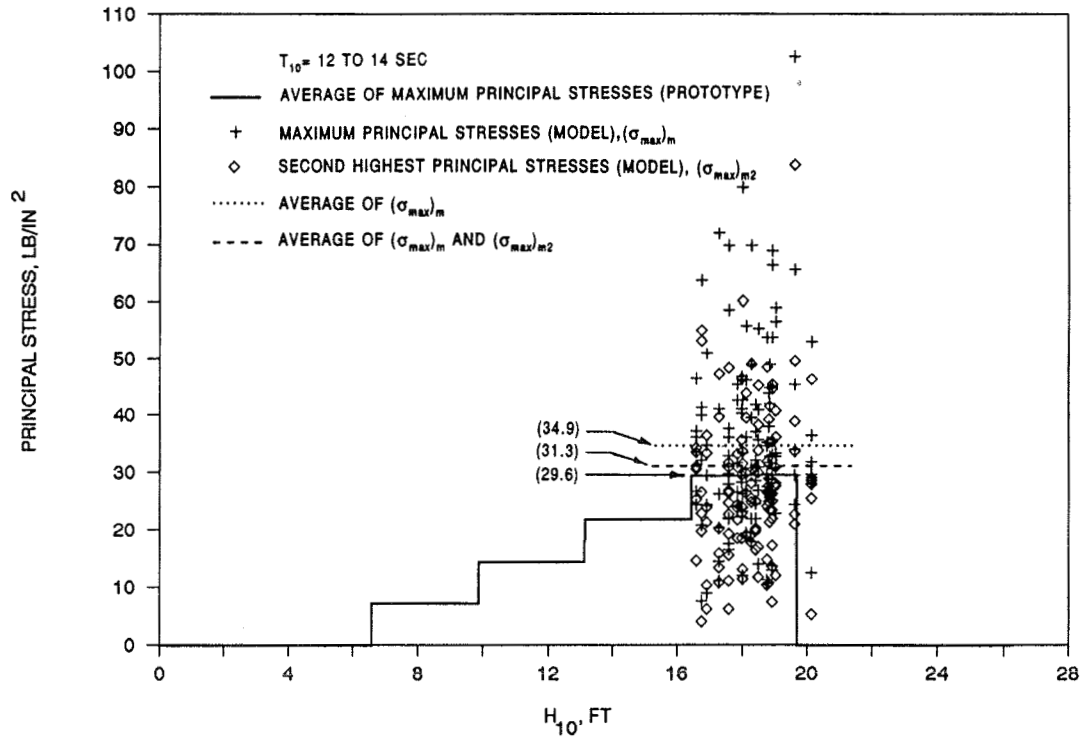


Figure 41. Model data of principal stress plotted against  $H_{10}$  and compared to average prototype values of maximum principal stress

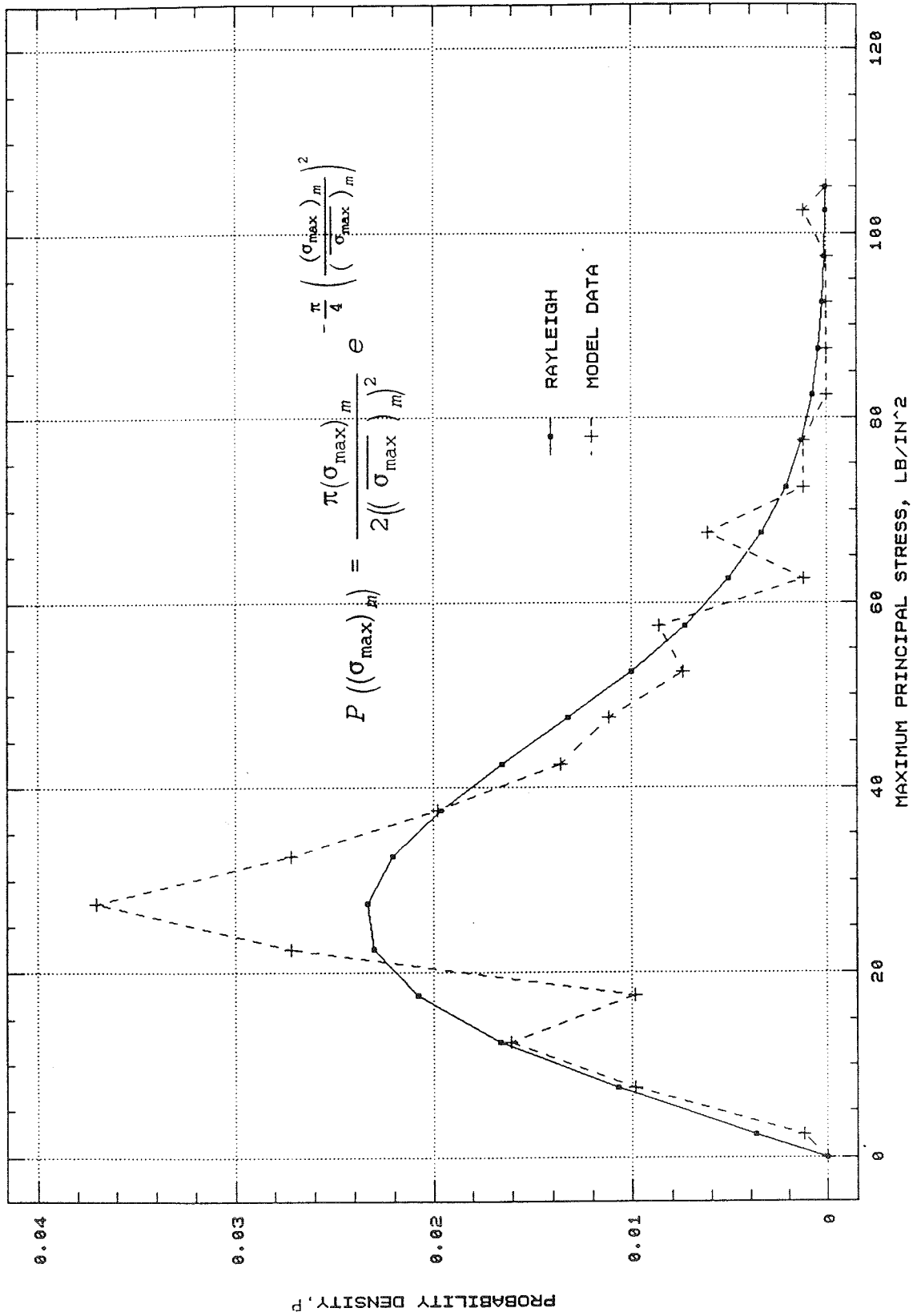


Figure 42. Probability density of maximum principal stress,  $(\sigma_{\max})_m$ , as measured in model and predicted by Rayleigh distribution

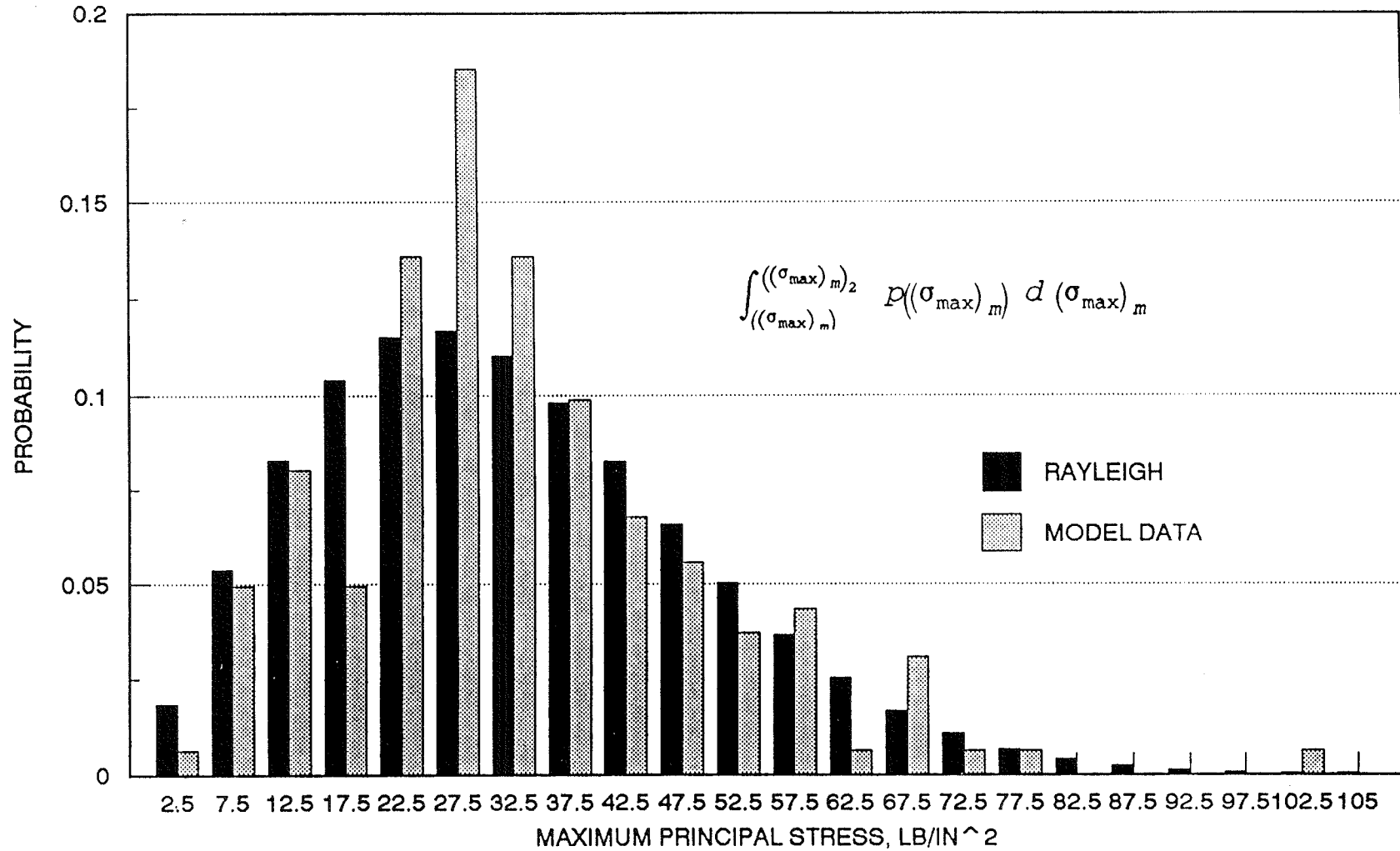


Figure 43. Probability of maximum principal stress,  $(\sigma_{max})_m$ , as measured in model and predicted by Rayleigh distribution

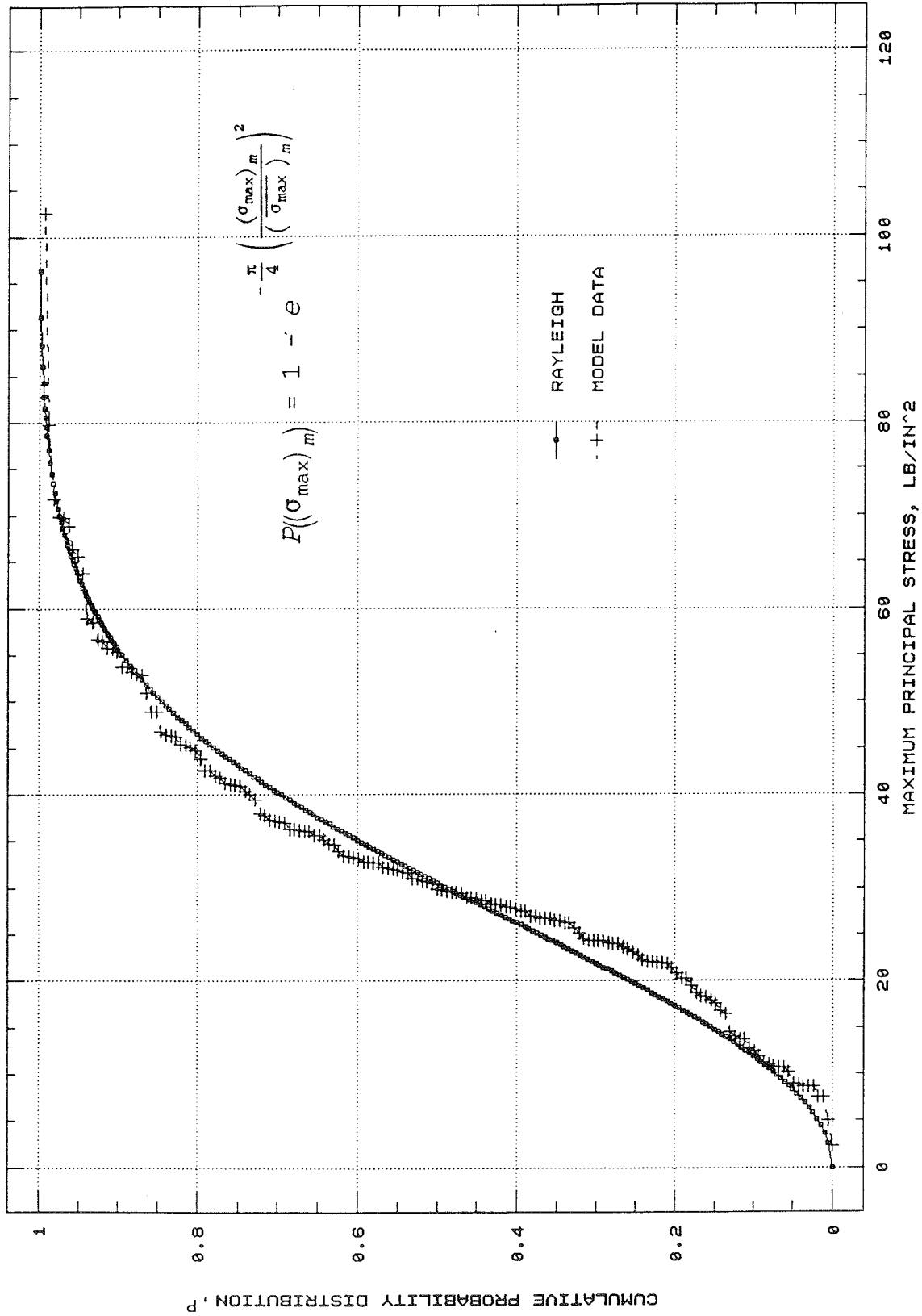


Figure 44. Cumulative probability distribution of maximum principal stress,  $(\sigma_{\max})_m$ , as measured in model and predicted by Rayleigh distribution

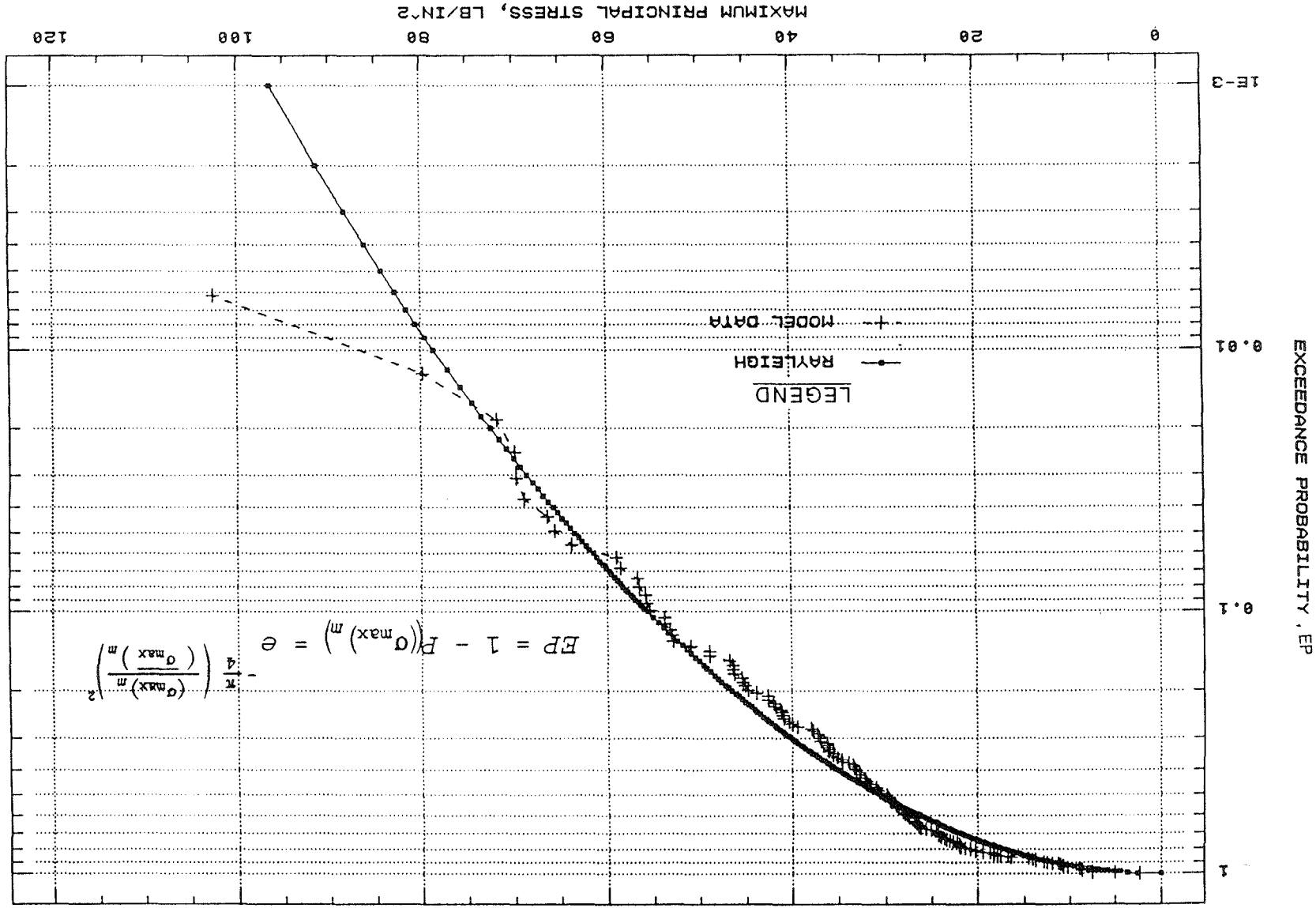


Figure 45. Exceedance probability of maximum principal stress,  $(\sigma_{max})_m$ , as measured in model and predicted by Rayleigh distribution

exceedance probabilities of maximum principal stresses associated with pulsating wave loadings.

48. Thus it has been shown that the instrumented model dolosse, when exposed to the same wave and structural environments as their prototype counterparts, can be used to determine average maximum principal stress values that very closely match the average maximum principal stress produced in the prototype dolosse. Like the prototype, the distribution of maximum principal stress values, measured using the instrumented model dolosse, is very closely approximated by a Rayleigh distribution function. With these validations against prototype data, the instrumented model dolosse can now be used to determine maximum principal stress distributions resulting from pulsating wave loadings for a range of geometric and environmental conditions that are not specific to the Crescent City breakwater.

#### PART IV: CONCLUSIONS

49. Based on the test conditions and test results reported herein it is concluded that the instrumented model dolosse, when built as described herein and used in a manner that provides for maintenance of high quality data devoid of noise, can be used to determine moment and torque values associated with pulsating wave loadings and these data can be used to determine the average, as well as the probability distributions, of maximum principal stress.

## REFERENCES

- Baumgartner, R. C., Carver, R. D., and Davidson, D. D. 1985 (Nov). "Breakwater Rehabilitation Study, Crescent City Harbor, California; Coastal Model Investigation," Technical Report CERC-85-8, US Army Engineer Waterways Experiment Station, Vicksburg, MS.
- Burcharth, H. F., and Howell, G. L. 1988 (Jun). "On Methods of Establishing Design Diagrams for Structural Integrity of Slender Complex Types of Breakwater Armour Units," Seminaire International Entretien des Infrastructures Maritimes, Casablanca, Morocco.
- Delft Hydraulics Laboratory. 1980 (Mar). "Recent Developments in Instrumentation: Load Measurements," hydro delft, Delft, The Netherlands.
- Hales, L. Z. 1985 (Mar). "Water Wave Refraction/Diffraction/Shoaling Investigation, Crescent City, California," Miscellaneous Paper CERC-85-3, US Army Engineer Waterways Experiment Station, Vicksburg, MS.
- Howell, G. L., et al. "Crescent City Prototype Dolosse Study," in preparation, US Army Engineer Waterways Experiment Station, Vicksburg, MS.
- Hudson, R. Y. 1975 (Jun). "Reliability of Rubble-Mound Breakwater Stability Models," Miscellaneous Paper H-75-5, US Army Engineer Waterways Experiment Station, Vicksburg, MS.
- Hudson, R. Y., and Jackson, R. A. 1955 (Jun). "Design of Tetrapod Cover Layer for Rubble-Mound Breakwater, Crescent City Harbor, Crescent City, California; Hydraulic Model Investigation," Technical Memorandum 2-413, US Army Engineer Waterways Experiment Station, Vicksburg, MS.
- \_\_\_\_\_. 1956 (Apr). "Stability of Crescent City Harbor Breakwater, Crescent City, California," Miscellaneous Paper 2-171, US Army Engineer Waterways Experiment Station, Vicksburg, MS.
- Markle, D. G., and Davidson, D. D. 1984 (Mar). "Breakage of Concrete Armor Units; Survey of Existing Corps Structures," Miscellaneous Paper CERC-84-2, US Army Engineer Waterways Experiment Station, Vicksburg, MS.
- Scott, R. D. 1986 (Dec). "The Analysis of Concrete Armour Units in a Breakwater," Ph.D. Thesis, Queen's University, Kingston, Ontario, Canada.
- Scott, R. D., Turke, D. J., and Baird, W. F. 1986 (Nov). "A Unique Instrumentation Scheme for Measuring Loads in Model Dolos Units," 20th International Conference on Coastal Engineering, Taiwan.
- Stevens, J. C., et al. 1942. "Hydraulic Models," Manuals on Engineering Practice No. 25, American Society of Civil Engineers, New York.

Table 1  
Capacitance Wave Rod, Channel No. 5  
Long Tem Stability Test

Calibration Range (in)	Date	Water Temperature deg F	Air Temperature deg F	Linear Maximum Deviation	Quadriatic Max. Dev.	Linear	
						b E+2	m E-2
8	12-09-86	50	55	.01129	.00373	-.1724	.6422
8	12-09-86	54	55	.00873	.00156	-.1733	.6440
8	12-10-86	55	51	.00955	.00239	-.1722	.6430
8	12-10-86	55	50	.00114	.00331	-.1714	.6389
6	12-11-86	53	46	.00445	.00128	-.1734	.6462
6	12-11-86	53	50	.00464	.00149	-.1741	.6472
4	12-12-86			.01024	.00243	-.1718	.6416
8	12-12-86			.00855	.00183	-.1727	.6427
8	12-17-86	55	57	.00476	.00282	-.1734	.6487
8	12-17-86	55	58	.01054	.00317	-.1720	.6420
8	12-18-86	54	53	.00410	.00350	-.1734	.6488
8	12-18-86	54	53	.00900	.00235	-.1717	.6420
8	12-19-86	54	51	.00670	.00120	-.1720	.6441
8	12-19-86			.00600	.00163	-.1765	.6493
6	12-30-86	48	52	.00312	.00087	-.1753	.6505
6	12-30-86	48	52	.00324	.00093	-.1758	.6502
6	01-05-87	46	42	.00282	.00067	-.1753	.6499
6	01-05-87	46	50	.00377	.00168	-.1753	.6490
6	01-06-87	46	42	.00380	.00116	-.1754	.6506
6	01-06-87	50	55	.00359	.00093	-.1755	.6506
6	01-07-87	46	50	.00378	.00110	-.1752	.6504
6	01-07-87	50	58	.00476	.00142	-.1754	.6486
6	01-08-87	48	45	.00241	.00094	-.1747	.6579
6	01-08-87			.00259	.00078	-.1747	.6478

Table 2

Availability of Prototype Dolos Data

<u>Date</u>	<u>Storm Hour</u>	<u>Prototype Dolos Number and Alpha Character</u>					
		<u>3[E] Ch. 1-3*</u>	<u>5[G] Ch. 1-3</u>	<u>8[D]* Ch. 2&amp;3</u>	<u>9[N] Ch. 1-3</u>	<u>12[P] Ch. 1-3</u>	<u>16[M] Ch. 1-3</u>
11-Jan-88	00	YES	NO	YES	YES	YES	YES
11-Jan-88	01	YES	YES	YES	YES	YES	YES
11-Jan-88	02	NO	YES	NO	NO	YES	YES
11-Jan-88	03	YES	NO	NO	NO	NO	NO
11-Jan-88	04	NO	NO	NO	NO	NO	NO

---

\* Channel 1 = Torque; Channel 2 = Vertical Moment; Channel 3 = Vertical Moment

Table 3

Wave And Water Level Data From Storm of 11 January 1988

Storm Hour	Proto. Wave Gage	H <sub>max</sub> Ft	H <sub>s</sub> Ft	T <sub>s</sub> Sec	H <sub>10</sub> Ft	T <sub>10</sub> Sec	H <sub>avg</sub> Ft	T <sub>avg</sub> Sec	H <sub>mo</sub> 4*(E) <sup>1/2</sup> Ft	Peak Freq Hz	Perk Period Sec	Still Water Level Ft. mllw
<u>As Measured in the Prototype</u>												
0	2	21.85	12.17	9.61	15.98	10.54	7.68	6.96	12.89	0.08	12.04	3.35
1	2	20.54	12.73	9.83	16.24	10.52	7.78	6.93	13.32	0.07	13.43	4.41
2	2	24.34	13.76	11.31	17.72	11.34	8.73	8.22	14.70	0.07	13.76	5.19
3	2	27.25	14.54	11.81	17.52	11.01	8.83	8.44	13.88	0.07	14.50	5.65
4	2	24.44	14.86	10.90	18.64	10.72	9.07	7.99	15.15	0.07	14.50	6.86
0	3	22.47	14.18	10.33	17.59	11.28	8.72	7.77	14.67	0.07	13.88	3.35
1	3	30.34	16.22	11.43	20.70	12.00	9.85	8.17	17.21	0.07	13.65	4.41
2	3	25.25	16.49	11.78	20.44	12.11	10.24	8.66	17.42	0.07	15.31	5.19
3	3	27.41	17.28	10.83	22.38	11.58	10.66	8.15	18.40	0.07	14.89	5.65
4	3	30.42	19.14	11.94	24.61	12.09	11.62	8.68	20.16	0.07	14.62	6.86
<u>As Measured in the Prototype</u>												
0	2	21.97	12.96	10.91	16.19	11.11	8.28	8.73	13.14	0.08	11.91	3.32
1	2	22.02	13.36	11.03	16.83	11.82	8.59	8.86	13.39	0.07	13.37	4.34
2	2	23.35	13.73	11.81	17.98	12.11	8.52	9.47	13.43	0.07	14.82	5.10
3	2	22.77	14.35	11.97	18.29	12.48	8.96	9.36	14.44	0.07	13.57	5.59
4	2	22.89	15.14	11.60	19.25	12.34	9.37	9.14	14.86	0.07	14.56	6.85
0	3	19.95	13.51	10.75	16.92	10.96	8.53	8.80	13.41	0.08	13.15	3.32
1	3	22.25	14.19	11.47	17.40	10.81	9.11	9.14	13.66	0.08	13.15	4.34
2	3	21.97	14.33	11.75	16.77	11.95	9.25	10.06	13.89	0.08	13.15	5.10
3	3	23.46	14.96	12.51	17.83	12.69	9.69	10.09	14.71	0.08	13.15	5.59
4	3	28.18	15.61	11.37	21.02	11.25	9.94	9.47	15.21	0.08	13.15	6.85

\* As measured at tide gage in lee of inner crescent city breakwater.

\*\* As measured at water level gage placed on lee side of model breakwater.

Table 4  
Prototype and Model Surveys  
of Dolosse

<u>Model Dolos Number</u>	<u>Prototype Dolos Number</u>	<u>Dolos Survey Elevation</u> ft. mllw	
		<u>Prototype</u>	<u>Model</u>
April 1987			
7	C1	12.69	10.7
	C2	18.62	16.6
	C3	13.43	12.9
8	E1	20.99	18.6
	E2	13.29	14.9
	E3	11.86	11.75
11	G1	15.98	15.85
	G2	14.30	17.0
	G3	20.39	20.75
9	N1	13.86	13.2
	N2	14.08	13.7
	N3	14.23	14.7
6	P1	13.13	14.35
	P2	11.16	14.3
	P3	11.60	12.3
Jananuary 1987			
5	D1	8.70	6.5
	D2	11.78	
	D3	11.68	8.65
10	M1	8.12	9.3
	M2	8.77	10.4
	M3	15.17	17.0

Table 5

Wave Period And Height and Maximum Principal Stress Data from Model Tests

Model Dolos No.	Test No.	Wave Period $T_{10}$ , sec	Wave Height $H_{10}$ , ft	Maximum Principal Stress $(\sigma_{\max})_m$ , lb/in. <sup>2</sup>	Second Highest Principal Stress $(\sigma_{\max})_m$ , lb/in. <sup>2</sup>
9	67	16.19	10.91	22.033	19.721
10	67	16.19	10.91	16.743	15.534
8	67	16.19	10.91	10.810	10.663
6	67	16.19	10.91	20.281	15.575
11	67	16.19	10.91	5.019	4.399
5	67	16.19	10.91	36.275	30.932
9	79	16.83	11.06	24.333	23.926
11	79	16.83	11.06	8.657	8.646
10	79	16.83	11.06	52.847	35.155
8	79	16.83	11.06	8.593	8.298
5	79	16.83	11.06	36.983	29.122
6	79	16.83	11.06	13.670	11.877
9	62	16.20	11.41	18.677	12.444
6	62	16.20	11.41	7.519	6.304
10	62	16.20	11.41	56.680	36.375
11	62	16.20	11.41	2.300	2.282
5	62	16.20	11.41	23.431	18.954
8	62	16.20	11.41	8.622	7.855
9	71	19.21	11.83	53.218	38.357
6	71	19.21	11.83	55.666	55.625
11	71	19.21	11.83	18.223	13.358
10	71	19.21	11.83	28.897	23.147
8	71	19.21	11.83	27.730	27.276
5	71	19.21	11.83	32.176	22.953
6	71	19.21	11.83	55.666	55.625
9	89	16.40	10.79	10.277	6.898
10	89	16.40	10.79	25.665	23.924
6	89	16.40	10.79	28.210	20.750
5	89	16.40	10.79	28.314	27.162
8	89	16.40	10.79	32.731	26.624
11	89	16.40	10.79	26.926	20.219
9	94	17.25	10.96	8.827	8.306
8	94	17.25	10.96	10.705	10.594
5	94	17.25	10.96	23.621	21.463
10	94	17.25	10.96	37.333	33.973
11	94	72.25	10.96	18.378	15.561
6	94	17.25	10.96	21.352	20.706
10	64	17.56	12.00	69.843	48.318
5	64	17.56	12.00	37.714	30.773
9	64	17.56	12.00	21.921	22.682
11	64	17.56	12.00	16.466	6.169

(Continued)

(Sheet 1 of 4)

Table 5 (Continued)

Model Dolos No.	Test No.	Wave Period $T_{10}$ , sec	Wave Height $H_{10}$ , ft	Maximum Principal Stress $(\sigma_{\max})_m$ , lb/in. <sup>2</sup>	Second Highest Principal Stress $(\sigma_{\max})_m$ , lb/in. <sup>2</sup>
8	64	17.56	12.00	58.508	26.344
6	64	17.56	12.00	22.080	19.296
9	63	16.73	12.14	39.955	26.538
10	63	16.73	12.14	41.282	53.130
11	63	16.73	12.14	7.519	4.046
8	63	16.73	12.14	63.775	54.935
6	63	16.73	12.14	20.842	19.804
5	63	16.73	12.14	31.999	22.817
9	68	16.89	12.18	50.889	36.316
5	68	16.89	12.18	24.144	23.885
10	68	16.89	12.18	34.665	32.226
11	68	16.89	12.18	8.976	6.186
8	68	16.89	12.18	29.505	10.256
6	68	16.89	12.18	24.292	21.260
11	85	18.01	12.21	11.966	11.288
9	85	18.01	12.21	26.238	23.920
6	85	18.01	12.21	33.291	31.522
10	85	18.01	12.21	79.798	60.160
8	85	18.01	12.21	23.100	13.098
5	85	18.01	12.21	42.538	33.615
6	82	18.91	12.22	66.376	28.549
8	82	18.91	12.22	25.076	17.191
10	82	18.91	12.22	53.773	45.351
5	82	18.91	12.22	30.460	26.285
11	82	18.91	12.22	12.874	13.470
9	82	18.91	12.22	28.650	23.372
9	81	18.76	12.26	35.113	31.764
5	81	18.76	12.26	34.624	26.432
8	81	18.76	12.26	27.470	14.797
10	81	18.76	12.26	53.761	48.542
6	81	18.76	12.26	29.794	24.126
11	81	18.76	12.26	11.246	10.309
5	88	20.13	12.36	28.909	27.913
10	88	20.13	12.36	52.983	46.218
11	88	20.13	12.36	12.438	5.266
9	88	20.13	12.36	29.652	29.057
6	88	20.13	12.36	31.834	28.561
8	88	20.13	12.36	36.311	25.383
8	86	18.50	12.58	26.892	16.896
6	86	18.50	12.58	30.785	29.906
5	86	18.50	12.58	35.638	33.828
10	86	18.50	12.58	55.294	45.245
11	86	18.50	12.58	14.024	11.742
9	86	18.50	12.58	40.857	38.204

(Continued)

(Sheet 2 of 4)

Table 5 (Continued)

Model Dolos No.	Test No.	Wave Period $T_{10}$ , sec	Wave Height $H_{10}$ , ft	Maximum Principal Stress $(\sigma_{\max})_m$ , lb/in. <sup>2</sup>	Second Highest Principal Stress $(\sigma_{\max})_m$ , lb/in. <sup>2</sup>
10	65	18.11	12.59	55.737	39.513
9	65	18.11	12.59	29.487	29.900
11	65	18.11	12.59	19.467	19.049
8	65	18.11	12.59	46.147	43.906
5	65	18.11	12.59	26.698	26.326
6	65	18.11	12.59	36.063	29.794
6	66	19.61	12.66	45.410	38.929
5	66	19.61	12.66	29.416	33.539
10	66	19.61	12.66	65.638	49.479
8	66	19.61	12.66	102.539	83.655
9	66	19.61	12.66	24.292	22.617
11	66	19.61	12.66	33.875	20.906
9	87	18.92	12.74	45.027	35.290
5	87	18.92	12.74	27.977	24.899
11	87	18.92	12.74	13.700	7.307
10	87	18.92	12.74	68.882	44.585
8	87	18.92	12.74	35.621	21.962
6	87	18.92	12.74	33.073	31.994
6	80	17.28	12.92	26.261	15.911
9	80	17.28	12.92	20.240	20.193
10	80	17.28	12.92	71.843	47.268
11	80	17.28	12.92	11.022	10.757
8	80	17.28	12.92	14.484	13.346
5	80	17.28	12.92	41.076	39.631
6	91	17.97	12.16	40.956	29.423
10	91	17.97	12.16	40.298	22.805
5	91	17.97	12.16	46.723	46.431
9	91	17.97	12.16	22.246	18.418
8	91	17.97	12.16	28.159	23.963
11	91	17.97	12.16	46.354	35.622
5	95	17.59	12.21	27.959	24.633
10	95	17.59	12.21	32.809	31.556
6	95	17.59	12.21	29.753	26.732
9	95	17.59	12.21	17.568	15.519
8	95	17.59	12.21	30.945	11.090
11	95	17.59	12.21	36.103	26.617
5	98	18.40	12.25	21.922	19.785
10	98	18.40	12.25	32.051	30.845
6	98	18.40	12.25	28.566	24.884
9	98	18.40	12.25	24.547	16.509
8	98	18.40	12.25	41.830	20.224
11	98	18.40	12.25	37.034	24.953
5	96	18.84	12.25	26.715	26.663
9	96	18.84	12.25	26.498	21.253

(Continued)

(Sheet 3 of 4)

Table 5 (Concluded)

Model Dolos No.	Test No.	Wave Period $T_{10}$ , sec	Wave Height $H_{10}$ , ft	Maximum Principal Stress $(\sigma_{\max})_m$ , lb/in. <sup>2</sup>	Second Highest Principal Stress $(\sigma_{\max})_m$ , lb/in. <sup>2</sup>
6	96	18.84	12.25	48.918	23.399
10	96	18.84	12.25	44.751	25.648
11	96	18.84	12.25	32.654	26.206
8	96	18.84	12.25	42.050	41.485
9	93	18.81	12.28	28.785	27.637
6	93	18.81	12.28	10.725	10.606
5	93	18.81	12.28	31.597	28.826
10	93	18.81	12.28	43.842	39.149
11	93	18.81	12.28	27.448	24.815
8	93	18.81	12.28	38.006	35.079
6	99	19.02	12.30	32.657	27.641
10	99	19.02	12.30	56.496	40.771
5	99	19.02	12.30	22.764	11.975
9	99	19.02	12.30	33.264	28.100
8	99	19.02	12.30	58.969	36.038
11	99	19.02	12.30	30.926	30.840
5	97	17.86	12.45	26.503	21.783
10	97	17.86	12.45	31.658	30.828
6	97	17.86	12.45	42.637	24.355
9	97	17.86	12.45	23.975	18.395
8	97	17.86	12.45	45.349	33.115
11	97	17.86	12.45	24.022	23.736
10	92	18.28	12.61	39.467	28.018
5	92	18.28	12.61	30.649	24.859
9	92	18.28	12.61	21.850	19.167
11	92	18.28	12.61	48.914	25.372
6	92	18.28	12.61	17.877	17.698
8	92	18.28	12.61	69.810	49.009
6	90	16.58	12.68	26.640	25.242
9	90	16.58	12.68	24.292	14.578
8	90	16.58	12.68	37.180	34.177
11	90	16.58	12.68	36.111	30.534
5	90	16.58	12.68	33.509	31.048
10	90	16.58	12.68	46.460	33.426

APPENDIX A: NOTATION

APPENDIX A: NOTATION

A	Area, ft <sup>2</sup>
EP(x)	Exceedance probability
H	Wave height, ft
H <sub>avg</sub>	Average wave height, ft
(H <sub>m</sub> ) <sub>z</sub>	Horizontal moment, ft-lb
H <sub>max</sub>	Maximum wave height, ft
H <sub>mo</sub>	Zeroth moment wave height equal to $4(E)^{\frac{1}{2}}$ , where E equals the area under the curve in the spectral energy density versus frequency plot, ft
H <sub>s</sub>	Significant wave height (average of the highest 1/3 of the waves), ft
H <sub>10</sub>	Average of the highest 10 percent of the waves in a wave train, ft
F	Force, lb
I	Moment of inertia, ft <sup>4</sup>
J	Polar moment of inertia, ft <sup>4</sup>
L	Length, linear scale, ft
mllw	Mean lower low water
p(x)	Probability density
P(x)	Cumulative probability
r	Distance from center to where two sides of octagon join, ft
r <sub>1</sub>	Length of line that joins center and side of octagon and is perpendicular to the side, ft
r <sub>2</sub>	Radius of a circle which has same moment of inertia as the octagon defined by the cross section of a dolos shank, ft
S	Specific gravity
sta	Station, survey location where observations are taken
T	Wave period, time, sec
T <sub>avg</sub>	Wave period associated with H <sub>avg</sub> , sec
T <sub>p</sub>	Wave period associated with peak spectral energy density, sec
T <sub>q</sub>	Torque, ft-lb
T <sub>s</sub>	Wave period associated with H <sub>s</sub> , sec
T <sub>10</sub>	Wave period associated with H <sub>10</sub> , sec
t <sub>1</sub>	Data acquisition time-step
V	Volume, ft <sup>3</sup>

$(V_m)_y$	Vertical moment, ft-lb
W	Weight, lb
y	Distance measured along y axis, feet
z	Distance measured along z axis, feet
$\alpha$	One half of the angle subtended by one side of an octagon, 22.5 deg
$\beta$	Angle defined by two adjoining vectors
$\gamma$	Specific weight, pcf
$\theta$	Angle measured counterclockwise from the y axis, degrees
$\sigma$	Principal stress, lb/in <sup>2</sup>
$\sigma_x$	Normal stress, lb/in <sup>2</sup>
$\sigma_{max}$	Maximum principal stress, lb/in <sup>2</sup>
$(\sigma_x)_{max}$	Maximum normal stress, lb/in <sup>2</sup>
$(\sigma_{max})_m$	Maximum value in a maximum principal stress time series, lb/in <sup>2</sup>
$(\sigma_{max})_{m2}$	Second highest value in a maximum principal stress time series, lb/in <sup>2</sup>
$\tau$	Shear stress, lb/in <sup>2</sup>

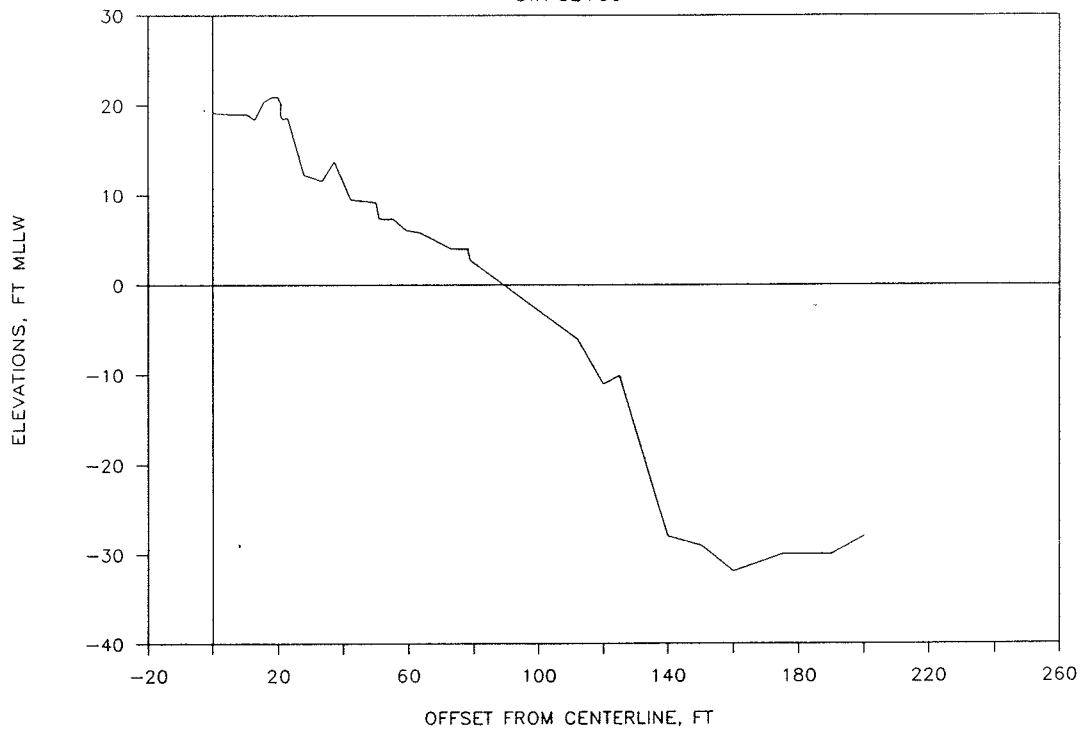
#### Subscripts

a	Refers to armor units of stones
r	Refers to ratio of model quantities to prototype quantities (i.e., $r=m/p$ )
w	Refers to water

APPENDIX B: PROTOTYPE BREAKWATER AND BATHYMETRY DATA

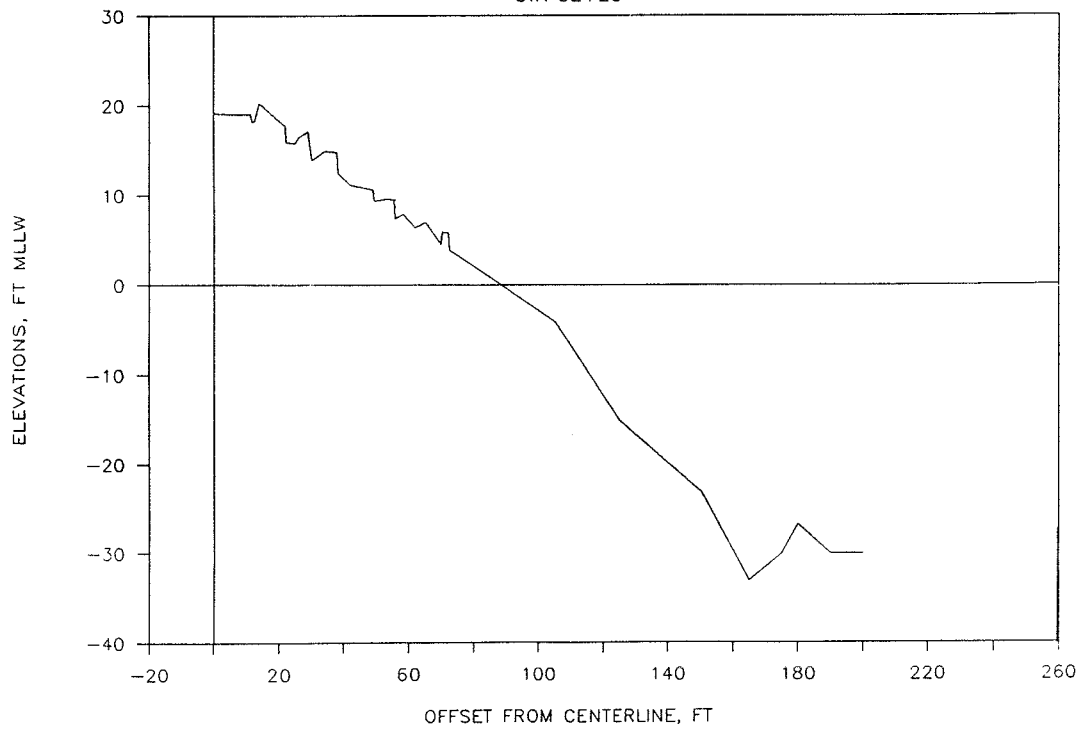
# BREAKWATER X-SECTIONS : CRESCENT CITY

STA 32+00



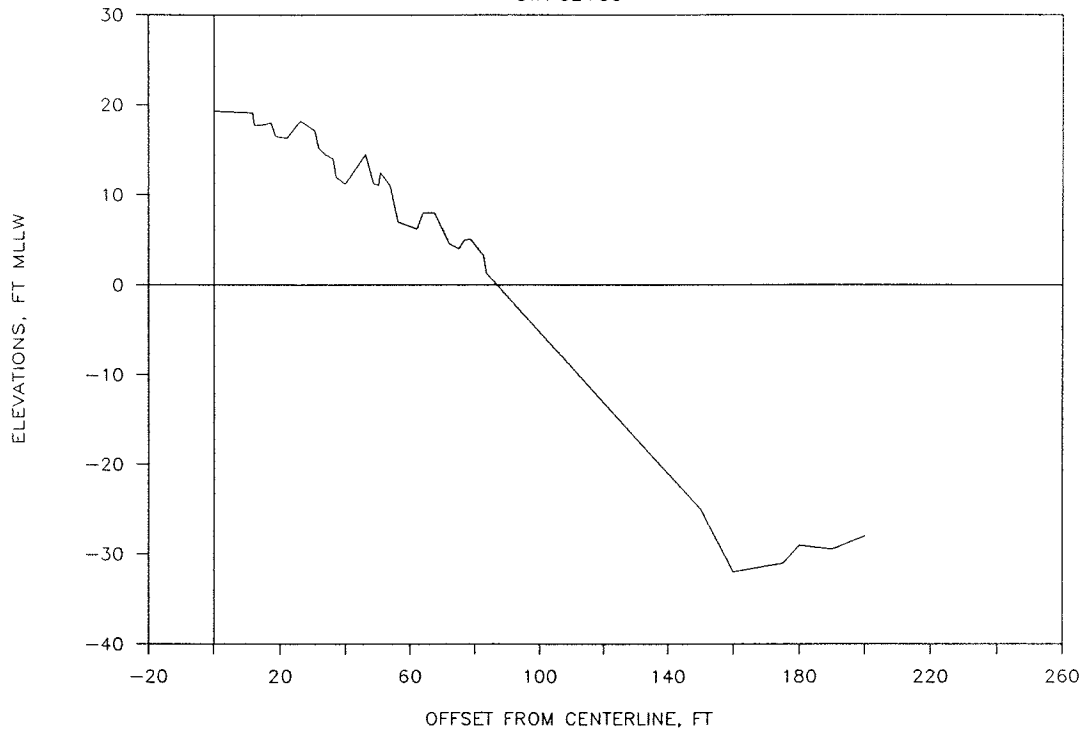
# BREAKWATER X-SECTIONS : CRESCENT CITY

STA 32+25



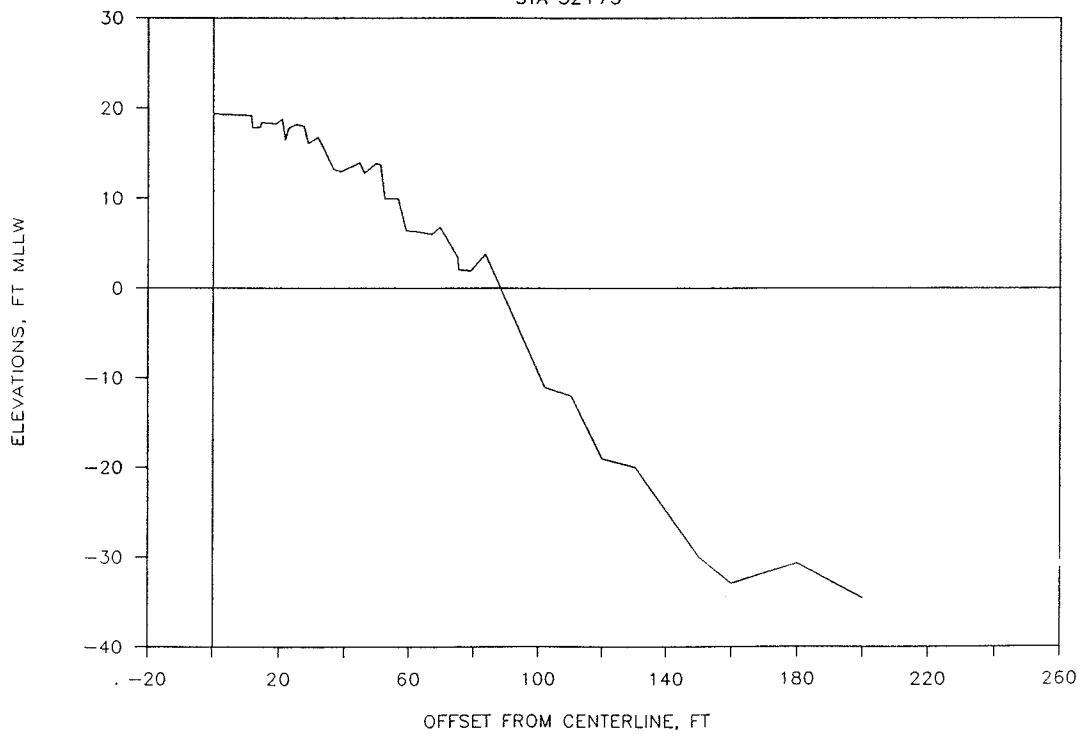
# BREAKWATER X-SECTIONS : CRESCENT CITY

STA 32+50



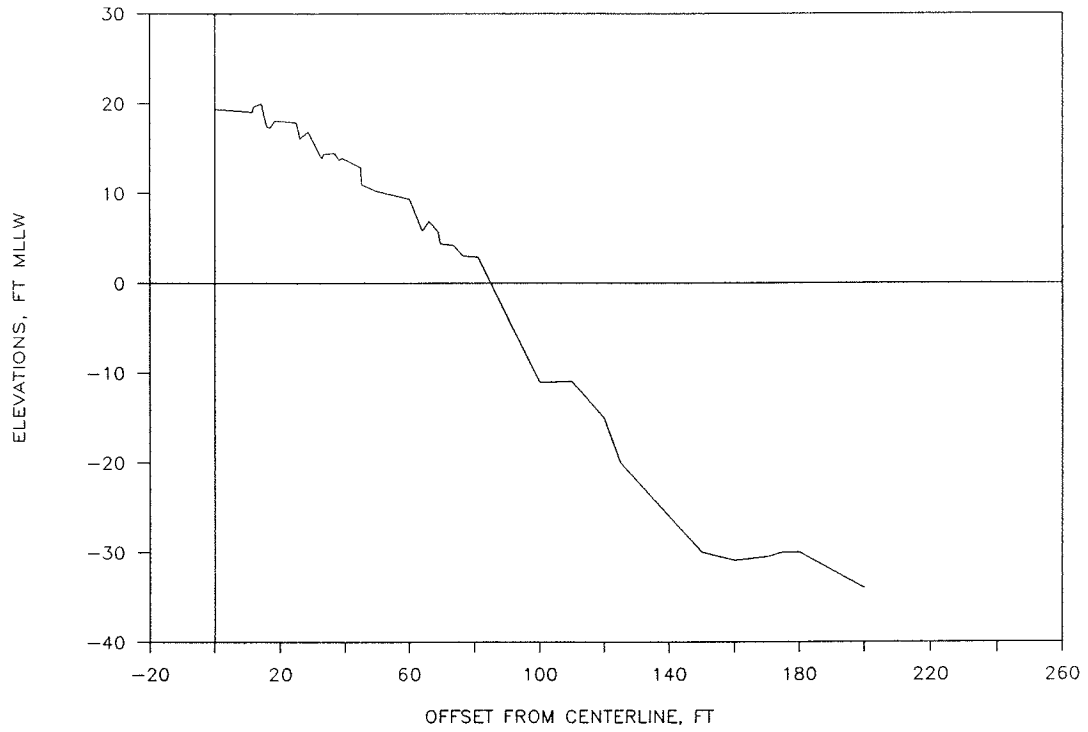
# BREAKWATER X-SECTIONS : CRESCENT CITY

STA 32+75



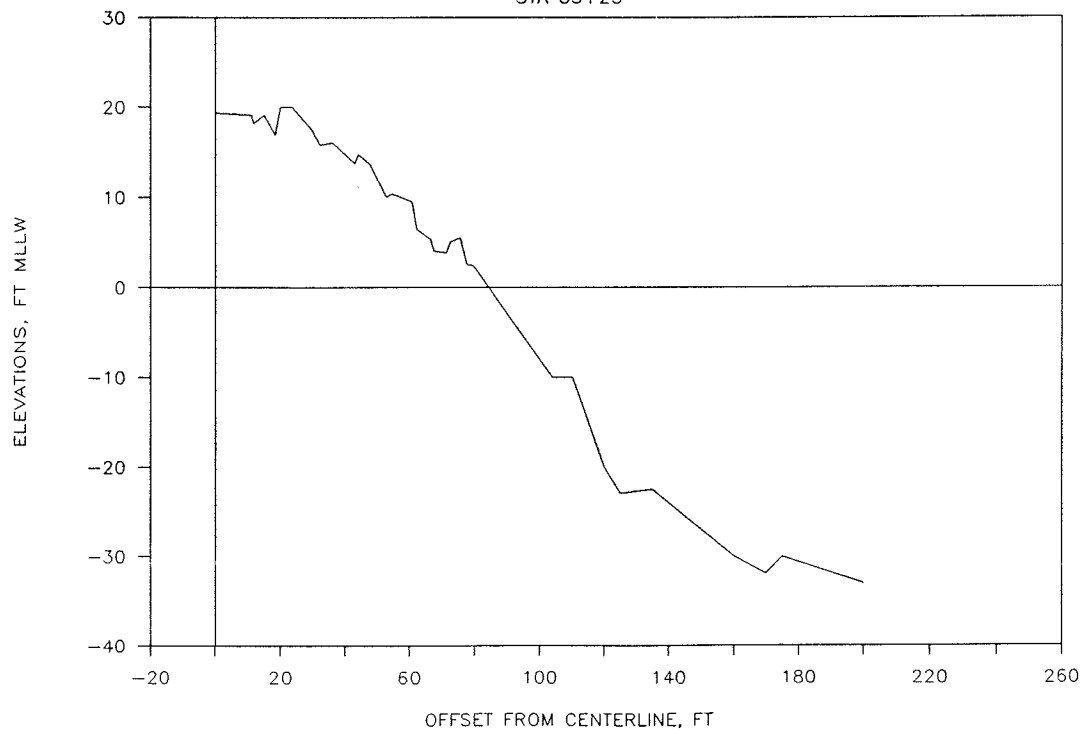
# BREAKWATER X-SECTIONS : CRESCENT CITY

STA 33+00



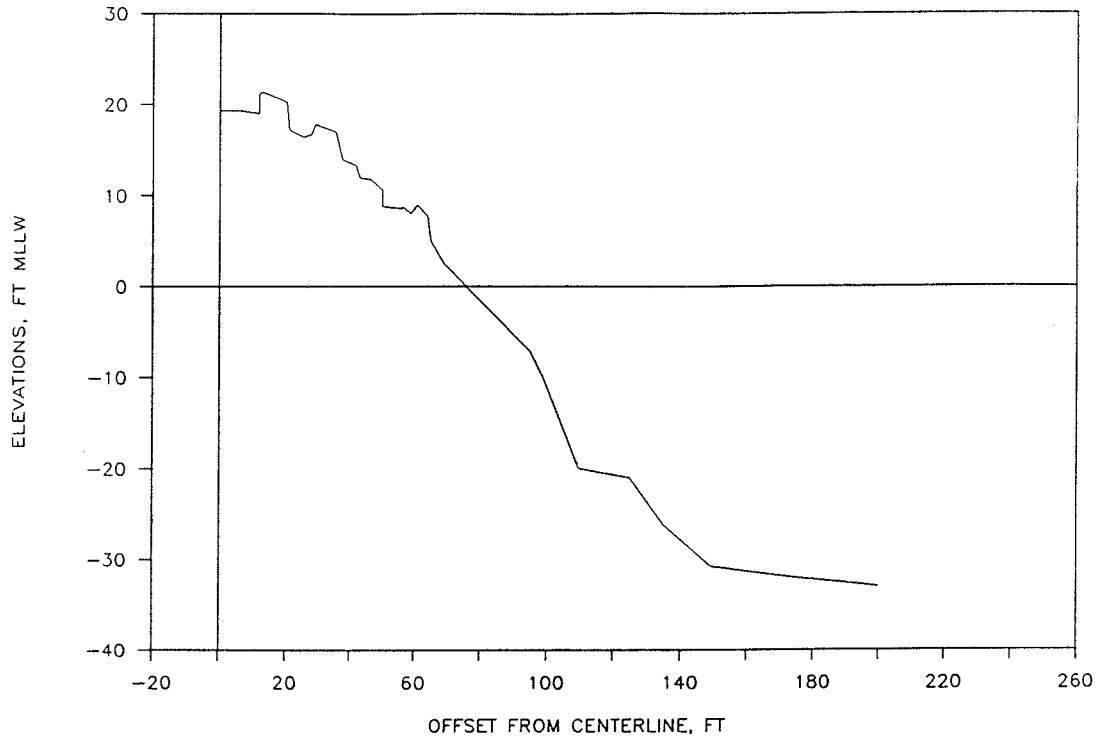
# BREAKWATER X-SECTIONS : CRESCENT CITY

STA 33+25



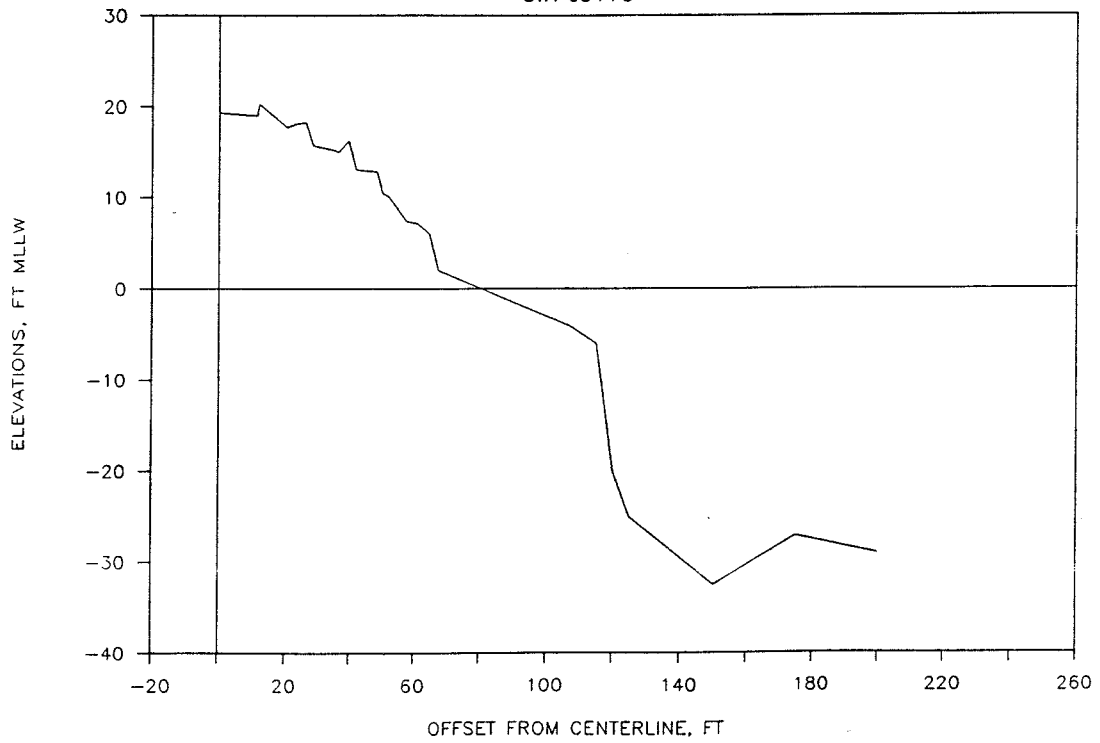
# BREAKWATER X-SECTIONS : CRESCENT CITY

STA 33+50



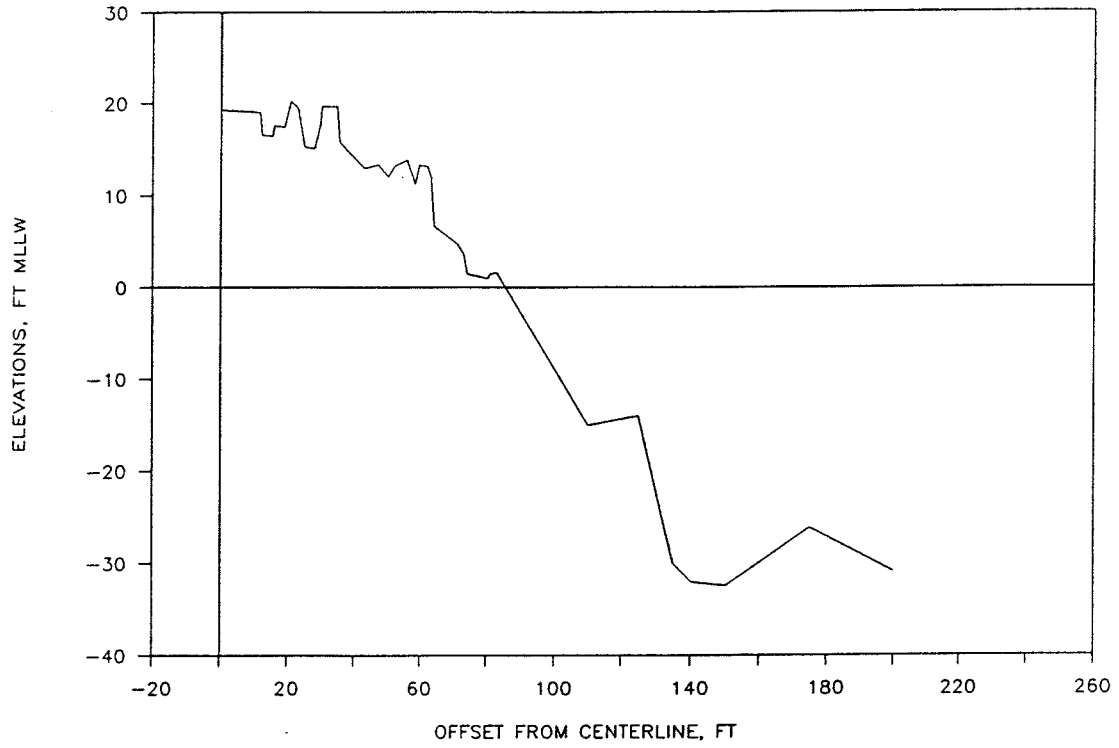
# BREAKWATER X-SECTIONS : CRESCENT CITY

STA 33+75



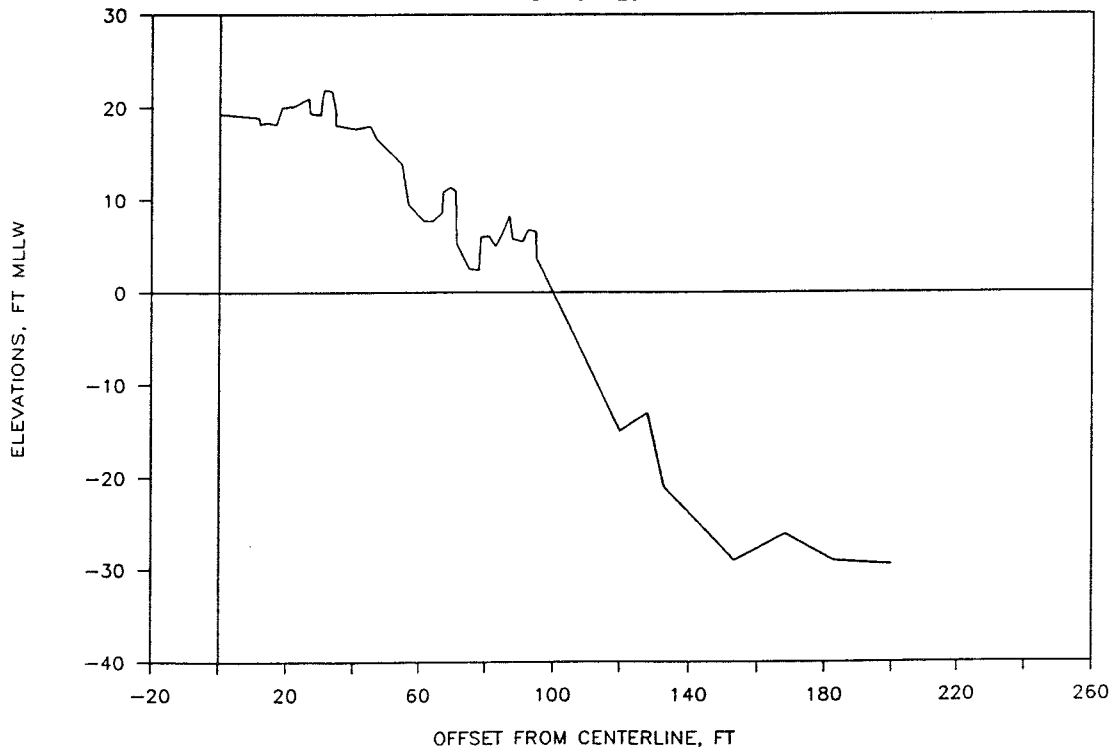
# BREAKWATER X-SECTIONS : CRESCENT CITY

STA 34+00



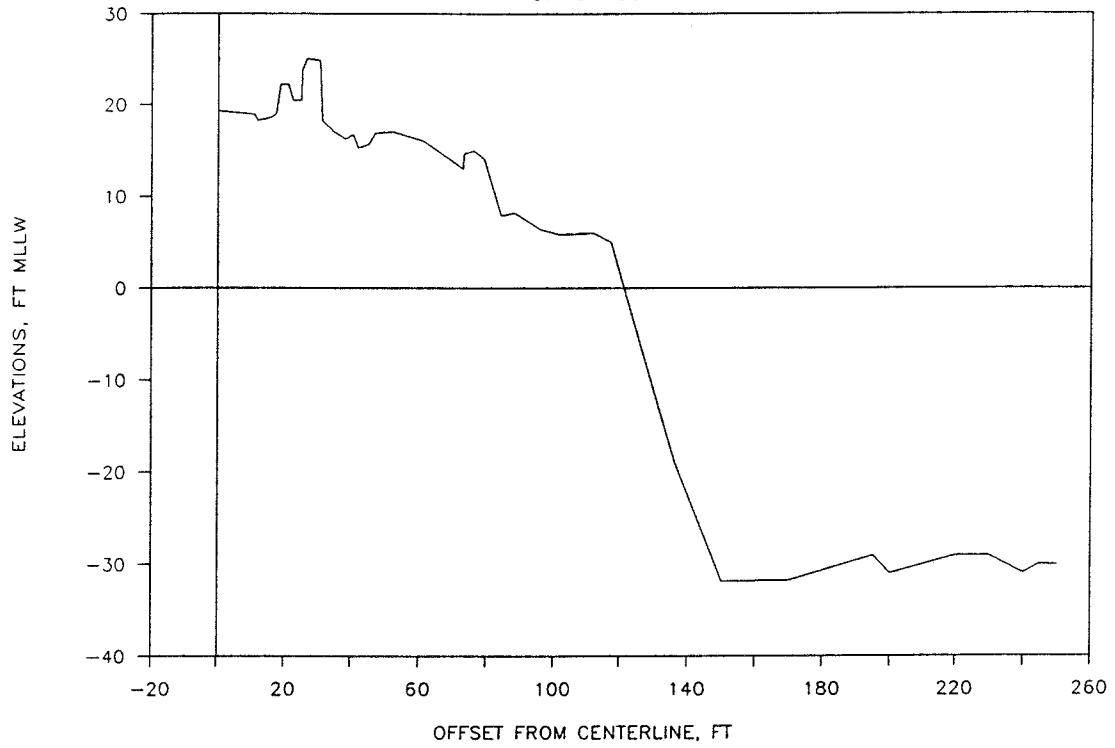
# BREAKWATER X-SECTIONS : CRESCENT CITY

STA 34+25



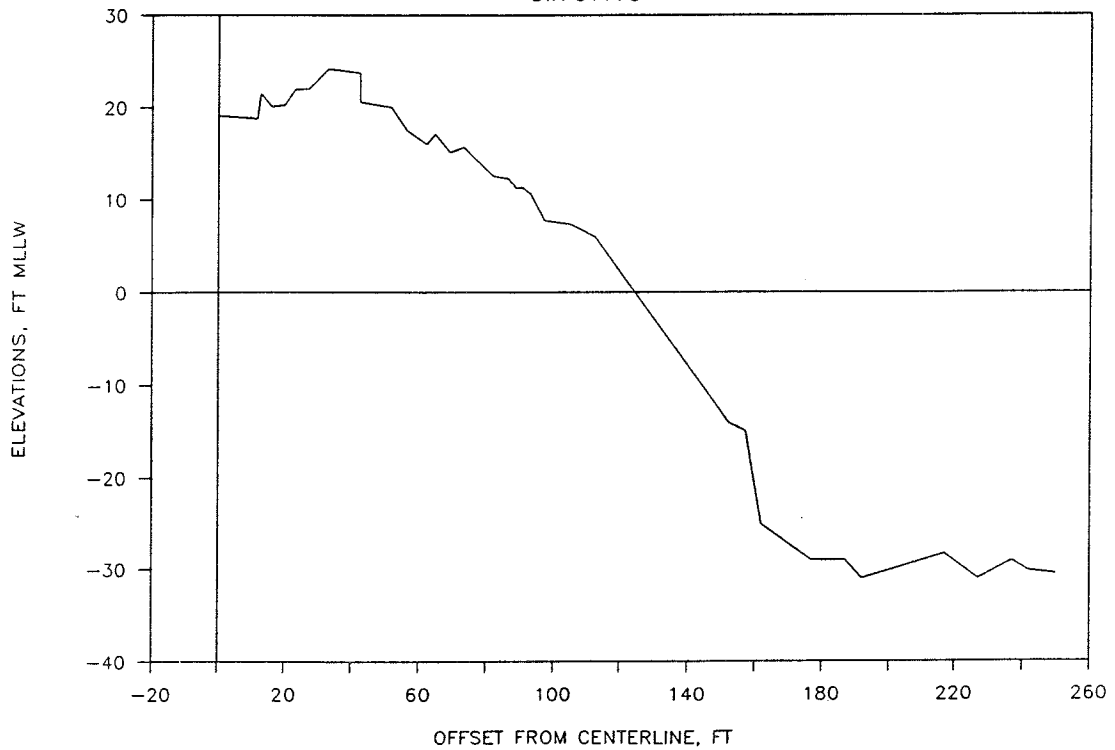
# BREAKWATER X-SECTIONS : CRESCENT CITY

STA 34+50



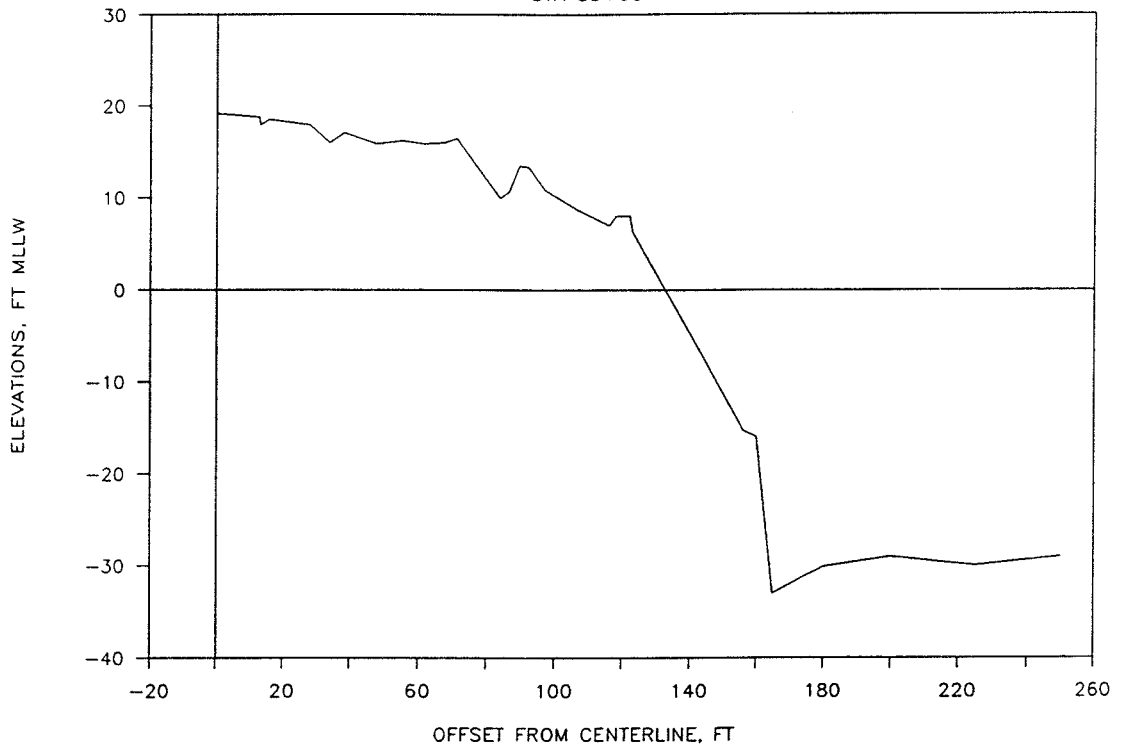
# BREAKWATER X-SECTIONS : CRESCENT CITY

STA 34+75



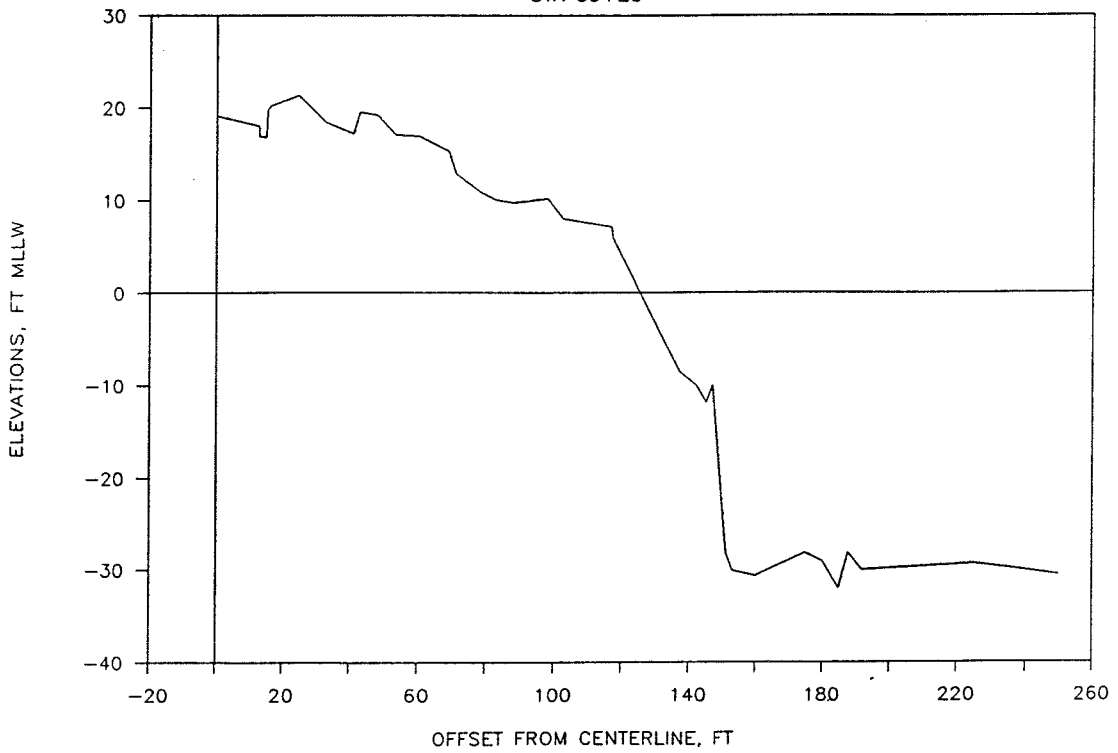
# BREAKWATER X-SECTIONS : CRESCENT CITY

STA 35+00



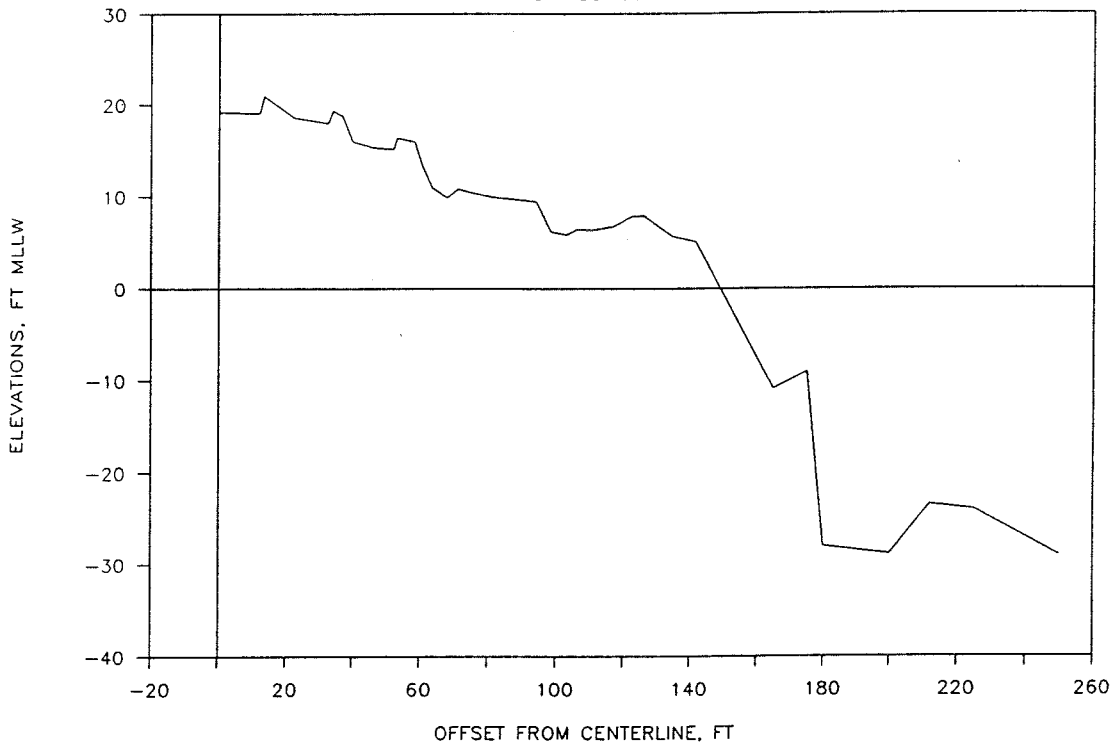
# BREAKWATER X-SECTIONS : CRESCENT CITY

STA 35+25



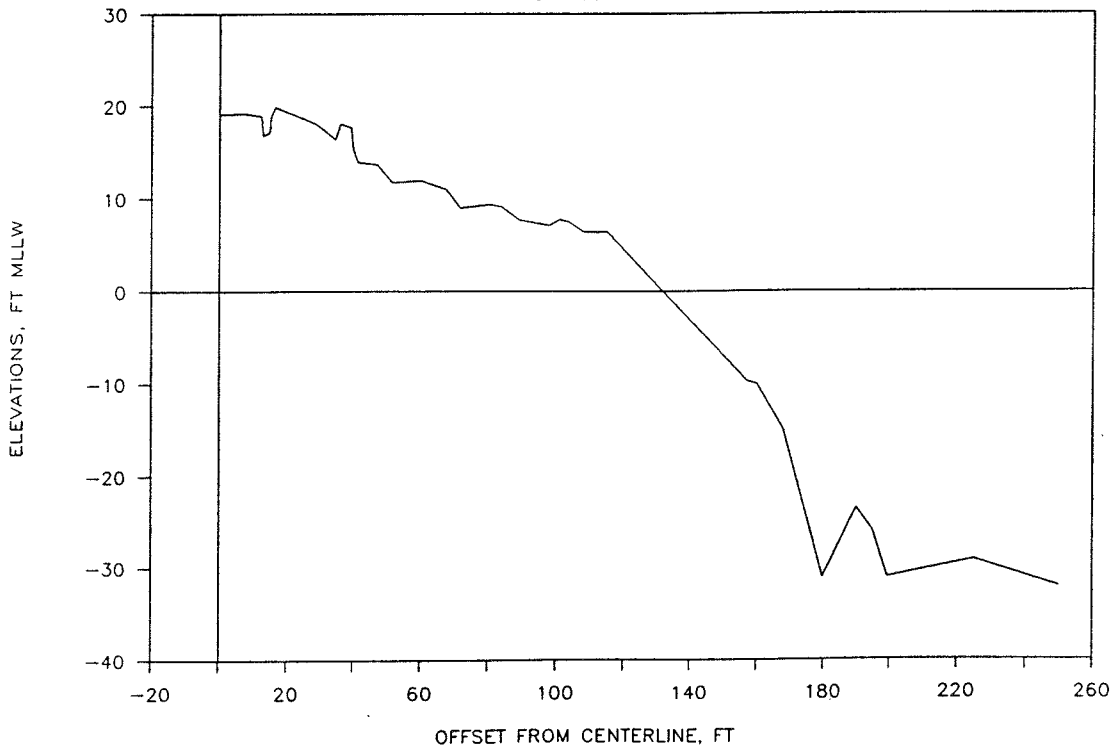
# BREAKWATER X-SECTIONS : CRESCENT CITY

STA 35+50



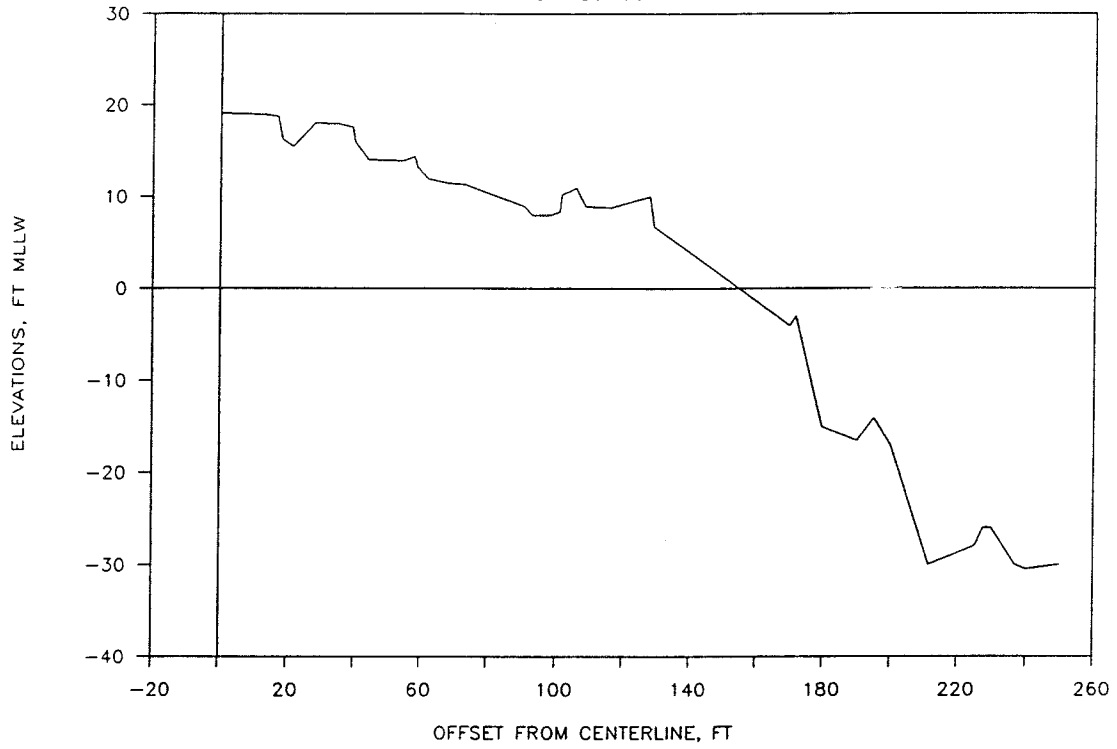
# BREAKWATER X-SECTIONS : CRESCENT CITY

STA 35+75



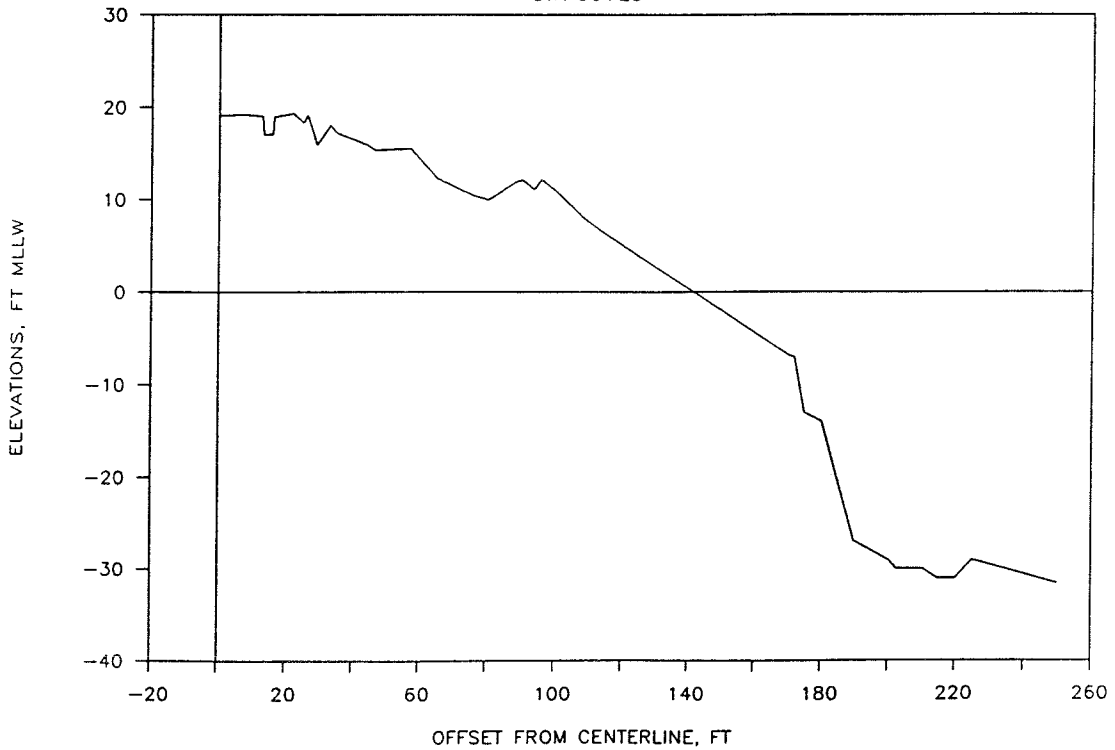
# BREAKWATER X-SECTIONS : CRESCENT CITY

STA 36+00



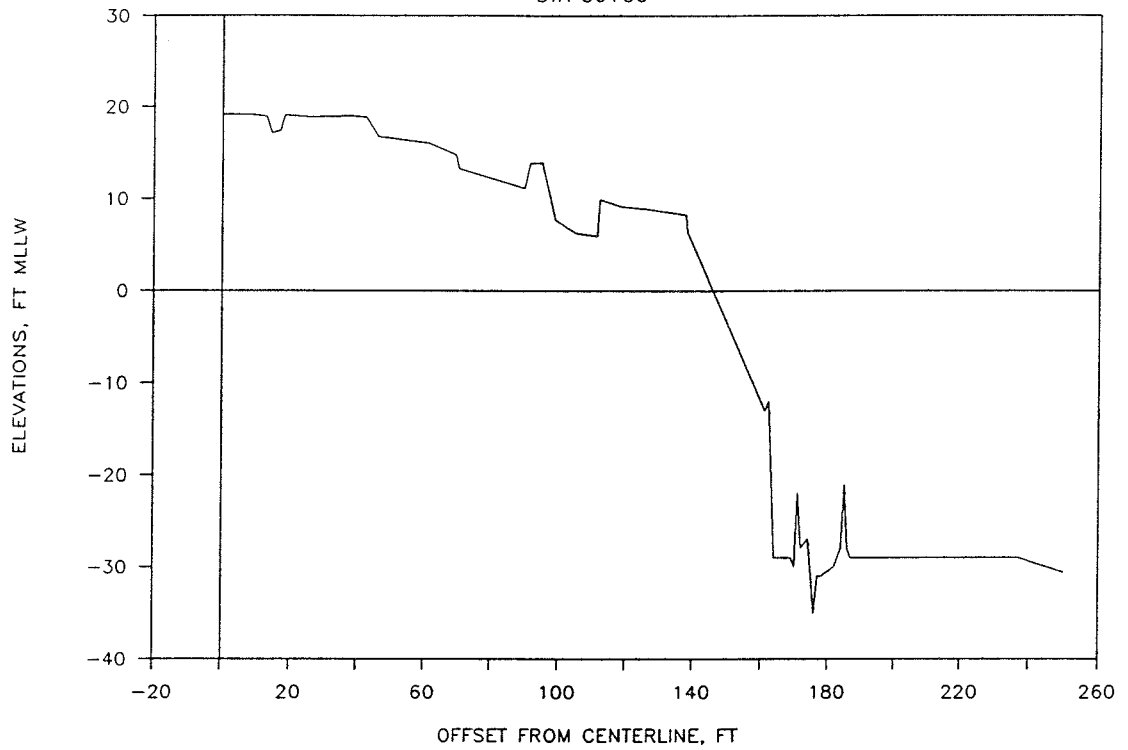
# BREAKWATER X-SECTIONS : CRESCENT CITY

STA 36+25



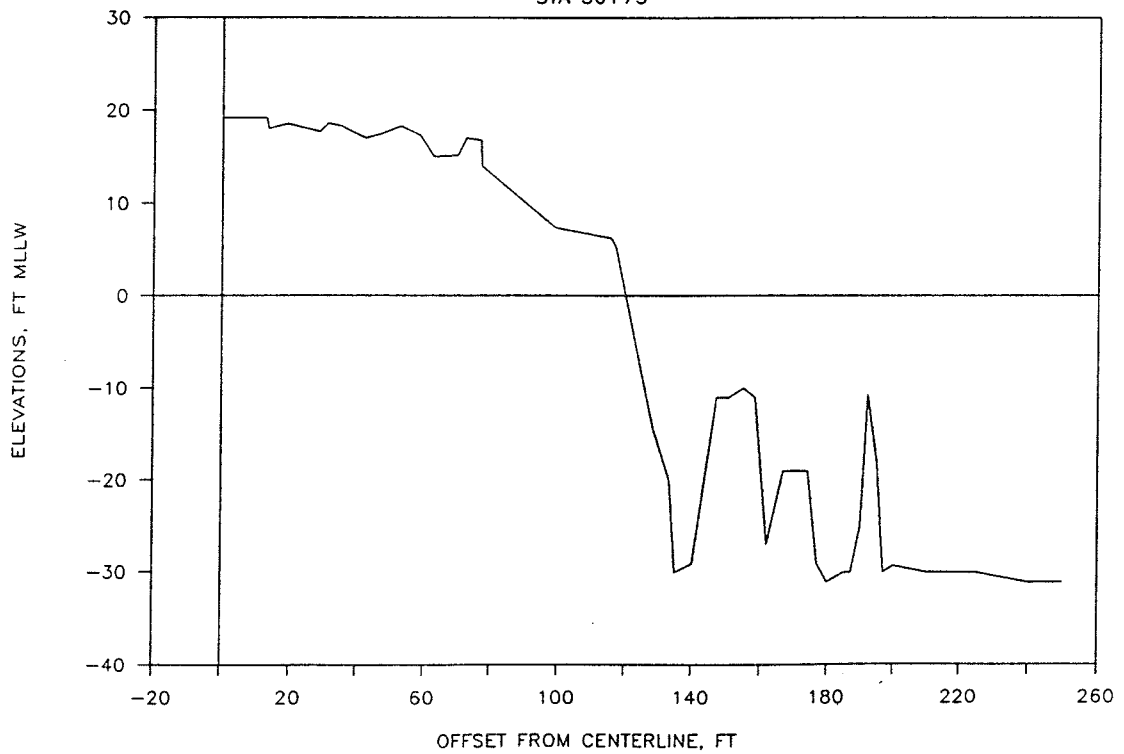
# BREAKWATER X-SECTIONS : CRESCENT CITY

STA 36+50

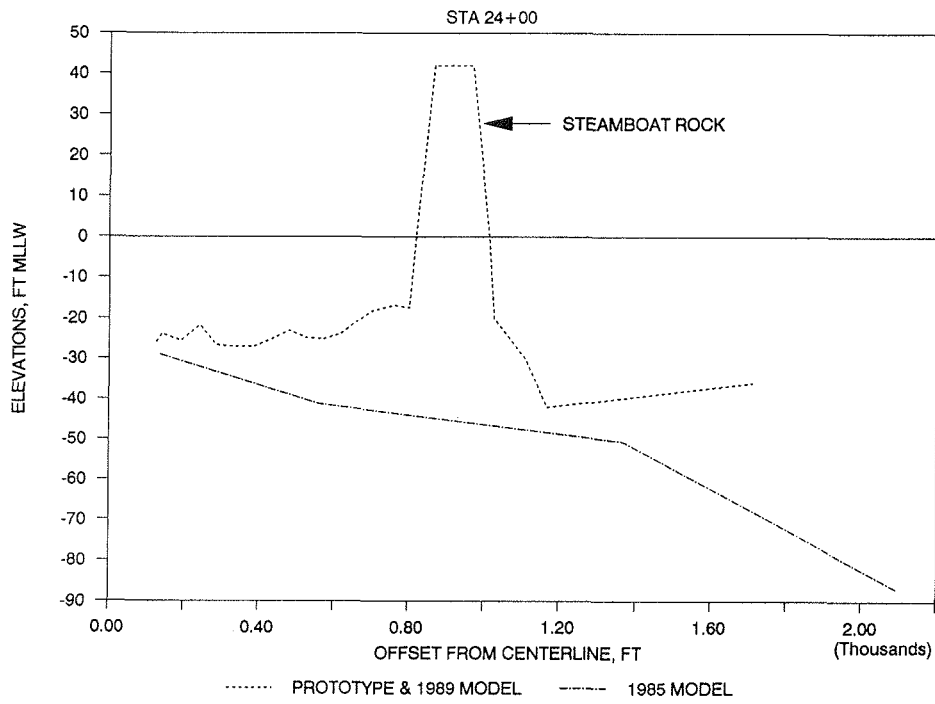


# BREAKWATER X-SECTIONS : CRESCENT CITY

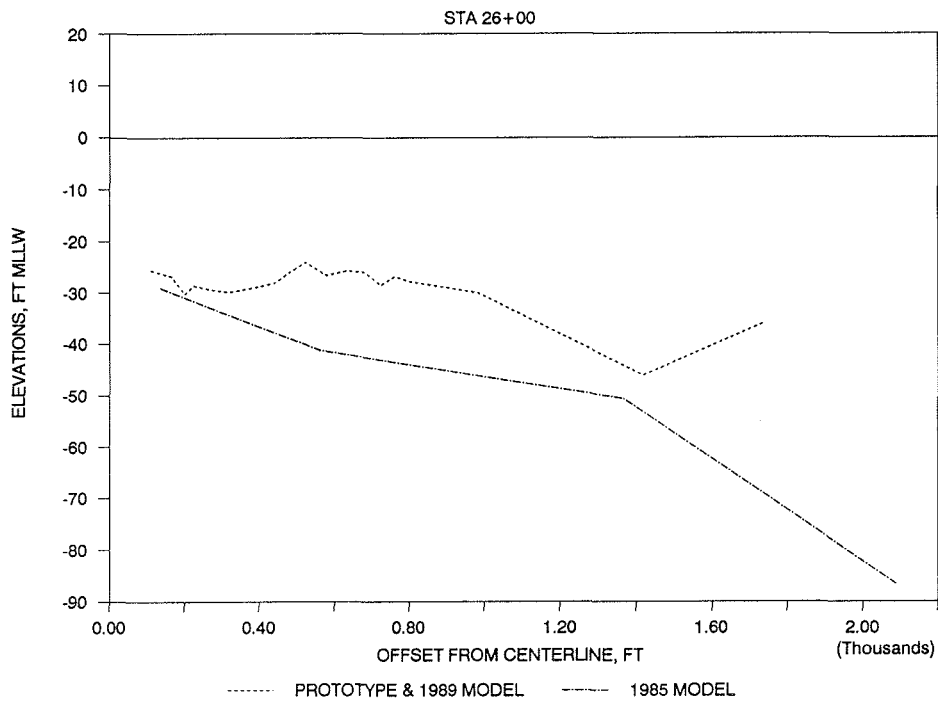
STA 36+75



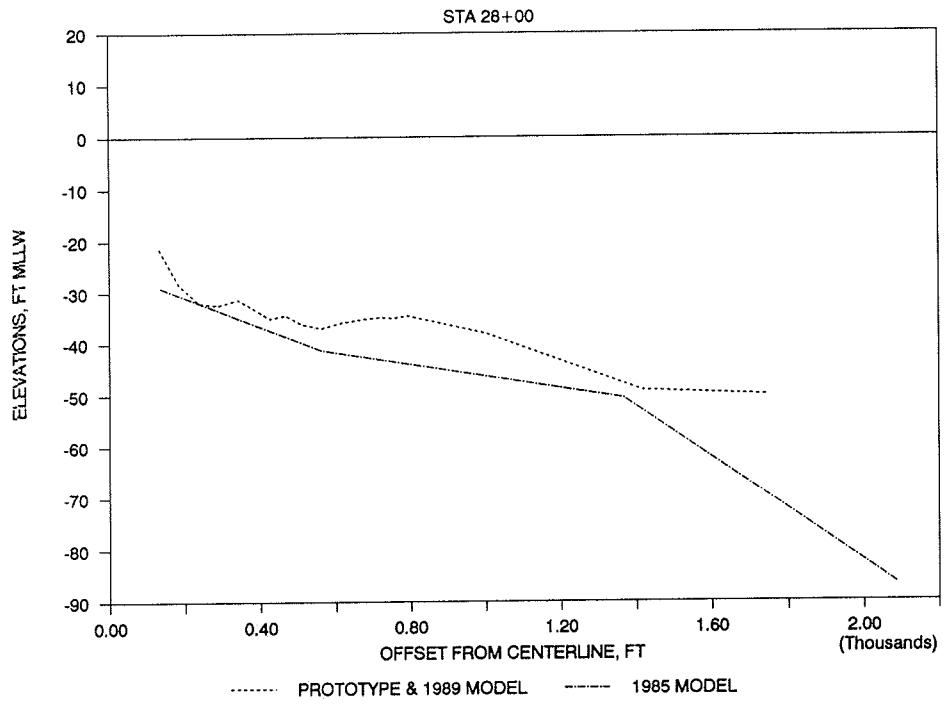
### MODEL AND PROTOTYPE BATHYMETRIES



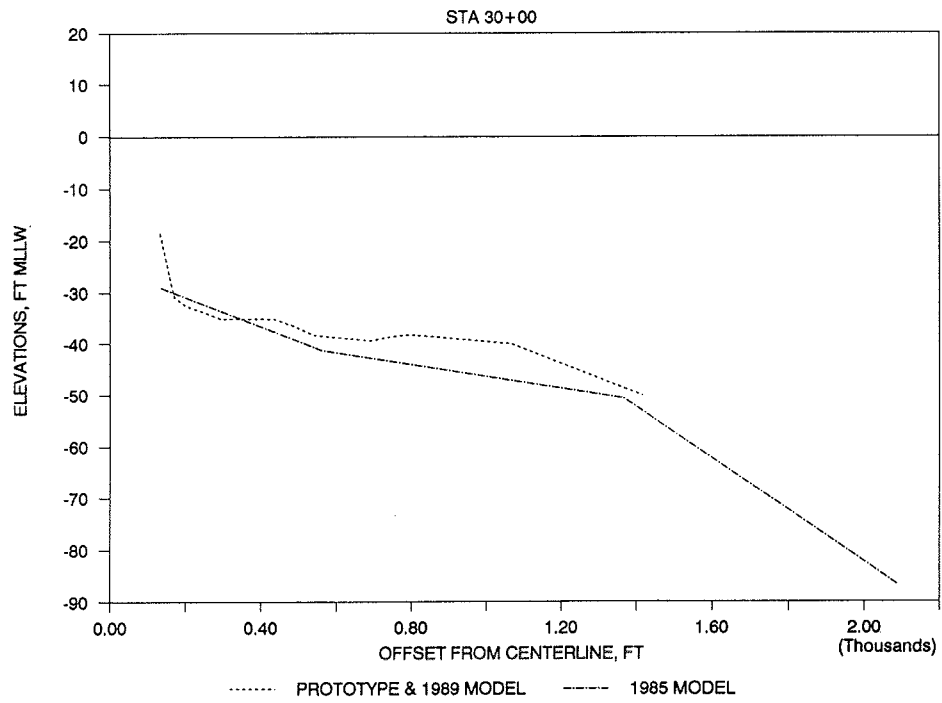
### MODEL AND PROTOTYPE BATHYMETRIES



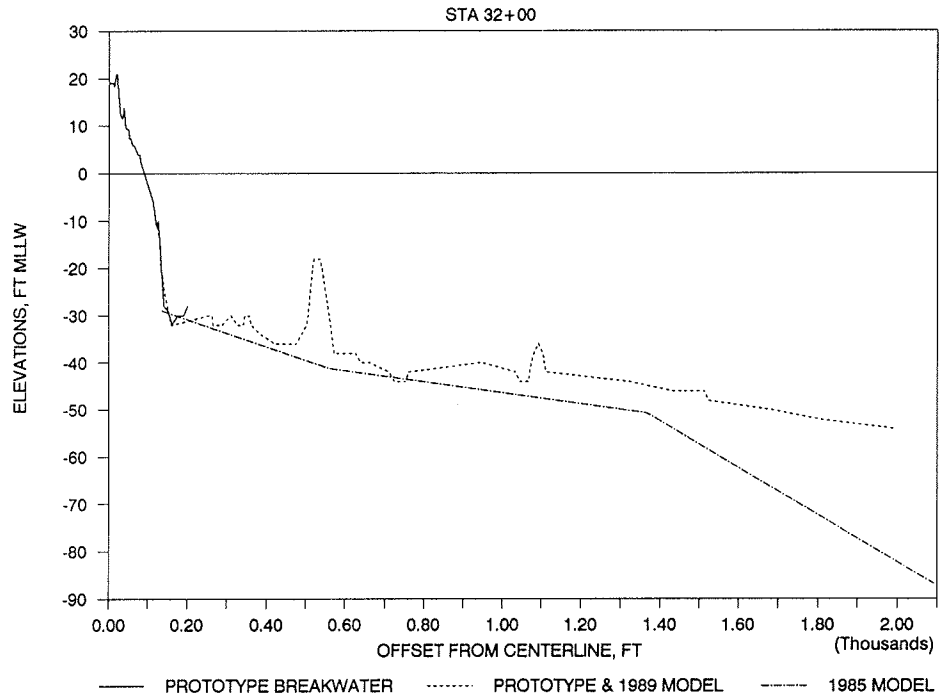
# MODEL AND PROTOTYPE BATHYMETRIES



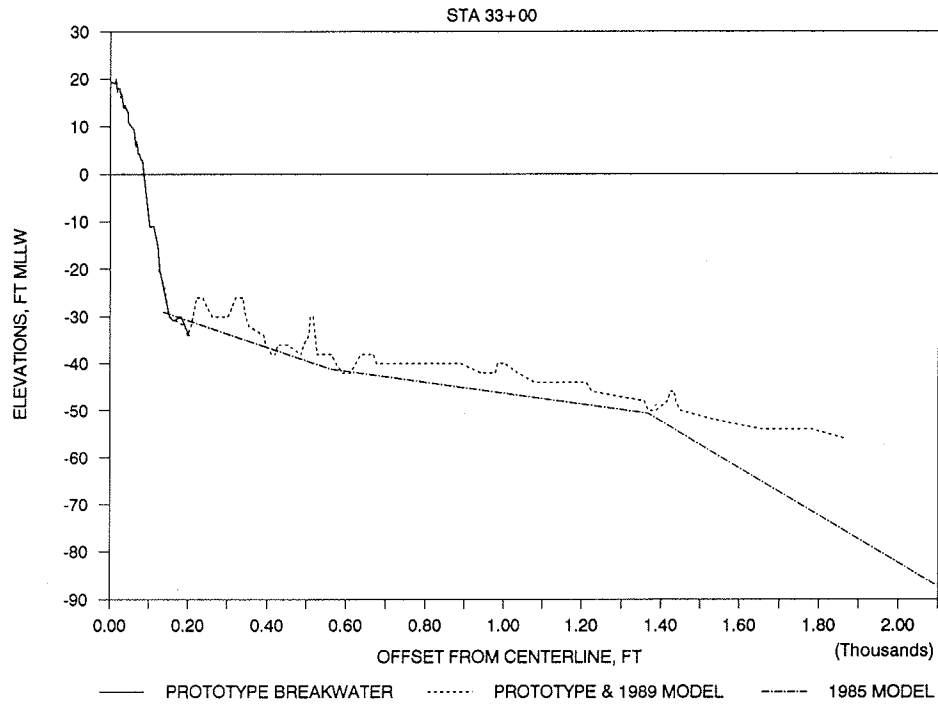
# MODEL AND PROTOTYPE BATHYMETRIES



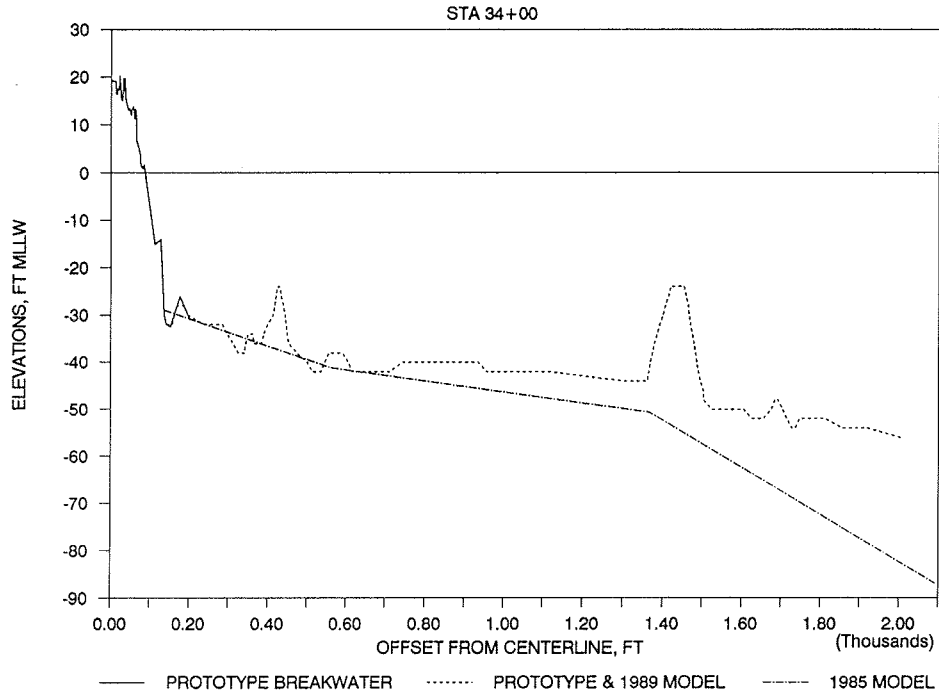
## BREAKWATER CROSS SECTION & BATHYMETRIES



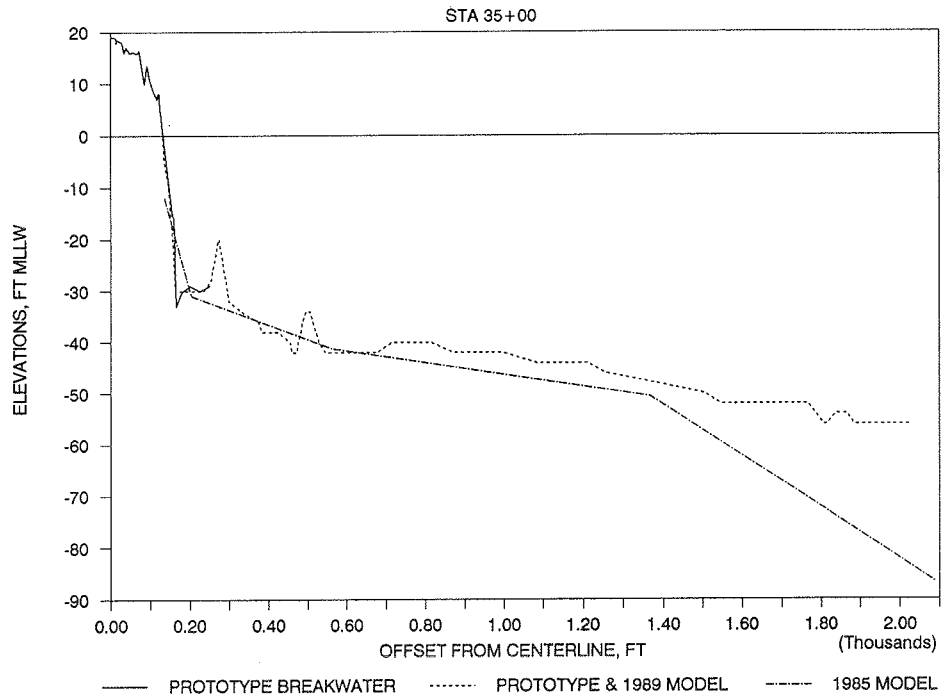
## BREAKWATER CROSS SECTION & BATHYMETRIES



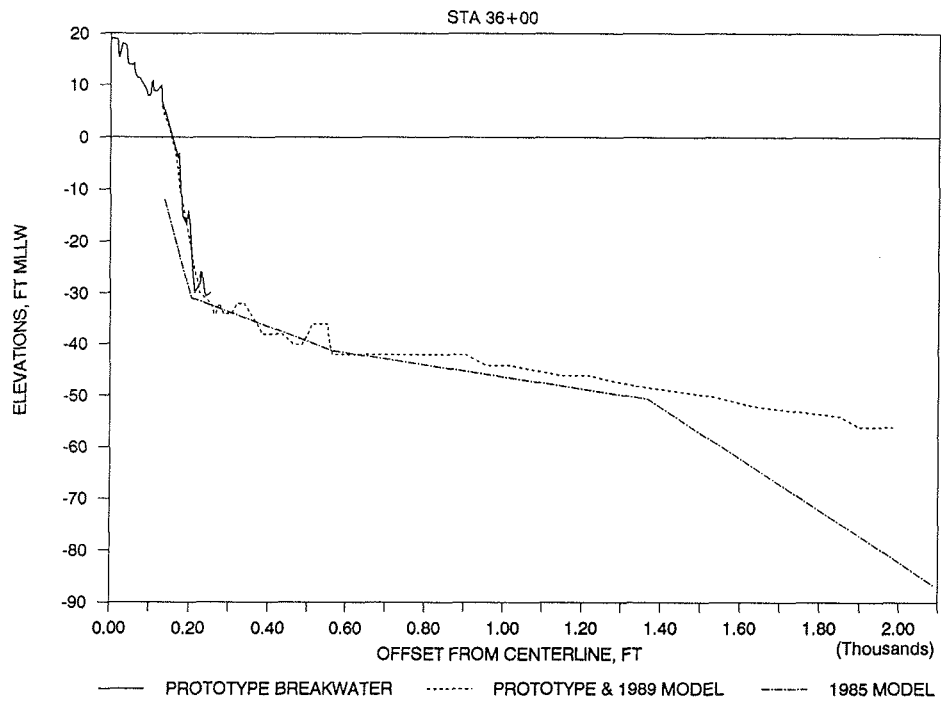
## BREAKWATER CROSS SECTION & BATHYMETRIES



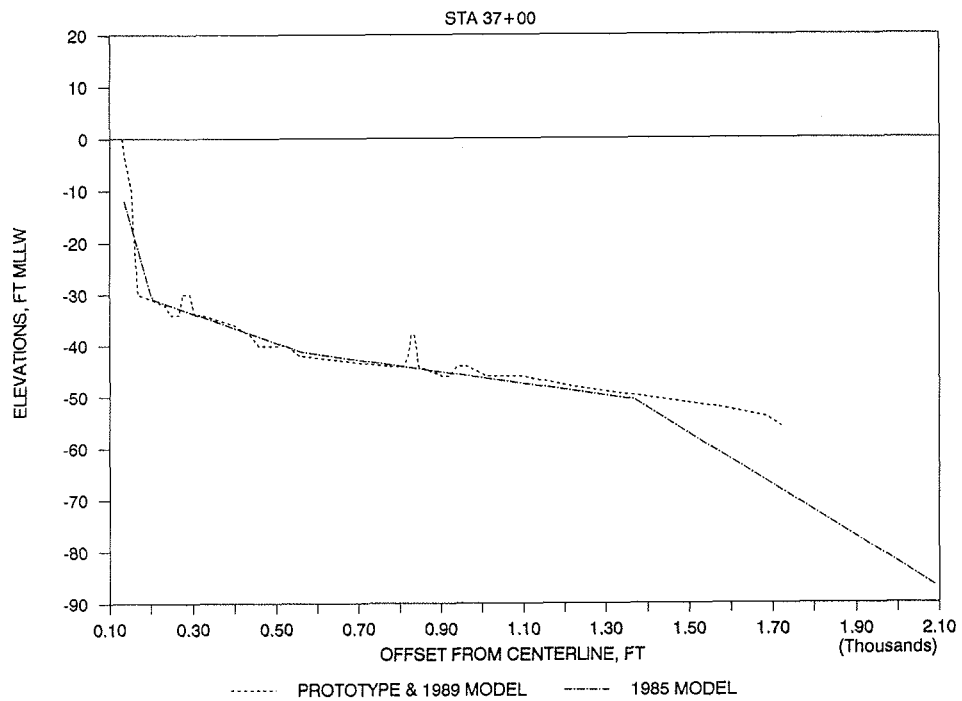
## BREAKWATER CROSS SECTION & BATHYMETRIES



## BREAKWATER CROSS SECTION & BATHYMETRIES



## MODEL AND PROTOTYPE BATHYMETRIES



APPENDIX C: ADACS

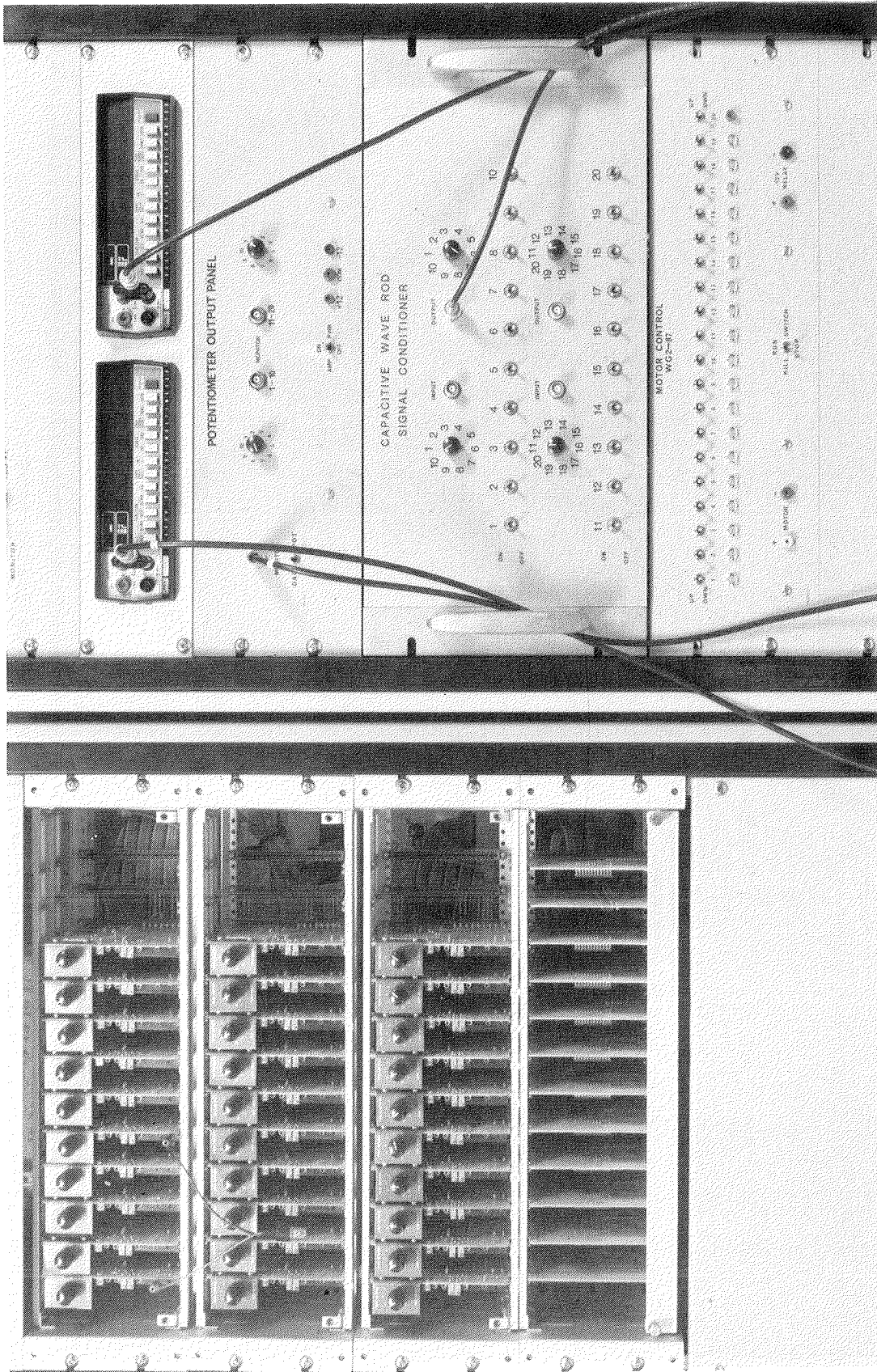


Figure C1. Dolos load cell amplifier panel (left) and wave gage amplifier and controller panels (right)

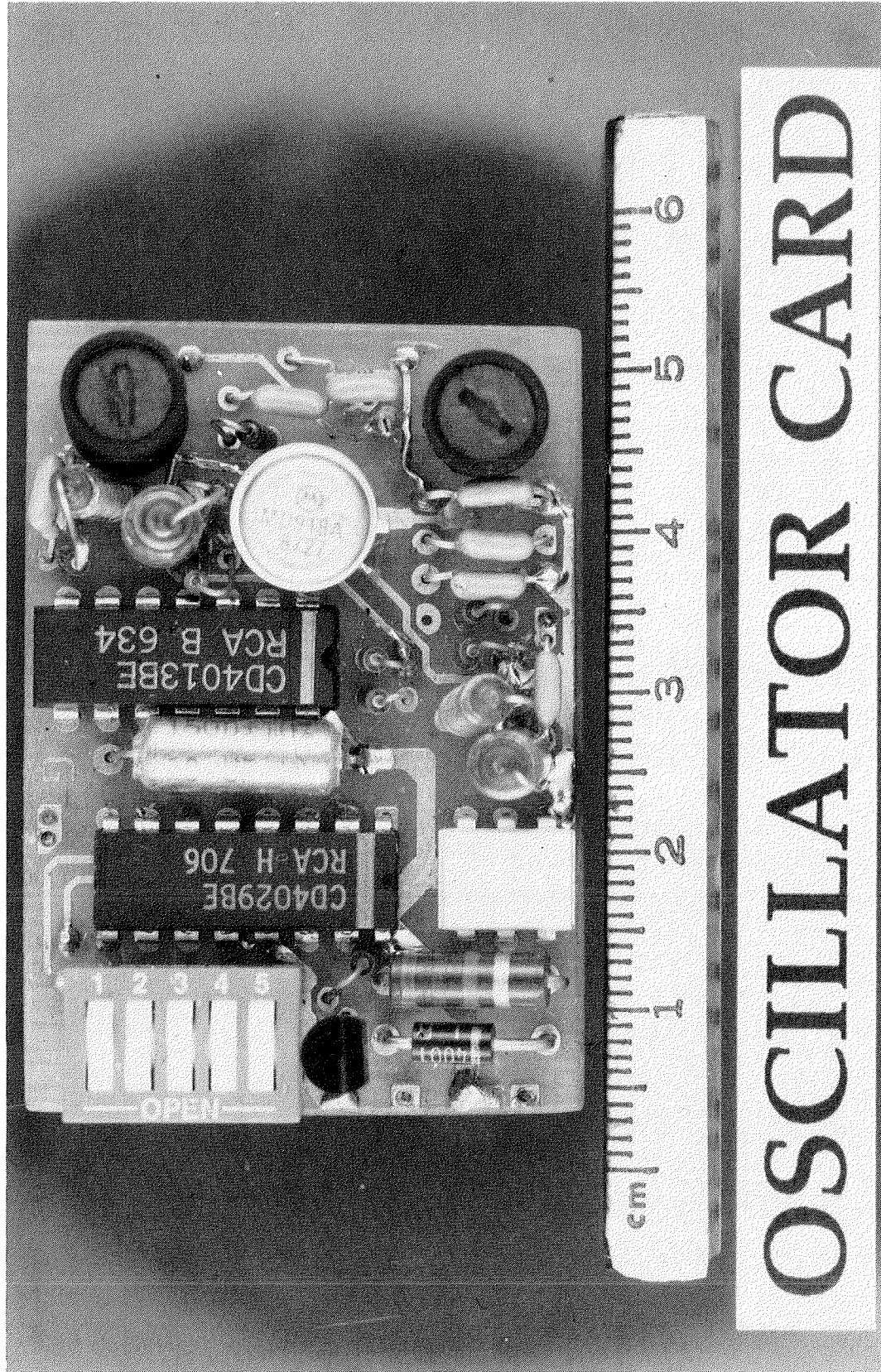


Figure C2. Wave gage oscillator card

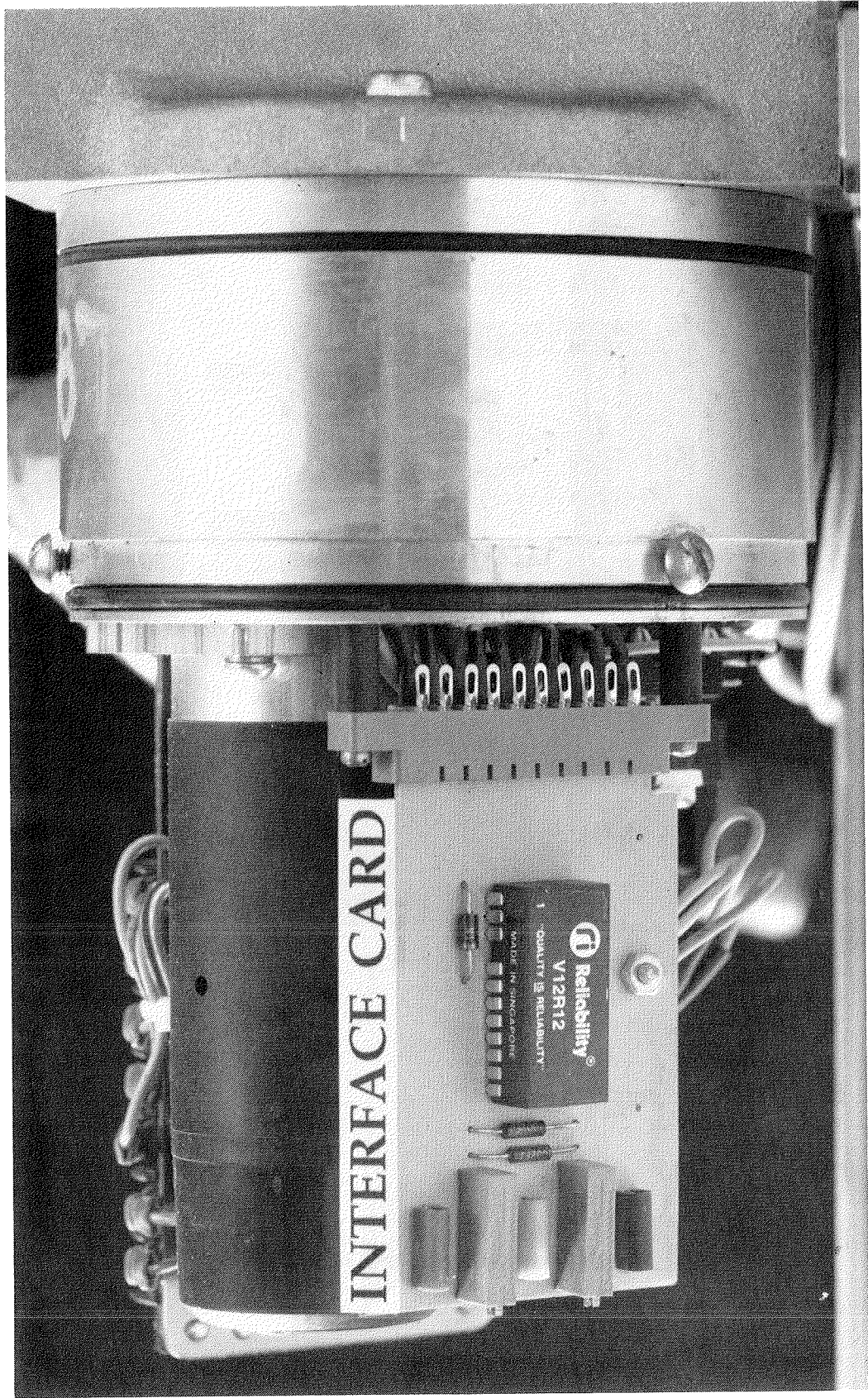


Figure C3. Wave gage interface card

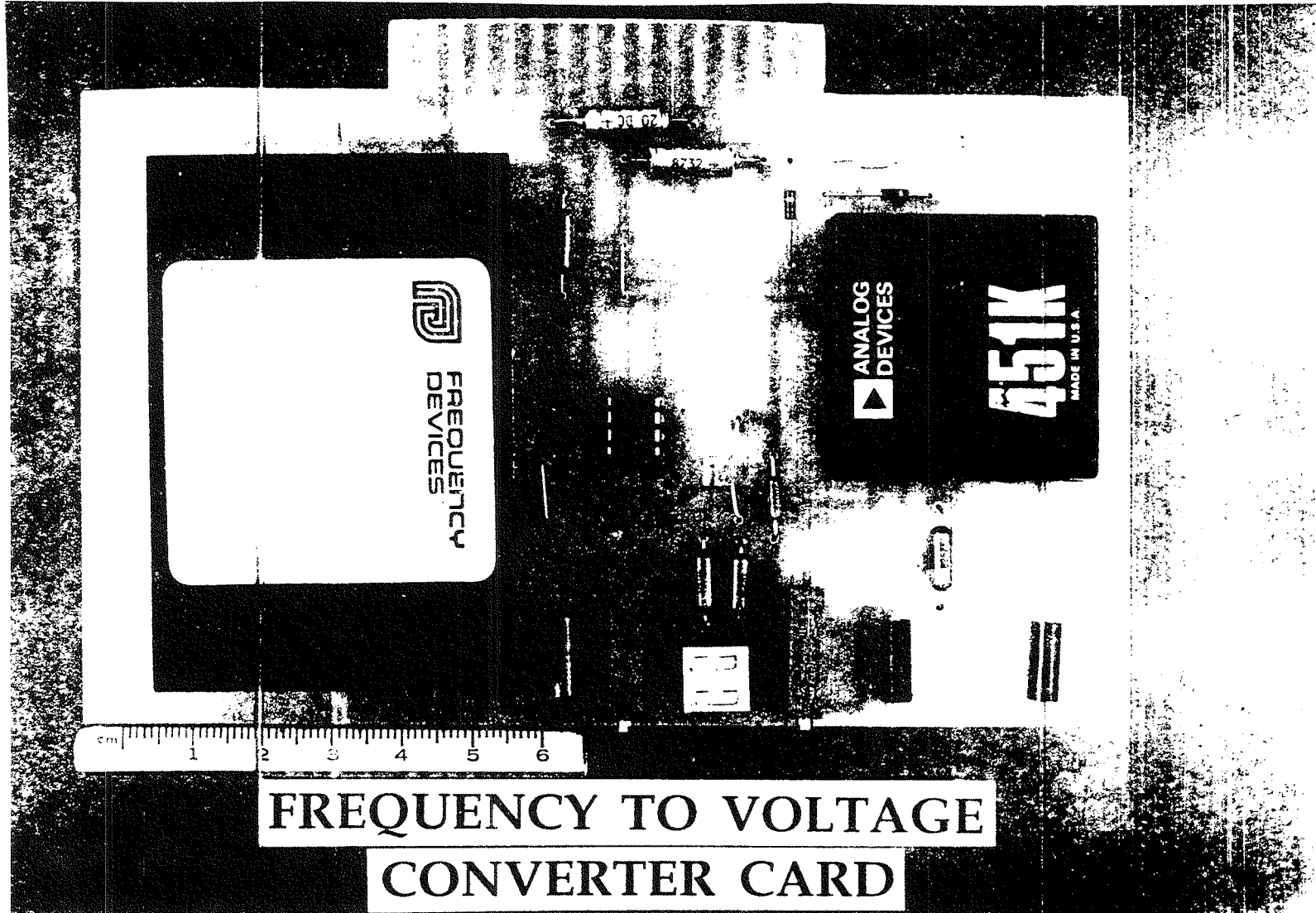
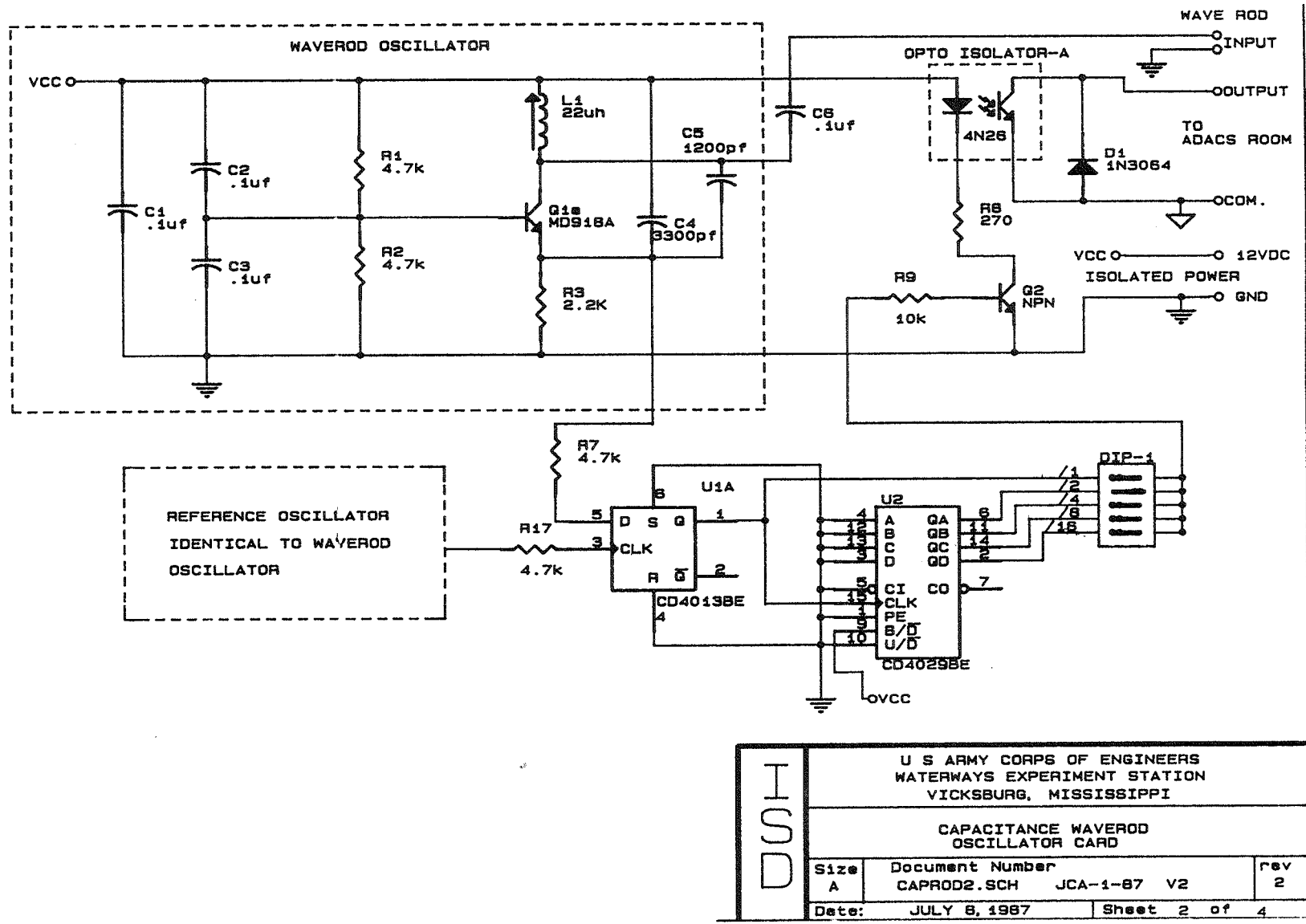


Figure C4. Wave gage frequency-to-voltage card

C7



DISI	U S ARMY CORPS OF ENGINEERS WATERWAYS EXPERIMENT STATION VICKSBURG, MISSISSIPPI		
	CAPACITANCE WAVEROD OSCILLATOR CARD		
	Size A	Document Number CAPROD2.SCH JCA-1-87 V2	rev 2
	Date:	JULY 8, 1987	Sheet 2 of 4

Figure C5. Wave gage oscillator card electrical schematic

88

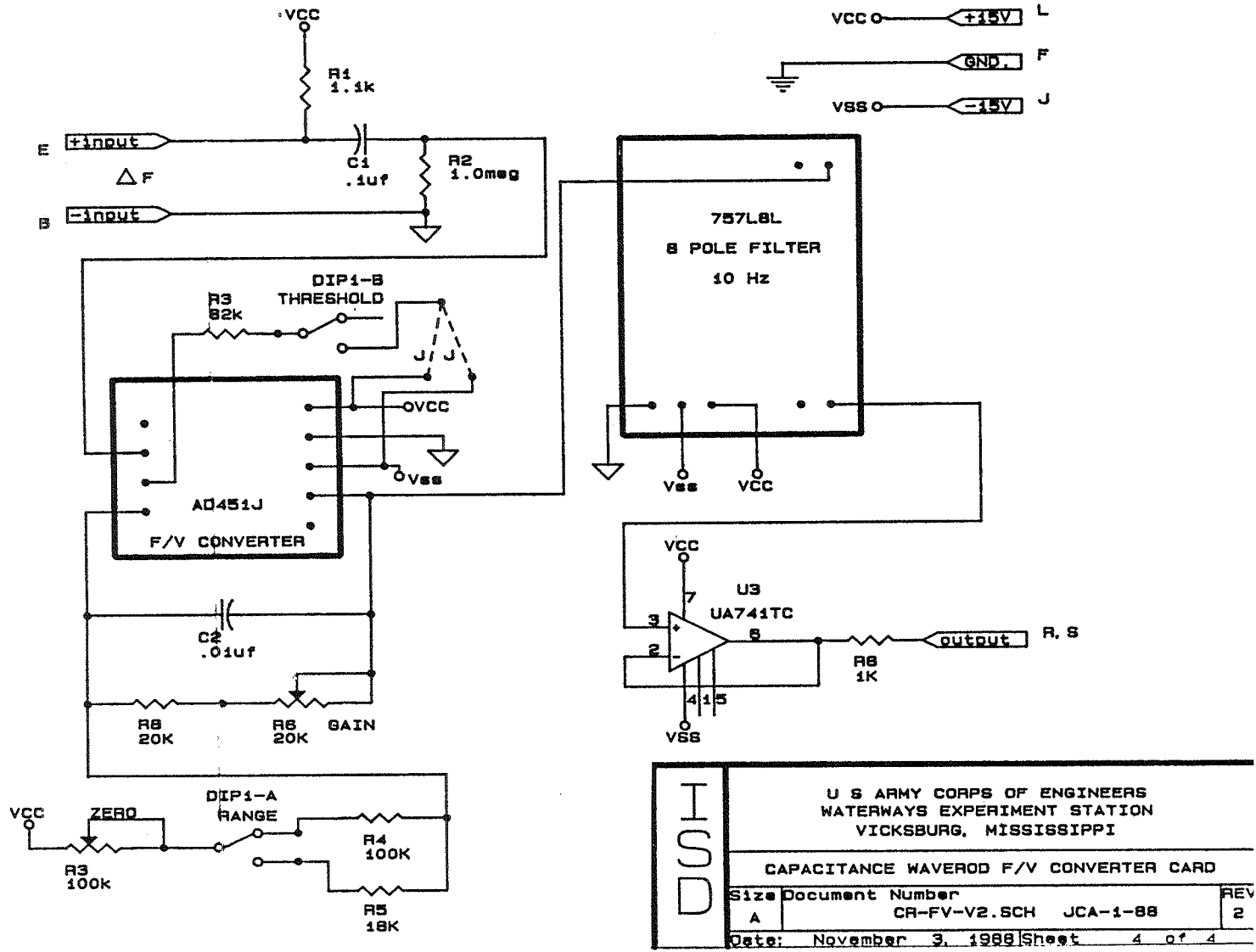
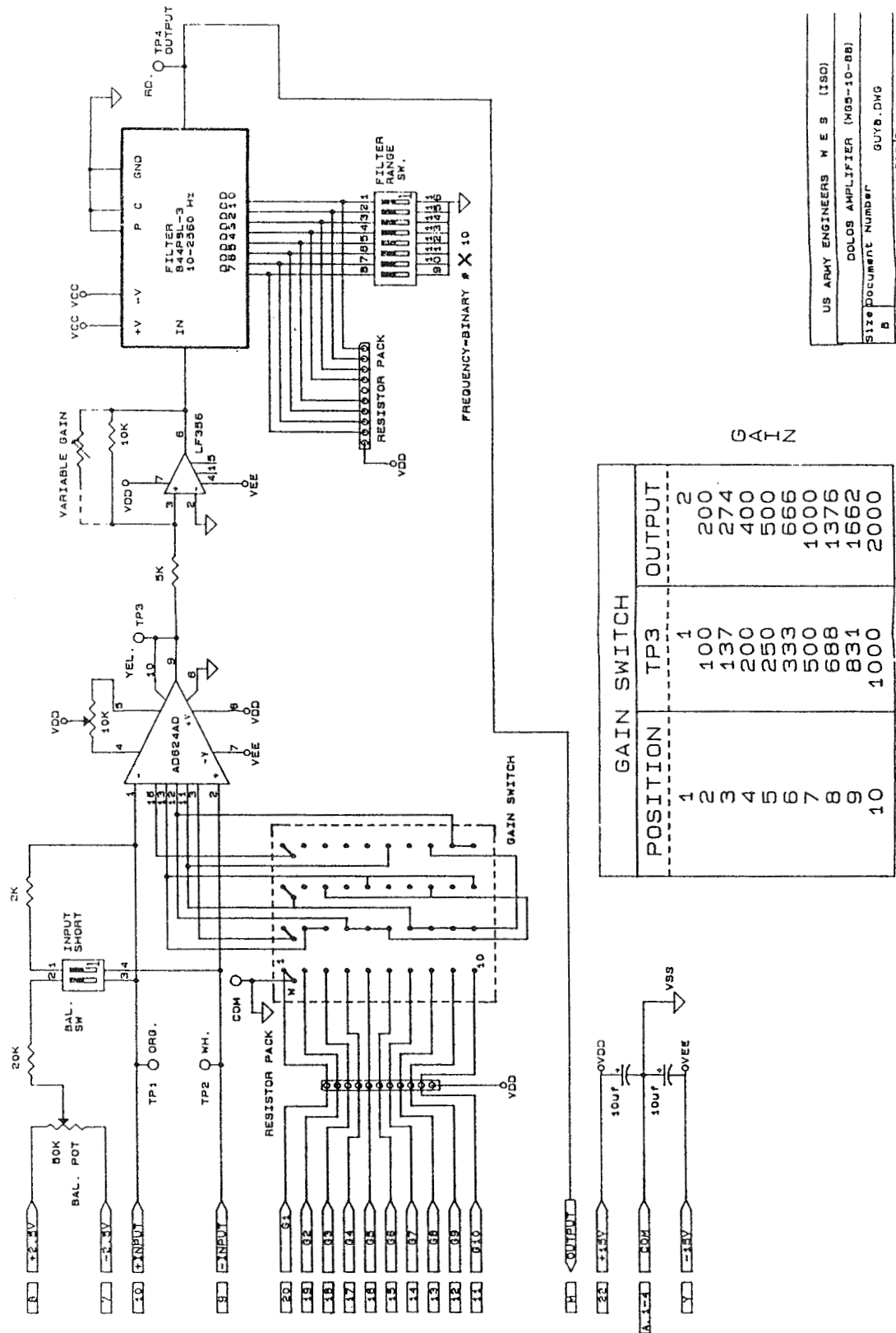


Figure C6. Wave gage frequency to voltage converter electrical schematic.





GAIN

POSITION	TP3	OUTPUT
1	100	200
2	137	274
3	200	400
4	250	500
5	333	666
6	500	1000
7	688	1376
8	831	1662
9	1000	2000
10		

US ARMY ENGINEERS M E S (ISO)  
 DOLOS AMPLIFIER (MOS-10-88)  
 Size/Document Number GUYB.DWG  
 Date: September 29, 1988 Sheet 1 of 3

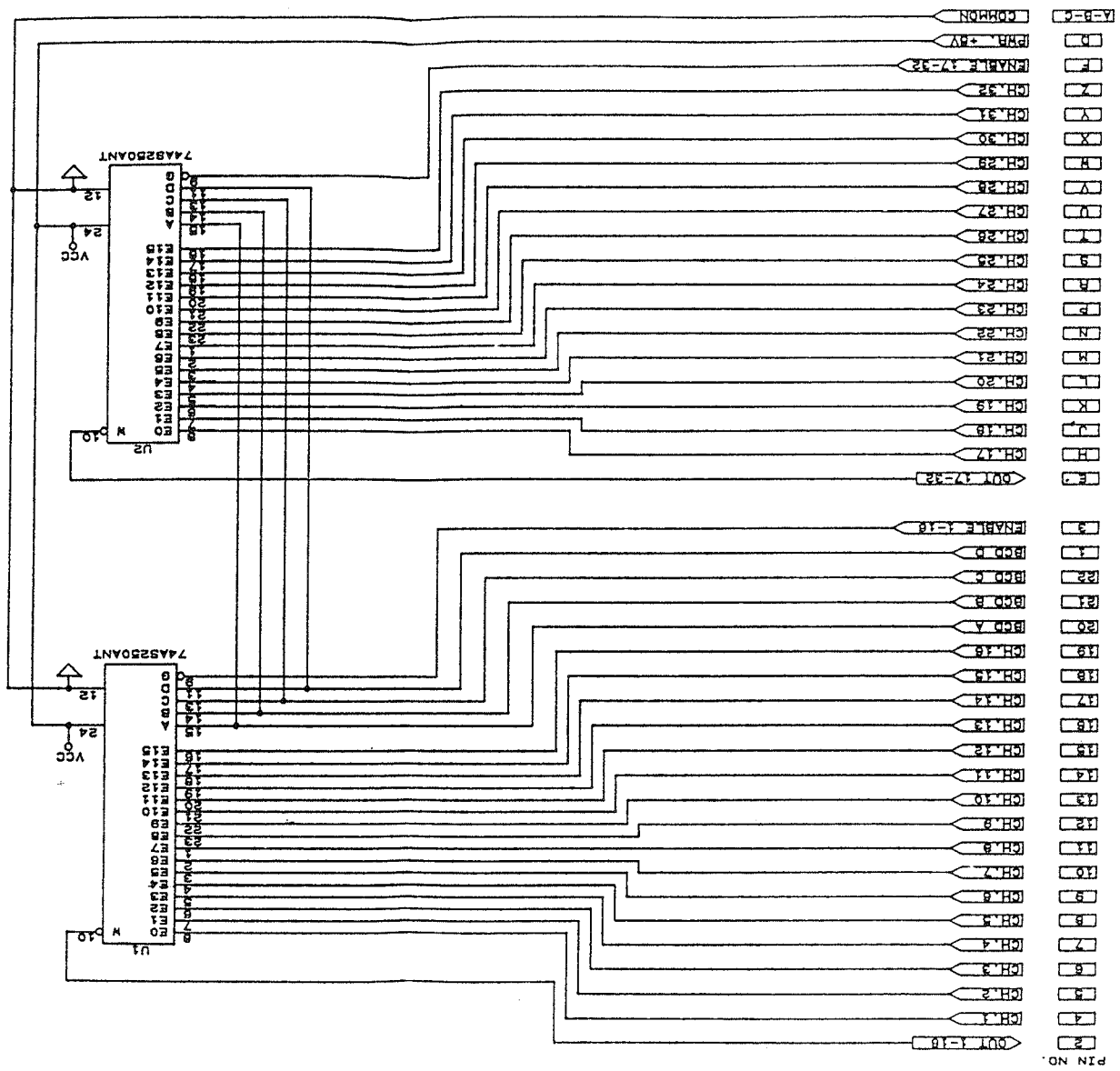
Figure C8. Electrical schematic of dolos load cell amplifier

COMPUTER CONTROL DIGITAL I/O LINES										
ENABLE	SELECT	STROBE			OUTPUT N	ENABLE OUTPUT	ENABLE S			
		A	B	C				D		
H	L	L	L	L	L	1-16	L			
H	L	L	L	L	2		L			
H	L	L	L	L	3		L			
H	L	L	L	L	4		L			
H	L	L	L	L	5		L			
H	L	L	L	L	6		L			
H	L	L	L	L	7		L			
H	L	L	L	L	8		L			
H	L	L	L	L	9		L			
H	L	L	L	L	10		L			
H	L	L	L	L	11		L			
H	L	L	L	L	12		L			
H	L	L	L	L	13		L			
H	L	L	L	L	14		L			
H	L	L	L	L	15		L			
H	L	L	L	L	16	1-16	L			
H	H	X	X	X	Z	7-32	H			
L	L	X	X	X	ISOLATED	ISOLATED	H			
H	H	L	L	L	17	17-32	L			
H	H	L	L	L	18		L			
H	H	L	L	L	19		L			
H	H	L	L	L	20		L			
H	H	L	L	L	21		L			
H	H	L	L	L	22		L			
H	H	L	L	L	23		L			
H	H	L	L	L	24		L			
H	H	L	L	L	25		L			
H	H	L	L	L	26		L			
H	H	L	L	L	27		L			
H	H	L	L	L	28		L			
H	H	L	L	L	29		L			
H	H	L	L	L	30		L			
H	H	L	L	L	31		L			
H	H	L	L	L	32	17-32	L			
H	L	X	X	X	Z	1-16	H			
L	L	X	X	X	ISOLATED	ISOLATED	H			

US ARMY ENGINEERS W E S (180)  
 TRUTH TABLE, DOLOS AMPLIFIER SYSTEM  
 Size Document Number 8049. TAB  
 Date: August 18, 1968 Sheet 1 of 1

Figure C9. Gain multiplexer truth table

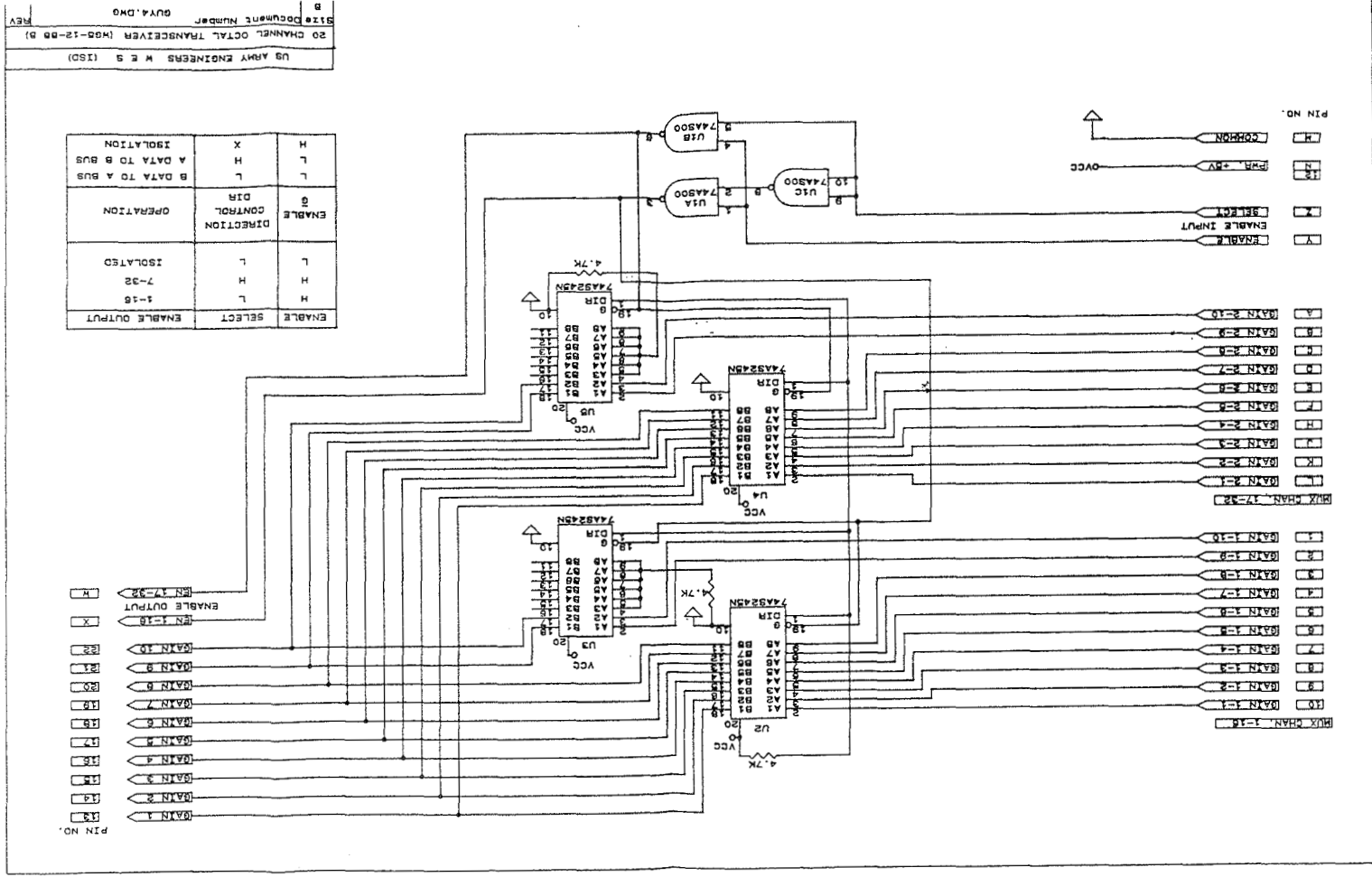
Figure C10. Electrical schematic for gain multiplexer, card 1



PIN NO.

US ARMY ENGINEERS M E S (18D)  
32 CHANNEL MULTIPLEXER (M08-12-BB)

Figure C11. Electrical schematic for gain multiplexer, card 2



### **Waterways Experiment Station Cataloging-in-Publication Data**

Markle, Dennis G.

Crescent City instrumented model dolos study : coastal model investigation / by Dennis G. Markle, Homer C. Greer, Coastal Engineering Research Center ; prepared for Department of the Army, US Army Corps of Engineers.

101 p. : ill. ; 28 cm. — (Technical report ; CERC-92-15)

Includes bibliographical references.

1. Breakwaters — California — Crescent City — Testing. 2. Embankments — Testing. 3. Embankments — Testing. 4. Hydraulic models. I. Greer, Homer C. II. United States. Army. Corps of Engineers. III. Coastal Engineering Research Center (U.S.) IV. U.S. Army Engineer Waterways Experiment Station. V. Title. VI. Series: Technical report (U.S. Army Engineer Waterways Experiment Station) ; CERC-92-15. TA7 W34 no.CERC-92-15